

EFFECTS OF MICROPLASTIC ON WATER FLOW AND CONTAMINANT TRANSPORT IN
WATER-SATURATED SAND



A Thesis Submitted in Partial Fulfillment of the Requirements
for the Degree of Master of Science in Earth Sciences

Department of Geology

FACULTY OF SCIENCE

Chulalongkorn University

Academic Year 2020

Copyright of Chulalongkorn University

ผลของไมโครพลาสติกต่อการไหลของน้ำและการเคลื่อนที่ของสารปนเปื้อนในทรายอ้อมตัวด้วยน้ำ



วิทยานิพนธ์นี้เป็นส่วนหนึ่งของการศึกษาตามหลักสูตรปริญญาวิทยาศาสตรมหาบัณฑิต

สาขาวิชาโลกศาสตร์ ภาควิชาธรณีวิทยา

คณะวิทยาศาสตร์ จุฬาลงกรณ์มหาวิทยาลัย

ปีการศึกษา 2563

ลิขสิทธิ์ของจุฬาลงกรณ์มหาวิทยาลัย

Thesis Title	EFFECTS OF MICROPLASTIC ON WATER FLOW AND CONTAMINANT TRANSPORT IN WATER-SATURATED SAND
By	Mr. Siravit Chanprasit
Field of Study	Earth Sciences
Thesis Advisor	Professor SRILERT CHOTPANTARAT, Ph.D.
Thesis Co Advisor	JENYUK LOHWACHARIN, Ph.D.

Accepted by the FACULTY OF SCIENCE, Chulalongkorn University in Partial
Fulfillment of the Requirement for the Master of Science

..... Dean of the FACULTY OF SCIENCE
(Professor POLKIT SANGVANICH, Ph.D.)

THESIS COMMITTEE

..... Chairman
(Assistant Professor AKKANEEWUT JIRAPINYAKUL, Ph.D.)

..... Thesis Advisor
(Professor SRILERT CHOTPANTARAT, Ph.D.)

..... Thesis Co-Advisor
(JENYUK LOHWACHARIN, Ph.D.)

..... Examiner
(Professor SANTI PAILOPLEE, Ph.D.)

..... External Examiner
(Pawee Klongvessa, D.Eng.)

ศิริวิทย์ จันทร์ประสิทธิ์ : ผลของไมโครพลาสติกต่อการไหลของน้ำและการเคลื่อนที่ของสารปนเปื้อน
 ในทรายอิ่มตัวด้วยน้ำ. (EFFECTS OF MICROPLASTIC ON WATER FLOW AND
 CONTAMINANT TRANSPORT IN WATER-SATURATED SAND) อ.ที่ปรึกษาหลัก : ศ. ดร.ศรีเลิศ
 โชติพันธุ์รัตน์, อ.ที่ปรึกษาร่วม : อ. ดร.เจนยุกต์ โล่ห์วัชรินทร์

ปัญหาการปนเปื้อนไมโครพลาสติกในสิ่งแวดล้อมทั่วโลกมีมานานหลายทศวรรษแล้ว ซึ่งผลของไมโครพลาสติกต่อสิ่งมีชีวิตได้มีการศึกษาวิจัยโดยละเอียด ในขณะที่ผลทางด้านชลศาสตร์ยังไม่ถูกกล่าวถึงมากนัก ดินเป็นปลายทางหนึ่งที่ยอมรับไมโครพลาสติกจากแหล่งอื่น จึงหลีกเลี่ยงไม่ได้ที่จะต้องเผชิญกับไมโครพลาสติกจำนวนมาก ซึ่งการเคลื่อนที่ของทรายผ่านไมโครพลาสติกและผลที่ตามมาอันยังไม่มีการศึกษาอย่างแน่ชัด งานวิจัยนี้มีจุดประสงค์เพื่อประเมินผลของไมโครพลาสติกต่อค่าสภาพนำชลศาสตร์ ค่าการแพร่กระจาย และสัมประสิทธิ์การแพร่กระจายของทราย โดยจะวัดจากการทดลองด้วยคอลัมน์ทรายขนาดเส้นผ่านศูนย์กลาง 7 เซนติเมตร โดยชั้นทรายมีความลึก 20 เซนติเมตร ครั้งหนึ่งของชั้นทรายจะถูกผสมด้วยไมโครพลาสติกเพื่อจำลองการปนเปื้อน ร่วมกับการใช้สารละลายตามรอยโบรไมด์ (ความเข้มข้น 1000 มิลลิกรัมต่อลิตร) เพื่อให้ควบคุมปัจจัยต่าง ๆ และทำการทดลองซ้ำได้ จากการทดลองทั้งสิ้น 15 คอลัมน์ของทรายที่ปนเปื้อนด้วยไมโครพลาสติกด้วยสัดส่วนที่แตกต่างกันตั้งแต่ร้อยละ 5 ถึง ร้อยละ 20 โดยมวล โดยมีทราย 3 ขนาด ได้แก่ 0.5-1.0 1.0-2.0 และ 2.0-4.0 มิลลิเมตร และ ไมโครพลาสติก 2 ขนาด ได้แก่ 0.25-0.5 และ 0.5-1.0 มิลลิเมตร ทำให้ได้ผลว่าการปนเปื้อนไมโครพลาสติกนั้นได้ส่งผลต่อทั้งค่าสภาพนำชลศาสตร์ของทรายและการแพร่กระจายของสารละลายตามรอยอย่างมีนัยสำคัญ นอกจากนี้ยังค้นพบความสัมพันธ์ระหว่างค่าสัมประสิทธิ์การแพร่กระจายกับค่าสภาพนำชลศาสตร์ และความสัมพันธ์ระหว่างค่าสัมประสิทธิ์การกระจายกับค่าการกระจายตัวซึ่งไม่เคยถูกกล่าวถึงในทฤษฎีใดมาก่อน ทั้งนี้ หลังจากการทดลองเสร็จสิ้นได้สังเกตการเคลื่อนที่ของไมโครพลาสติกที่ปนเปื้อนในคอลัมน์ทราย พบว่าไมโครพลาสติกไม่มีการรुक้าไปยังทรายชั้นอื่น

จุฬาลงกรณ์มหาวิทยาลัย
 CHULALONGKORN UNIVERSITY

สาขาวิชา โลกศาสตร์
 ปีการศึกษา 2563

ลายมือชื่อนิสิต
 ลายมือชื่อ อ.ที่ปรึกษาหลัก
 ลายมือชื่อ อ.ที่ปรึกษาร่วม

6172188023 : MAJOR EARTH SCIENCES

KEYWORD: Microplastics, Contaminant transport, Water flow, Water-saturated sand

Siravit Chanprasit : EFFECTS OF MICROPLASTIC ON WATER FLOW AND CONTAMINANT TRANSPORT IN WATER-SATURATED SAND. Advisor: Prof. SRILERT CHOTPANTARAT, Ph.D. Co-advisor: JENYUK LOHWACHARIN, Ph.D.

After decades of discovery of microplastic contamination over the world, effects of microplastic on organisms have been studied thoroughly, whereas ones on hydrological aspect are yet quite mentioned. As one of major microplastic sinks, soils are inevitable to face a number of microplastics; however, the movement of microplastic through soil and its consequence are still unknown. Then this research would be focusing on effects of microplastic contamination in soil sediment on hydraulic and transport parameters. Hydraulic conductivity (K), distribution coefficient (K_d), and dispersion coefficient (D) are the main parameters to be measured. The column experiment in column of diameter 7 cm and depth 20 cm of sand, half of which is contaminated with microplastic, together with bromide tracer solution (1000 mg/L) was chosen to be conducted for controllability, and replication. The total of 15 column experiments were conducted with microplastic contamination of microplastic in sand ranging from 5-20% by mass. Three size ranges of sand, 0.5-1.0, 1.0-2.0 and 2.0-4.0 millimeters, together with microplastic of size 0.25-0.5 and 0.5-1.0 millimeters, were used in the experiments. The result suggested that microplastic contamination has significantly affected hydraulic conductivity of the sand and dispersion of the solution. A relationship between hydraulic conductivity and dispersion coefficient, as well as one between distribution coefficient and dispersivity, was discovered. Those findings were mentioned in no prior theories. After each experiment, the movement, or migration, of microplastic was examined. The result suggested that there was no migration of microplastic to any other layers of sand.

Field of Study: Earth Sciences

Student's Signature

Academic Year: 2020

Advisor's Signature

Co-advisor's Signature

ACKNOWLEDGEMENTS

After two and a half years of hard work, this thesis has finally been complete with support and encouragement from my companions. Firstly, my advisor, who never gives up on me, no matter what kind of obstruction there is, guidance from him has led me to the right path. Secondly, all staffs and lecturers of the department, without whom my laboratory would never happen to finish, their technical support is worthier than any other one, especially in the middle of pandemic like this. Next, my family and my friends, who are always there for me when I needed their encouragement or even when I wanted to escape from stressful situations. Also, the university, for financial support, Ratchadapisek Sompoch Endowment Fund (2020) under Microplastic Cluster, Vidhayabundit Scholarship and Research Assistantship Scholarship, and Suntor Co. Ltd., for microplastic which I could not find somewhere else, without abovementioned supports, this thesis would not have even started. Lastly, I would appreciate myself, my best companion, for breaking through all difficulties, no matter how hard it is. You, I, we are cool, as we were, and shall be cooler hereafter.



จุฬาลงกรณ์มหาวิทยาลัย
CHULALONGKORN UNIVERSITY

Siravit Chanprasit

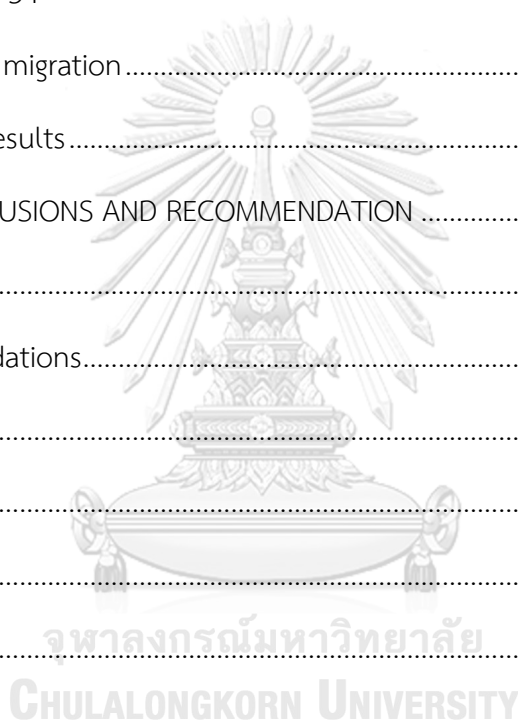
TABLE OF CONTENTS

	Page
.....	iii
ABSTRACT (THAI).....	iii
.....	iv
ABSTRACT (ENGLISH).....	iv
ACKNOWLEDGEMENTS.....	v
TABLE OF CONTENTS.....	vi
CHAPTER 1 INTRODUCTION.....	10
1.1 Rationale.....	10
1.2 Objectives.....	11
1.3 Hypothesis.....	11
1.4 Methodology.....	12
1.5 Research assumptions.....	12
1.6 Expected results.....	12
1.7 Organization of thesis.....	13
CHAPTER 2 LITERATURE REVIEW.....	14
2.1 Microplastic.....	14
2.2 Microplastic contamination in sandy beach.....	14
2.3 Microplastic contamination on sandy beaches on Gulf of Thailand.....	14
2.4 Vertical migration of microplastic in sand soil.....	14
2.5 Density separation.....	15
2.6 Influence of polyethylene microplastic.....	15

2.7 Pore volume and porosity	15
2.8 Seepage velocity	16
2.9 Hydraulic conductivity	16
2.10 Vertical hydraulic conductivity of stratified soil.....	17
2.11 Tracer transport in soil	18
2.12 Hydrodynamic dispersion	18
2.13 Peclet number	19
2.14 Sorption.....	19
2.15 Advection-Dispersion-Reaction equation.....	20
2.16 Electrical conductivity	20
2.16.1 EC and concentration.....	20
2.17 Breakthrough curve	21
2.17.1 Breakpoint.....	22
2.17.2 Adsorption capacity	22
2.18 Breakthrough curve fitting.....	23
2.19 HYDURS-1D.....	23
CHAPTER 3 METHODOLOGY	24
3.1 Flow chart	24
3.2 Material preparation.....	24
3.2.1 Column experiment.....	24
3.2.2 Sand	25
3.2.3 Microplastic.....	26
3.2.4 Bulk density measurement.....	26
3.2.5 EC meter.....	27

3.2.6 Tracer Solution.....	27
3.2.7 Sand and MP mixtures	27
3.2.8 Column packing	28
3.3 Column experiment procedure	29
3.3.1 EC measurement	29
3.3.2 Column experiment.....	29
3.3.3 Column section and sampling.....	31
3.3.4 Density separation.....	31
3.4 Data analysis	32
3.4.1 Hydraulic conductivity calculation	32
3.4.2 Breakthrough curve adjustment.....	33
3.4.3 Breakthrough curve fitting.....	33
3.4.4 Curve fitting with HYDRUS-1D	34
CHAPTER 4 RESULTS AND DISCUSSION	35
4.1 Basic hydraulic properties	35
4.1.1 Bulk density	35
4.1.2 Pore volume and porosity.....	35
4.1.3 Porosity and bulk density	36
4.1.4 Constant flow rate	37
4.1.5 Constant flow rate and bulk density.....	38
4.1.6 Constant flow rate and pore volume	39
4.1.7 Hydraulic conductivity of the column	39
4.1.8 Hydraulic conductivity of the middle layer	40
4.1.9 Hydraulic conductivity and grain size.....	41

4.2 Breakthrough curve analysis.....	43
4.2.1 Breakthrough curve fitting using spreadsheet software(Excel).....	43
(i) The parameters of breakthrough curve fitting.....	44
(ii) Usable capacity, total capacity, and usable fraction.....	46
4.2.2 Breakthrough curve fitting (HYDRUS-1D).....	48
4.2.3 The connection between two curve fitting methods (Excel and HYDRUS-1D) 54	
4.3 Microplastic migration.....	56
4.4 Additional results.....	58
CHAPTER 5 CONCLUSIONS AND RECOMMENDATION	59
5.1 Conclusions.....	59
5.2 Recommendations.....	60
APPENDIX A.....	61
APPENDIX B.....	71
APPENDIX C.....	73
APPENDIX D.....	97
APPENDIX E.....	118
REFERENCES	126
VITA.....	130



CHAPTER 1 INTRODUCTION

1.1 Rationale

After over 50 years of the first discovery, microplastic is nowadays one of the most well-known global contaminants. The plastic particles of size smaller than 5 millimeters (Xu et al. 2020; Bissen and Chawchai 2020; O'Connor et al. 2019), microplastics, could be categorized into two groups with respect to the origination. Primary microplastic refers to the intentionally produced microplastic, while secondary microplastic refers to the plastic particles originated from weathering and degradation of larger plastics, unintentionally (Royer et al. 2018). The plastic particle has been discovered contaminating the environment throughout the world, including seafloor (La Daana et al. 2018; Peng et al. 2020; Goodman et al. 2020), beaches (Urban-Malinga et al. 2020; Bissen and Chawchai 2020; Ballent et al. 2016), lakes (Su et al. 2016), estuaries (Zhang et al. 2019; Firdaus, Trihadiningrum, and Lestari 2020), groundwater (La Daana et al. 2018), rivers (Lestari et al. 2020) and so on. Even in Thailand, it was discovered that sandy beaches alongside the Gulf of Thailand have also been contaminated with microplastics (Bissen and Chawchai 2020; Thepwilai et al. 2021).

Nowadays, there have been a great number of studies about microplastic, in various aspects, namely, the discovery, the hazard to variety of aquatic organisms (Wu et al. 2020; Beyer et al. 2017; Schmid et al. 2018), etc. Yet the hydrogeological effects of microplastic contamination have not been thoroughly investigated. Once the comprehension of microplastic manner in such aspect is clear, it could lead to better microplastic regulation.

(Hüffer et al. 2019) has discovered that the transport of pesticides could be influenced by microplastic contamination, in this case mainly polyethylene one. Consequently, this study was aimed to simulate microplastic contamination in water-saturated sand column and investigate effects of the contamination on flow and transport, indicated by hydrogeological parameters, namely porosity (ϕ), hydraulic conductivity (K), dispersion coefficient (D), and distribution coefficient (K_d) which might have been affected according to microplastic disruption on

particle configuration, over various amount of microplastic in each batch. The representative microplastic in the experiment was selected to be low-density polyethylene according to tendency to degrade into secondary microplastic (Royer et al. 2018) as well as the availability in real situations (Saliu et al. 2018; Firdaus, Trihadiningrum, and Lestari 2020). The sand was used in three size ranges, 0.5-1.0, 1.0-2.0 and 2.0-4.0 mm, representing fine sand, coarse sand, and very coarse sand, respectively. Meanwhile, the microplastic was used in two size ranges, 0.25-0.5 and 0.5-1.0 mm which is discovered contaminating some environment (Urban-Malinga et al. 2020).

Empirical theory about hydrogeological effects of microplastic is expected to be the result of this study and the foundation of future microplastic contamination research.

1.2 Objectives

- To investigate hydrogeological effects of microplastic contamination in water-saturated sand by measuring porosity (ϕ), hydraulic conductivity (K), dispersion coefficient (D), and distribution coefficient (K_d) of columns with different amount of microplastic contaminant.
- To examine migration of microplastic in water-saturated sand columns under different amounts of microplastic contamination

1.3 Hypothesis

The hypothesis of this thesis is that the existence of microplastic contamination in sand columns would have effects on the hydraulic parameters (e.g., porosity (ϕ), hydraulic conductivity (K), dispersion coefficient (D), and distribution coefficient (K_d)) of the sand in the column. And there should be some trend over different concentrations of microplastic contaminant for each parameter. Moreover, with relatively smaller size the sand particle, the microplastic would have more tendency to migrate along the direction of water flow.

1.4 Methodology

This study was divided into 3 parts:

- Microplastic and sand were mixed with different sand size combination and concentrations, in the unit of mass percentage. The combination of sand size and microplastic concentration are as follows:
 - 1) Microplastic of size 0.25-0.5 mm was mixed with sand of size 0.5-1.0 mm at concentrations of 5%, 10%, 15% and 20%,
 - 2) Microplastic of size 0.5-1.0 mm was mixed with sand of size 0.5-1.0 mm at concentrations of 5%, 10%, 15% and 20%, and
 - 3) And microplastic of size 0.5-1.0 was mixed with sand of size 1.0-2.0 and 2.0-4.0 at concentrations of 5% and 15%
- Columns of microplastic-sand mixture were flown with deionized water and sodium bromide (NaBr) solution, as a tracer solution, to measure the hydraulic conductivity (K), dispersion coefficient (D), and distribution coefficient (K_d) of each column.
- The mixture in the columns, after flowing with water and NaBr solution, were sectioned into three main layers, sampled, and measured the concentrations of microplastic in each layer, in order to investigate the gradient of microplastic concentrations.

1.5 Research assumptions

In this research, it was assumed that sand-microplastic mixtures were packed into the column uniformly, i.e., the concentration at every point is equal. The mixtures reacted with neither water nor sodium bromide solution. The sand was water-saturated throughout the column experiment, and the flow in column was downward.

1.6 Expected results

The result of this study was expected to investigate effects of microplastic contamination in soil on the hydraulic properties.

1.7 Organization of thesis

This thesis composed of five chapters, including Chapter 1 Introduction, Chapter 2 Literature Review, Chapter 3 Methodology, Chapter 4 Results and Discussion, and Chapter 5 Conclusions and Recommendation, respectively.



CHAPTER 2 LITERATURE REVIEW

2.1 Microplastic

Microplastic (MP) is defined to be plastic particles of size, or length, less than 5 mm. Microplastics are divided into two main categories: primary microplastics, and secondary microplastics. Primary microplastics are those plastics whose dimension is intentionally produced smaller than 5 mm, e.g., microbeads. While secondary microplastics are originated from the degradation of larger plastic pieces caused by weathering (Royer et al. 2018). Microplastic could also be classified by the shape into microfilm, microfiber, microbead (granule), foam and fragment (debris).

2.2 Microplastic contamination in sandy beach

(Urban-Malinga et al. 2020) has revealed that there are microplastic contamination in sandy beaches of southern Baltic Sea. Moreover, the majority of plastic particle was of size 0.5-1.0 mm and color blue. The result suggested that high contamination sites were associated to plastic macrolitter pollution and anthropogenic activities, namely, fishery (microfibers from fishing net), and tourism (synthetic fibers from tourists' clothes).

2.3 Microplastic contamination on sandy beaches on Gulf of Thailand

(Bissen and Chawchai 2020; Thepwilai et al. 2021) have sampled sands from beaches alongside the shore of Gulf of Thailand and discovered abundance of MP in all 25 samples collected. Most of the MP found was of sheet and fiber shapes, and black. The amount of MP was discovered correlative to the surface circulation direction as well as the anthropogenic factors, such as fishing industries, and sewage system.

2.4 Vertical migration of microplastic in sand soil

(O'Connor et al. 2019) have conducted an experiment of tidal flow in the sand column. And the result came out that fine polyethylene microplastic (PE) had

migrated deepest among all microplastics used in the experiment. So, polyethylene microplastic was selected to be the representative due to high tendency of migration.

2.5 Density separation

Density separation is a simple but effective technique of extracting microplastic out of other substances. It relies on a simple buoyancy principle that a matter of lower density would float in a solution of higher density. Microplastics which have various density up to the type of plastic, shall require different density of solution for separation process. One of most widely used solutions is zinc chloride ($ZnCl_2$) due to the cost and wide range of solution density provided (up to 2.1 g/cm^3). However, sodium chloride ($NaCl$) and sodium iodide (NaI) could also be used.

2.6 Influence of polyethylene microplastic

(Hüffer et al. 2019) has discovered that contamination of polyethylene microplastic could have influence on the transport of some pesticides in soils. Distribution coefficient, together with sorption capacity of the MP was lower than one of the pure soil, implying that microplastic-contaminated soils would have lower distribution coefficient and sorption capacity. This was caused by the fact that molecular interactions between the pesticide and the PE was weaker than ones between the pesticide and soil particles.

2.7 Pore volume and porosity

Pore volume (PV) is one of the fundamental hydrological parameters referring to the volume of air, or void, in a material. In this study, PV was measured within column setting process, the sand and mixture were gradually set together with water into the column with lid at the lower end, in order to ensure that the media is completely saturated. When the setting was finished, the total volume of water used was taken to be the pore volume.

Porosity (ϕ) is the ratio of pore volume, or void space to the total volume of the material. Porosity could be calculated from Equation 2.1.

$$\phi = \frac{PV}{V_T} \quad [2.1]$$

Where PV stands for pore volume, and

V_T stands for the total volume of the material.

2.8 Seepage velocity

Seepage velocity, denoted by v_s , represents the actual velocity of the fluid flowing through the void space in the material. The seepage velocity could be represented in Equation 2.2.

$$v_s = \frac{v}{\phi} \quad [2.2]$$

Where v stands for discharge velocity.

ϕ stands for porosity.

2.9 Hydraulic conductivity

Hydraulic conductivity, K , describes the ability of a fluid flowing through a porous media. It is dependent on the permeability of the media, the saturation degree, the density and viscosity of the fluid. In this case, the experiment was conducted in saturated media, so a hydraulic conductivity measured was a saturated one. According to (Gefell, Larue, and Russell 2019), for vertical columns, the hydraulic conductivity could be represented in Equation 2.3.

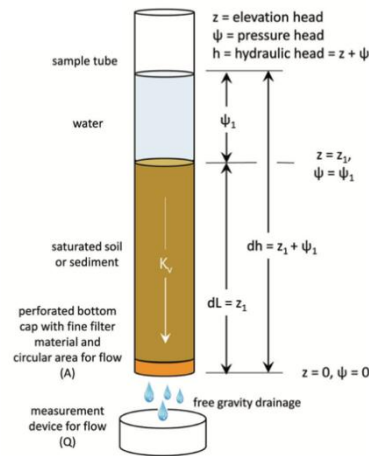


Figure 2.1 The vertical sand column with free gravity drainage (Gefell, Larue, and Russell 2019)

$$K_V = \frac{Q}{A \frac{dh}{dt}} \quad [2.3]$$

Where K_V stands for vertical hydraulic conductivity

Q stands for flow rate

A stands for cross section area of the column and.

$\frac{dh}{dt}$ stands for hydraulic gradient.

2.10 Vertical hydraulic conductivity of stratified soil

For a soil composing of layers of different types of soil, or different hydraulic conductivity, the equivalent vertical hydraulic conductivity of the whole system could be calculated by Equation 2.4.

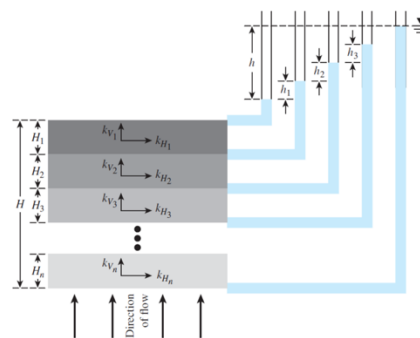


Figure 2.2 The hydraulic conductivity of stratified soil

$$K = \frac{H}{\frac{H_1}{K_{V_1}} + \frac{H_2}{K_{V_2}} + \dots + \frac{H_n}{K_{V_n}}} \quad [2.4]$$

Where K stands for the vertical hydraulic conductivity of the column

K_{V_i} stands for the vertical hydraulic conductivity of the i^{th} layer

$i = 1, 2, 3, \dots, n$

H stands for the depth of the in-column soil, and

H_i stands for the depth of the i^{th} layer, $i = 1, 2, 3, \dots, n$.

2.11 Tracer transport in soil

Sodium bromide (NaBr) solution is regarded as a non-reactive tracer, that is it does not react with soil particles and components and has low sorption to soil particles, moreover, salt tracers are suitable for small-scale experiments such as soil column (Treatise on Water Science), therefore, several studies have used it as tracer in soil columns. (Masipan, Chotpantararat, and Boonkaewwan 2016) conducted a vertical column experiment and used NaBr as a tracer to determine the dispersivity of the solution in the column. As a result, positive power correlation between column length and dispersivity was discovered. Also, bromide tracer was used by Kastrinos et al. (2019), Labrecque et al. (2021) (Kastrinos, Chiasson, and Ormond 2019; Labrecque and Blanford 2021) and many more. Furthermore, due to availability, NaBr was selected to be the tracer in this study.

2.12 Hydrodynamic dispersion

Molecular diffusion, diffusion process caused by the concentration gradient, and mechanical dispersion, diffusion process caused by movement of the solute front, are combined, and regarded as hydrodynamic dispersion (Fetter, Boving, and Kremer 1999). Up to three directions of dispersion could be put in consideration, however, in this study, only longitudinal dispersion, dispersion in the same direction as the flow of the solute, would be considered. Dispersion in such direction could be determined by the coefficient of longitudinal dispersion

(D_L). D_L could be represented as the sum of mechanical dispersion and molecular diffusion as shown in Equation 2.5.

$$D_L = \alpha_L v_s + D^* \quad [2.5]$$

Where D_L stands for hydrodynamic dispersion in longitudinal direction

α_L stands for longitudinal dispersivity

v_s stands for seepage velocity, and

D^* stands for molecular diffusion.

The value of D^* usually lies in the magnitude of $10^{-5} - 10^{-6}$ cm²/s (Cussler and Cussler 2009), so, if the term $\alpha_L v_s$ is greater than D^* , the term D^* could be omitted.

2.13 Peclet number

Peclet number (Pe_L) is a dimensionless ratio of advection rate over dispersion rate, showing the predominance of either of two, see Equation 2.6.

$$Pe_L = \frac{vL}{D_L} \quad [2.6]$$

Where Pe_L stands for Peclet number

v stands for advective velocity

L stands for characteristic length

D_L stands for longitudinal dispersion coefficient

2.14 Sorption

Sorption is the collective term of adsorption, chemisorption, absorption, and ion exchange. In this study, the sorption isotherm (see Figure 2.3), the relation between input concentration and the amount of sorbed solute, was assumed to be linear. Accordingly, the degree of sorption could be represented with the slope of the line called distribution coefficient (K_d).

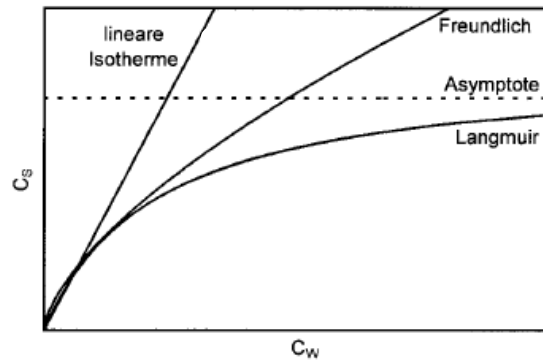


Figure 2.3 Sorption isotherm

2.15 Advection-Dispersion-Reaction equation

The equation (see Equation 2.7) describes the dispersing manner of a solution in a saturated homogeneous porous media.

$$\frac{\partial C}{\partial t} = D_L \frac{\partial^2 C}{\partial x^2} - v \frac{\partial C}{\partial x} - \frac{B_d}{\theta} \frac{\partial C^*}{\partial t} - \left(\frac{\partial C}{\partial t} \right)_{rxn} \quad [2.7]$$

Where C stands for the concentration

t stands for time

$D_L \frac{\partial^2 C}{\partial x^2}$ represents the dispersion process

$v \frac{\partial C}{\partial x}$ represents the advection process

$\frac{B_d}{\theta} \frac{\partial C^*}{\partial t}$ represents the sorption process, and

$\left(\frac{\partial C}{\partial t} \right)_{rxn}$ represents the reaction process.

2.16 Electrical conductivity

The electric conductivity (EC) of a solution could be measured by an EC meter.

The unit of conductivity is $\mu\text{S}/\text{cm}$.

2.16.1 EC and concentration

It is suggested that the electric conductivity and the concentration of an ion are linearly proportional (see Figure 2.4) (Richards 1954). When only the relative concentration was in consideration, it is eligible to regard the

conductivity as the concentration. Such calculation was previously done by (Hossain 2006) as shown in Equation 2.8.

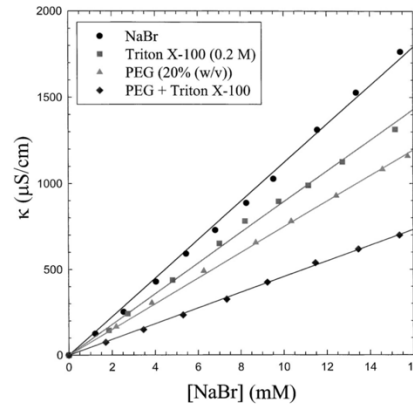


Figure 2.4 The relation between EC and the concentration (Polle and Chen 2015)

$$C/C_0 = \frac{EC_i - BG}{TR - BG} \quad [2.8]$$

Where C/C_0 stands for relative concentration of sodium bromide solution

EC_i stands for the EC value of the the i^{th} sample, $i = 0, 1, 2, 3, \dots$

BG stands for the background EC value, and

TR stands for the EC value of the sodium bromide solution.

2.17 Breakthrough curve

Breakthrough curve is a graph of relative concentration of outlet solution over time or flown volume (see Figure 2.5). Breakthrough curves may contain only ascending log of the graph, up to maximum concentration, but in this study, as pioneering research, the descending one was included to provide more precise information. In this study, after the effluent concentration have reached the maximum concentration for some time, the influent would be swapped back to pure water, causing the decline of the curve. The 'swap point' was set to be the end of ascending log and the start of descending log.

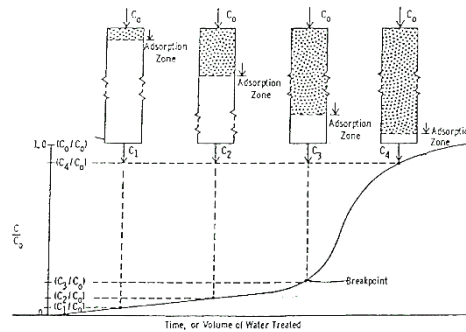


Figure 2.5 Breakthrough curve derived from sample collection

2.17.1 Breakpoint

Breakpoint is the point at which the relative concentration of the effluent solution approaches the value of 0.05 (5%) for the ascending log (see Figure 2.6).

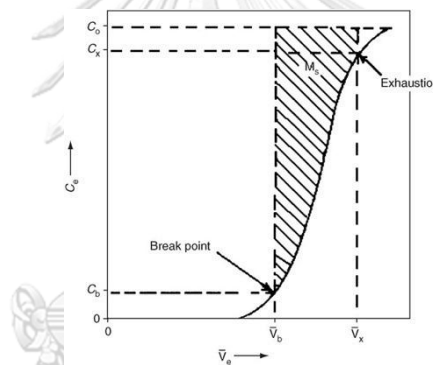


Figure 2.6 Breakpoint and exhaustion point of ascending log

2.17.2 Adsorption capacity

The capacity of soil adsorption could be determined by a ratio of breakpoint, or the area over the curve to the breakpoint itself, to the total capacity, the whole area over the curve. Note that only ascending log was considered in the following calculations.

$$x_B = \int_0^{t_B} (1 - C/C_0) dx \quad [2.9]$$

$$x_T = \int_0^{\infty} (1 - C/C_0) dx \quad [2.10]$$

The usable fraction, $\frac{x_B}{x_T}$, could represent the fraction of column used for adsorption of the solution.

2.18 Breakthrough curve fitting

Breakthrough curves were fitted by the function solver in Microsoft Excel. Each curve was divided into two sections, or logs, namely ascending and descending. Ascending log and descending log would be fitted by Equation 2.11 and 2.12 respectively.

$$C/C_0 = 1 - e^{-kt^n} \quad [2.11]$$

$$C/C_0 = e^{-kt^n} \quad [2.12]$$

Where k and n are constants, and t represents the cumulative volume of flown solution relative to pore volume. The first equation would fit the ascending section and the second one would fit the descending part.

Moreover, the curve would be fitted with HYDRUS-1D, to obtain the values of distribution coefficient (K_d), longitudinal dispersivity (α_L) and, consequently, dispersion coefficient (D_L) to interpret the constants k and n . Since such curve fitting was noticed in no prior studies, k and n might yet be interpreted or discovered correlating any other hydraulic parameter

2.19 HYDRUS-1D จุฬาลงกรณ์มหาวิทยาลัย

HYDRUS-1D is a program for simulation of one-dimensional movement of water, heat, and solutes in variably saturated media. By numerically solve Richard's equation for water flow, and Advection-Dispersion-Reaction equation for heat and solute transport (Source: <https://www.pc-progress.com/en/Default.aspx?h1d-description>), HYDRUS-1D could simulate the transport and consequently be used to fit breakthrough curves.

CHAPTER 3 METHODOLOGY

3.1 Flow chart

The working plan of this study is represented in figure 3.1.

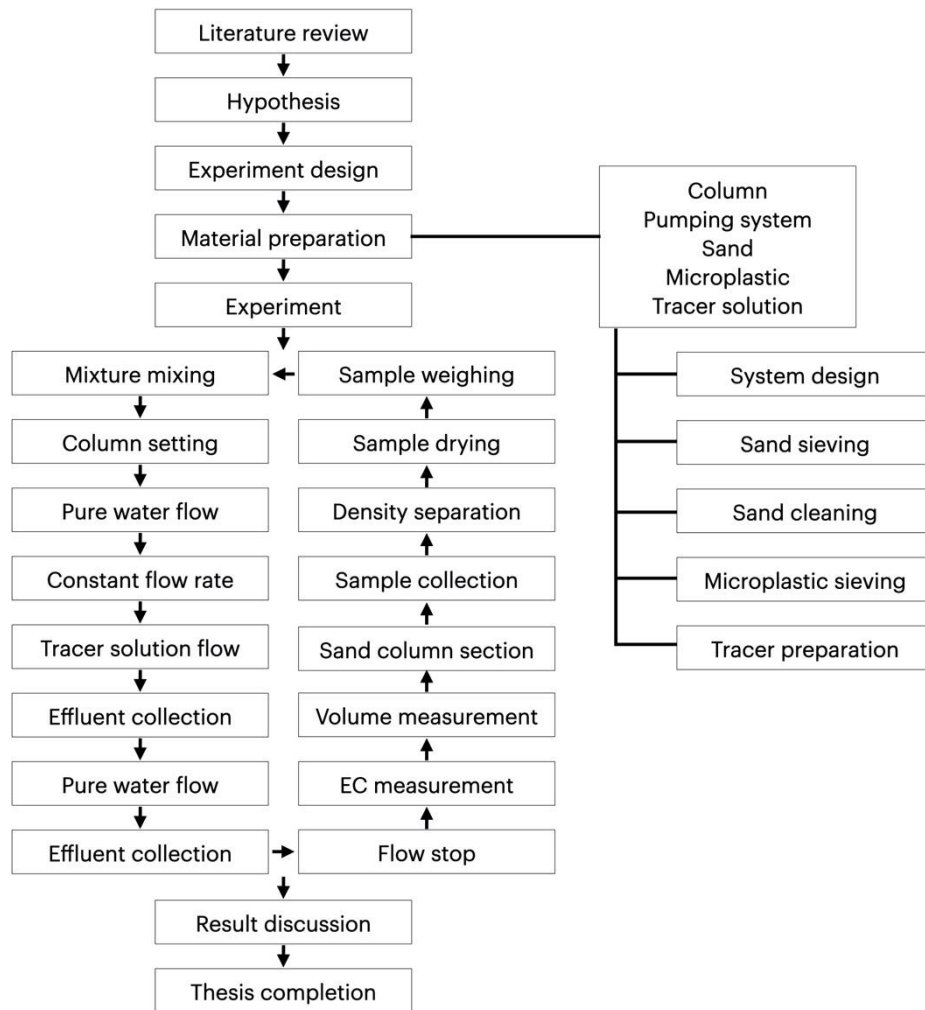


Figure 3.1 The workflow of the research

3.2 Material preparation

3.2.1 Column experiment

The column used in the experiment was made of a transparent acrylic tube of height 30 centimeters as shown in Figure 3.2, outer diameter of 7 centimeters and average inner diameter of 6.450 centimeters. Along the side, centimeter scale was marked, a hole was punctured at height of 21 centimeters, connected with a tube, to overflow the fluid, maintaining

constant ponding level. The bottom was dammed with a mesh and a cloth secured by cable ties. Also, a lid could be attached when the column was being set as shown in Figure 3.2.

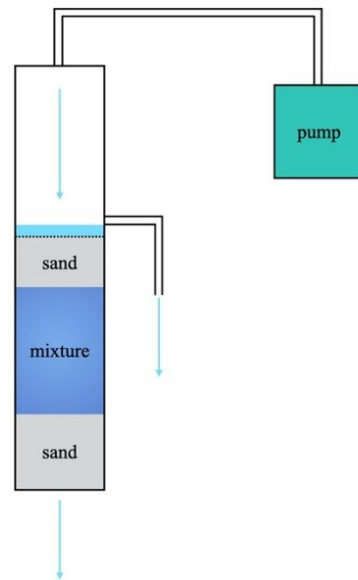


Figure 3.2 The column experiment and real column setting

3.2.2 Sand

Aquarium sand was purchased and sieved with meshes of size 0.25, 0.5, 1.0, 2.0 and 4.0 mm, most of the sand was of three size ranges, 0.5-1.0, 1.0-2.0 and 2.0-4.0 mm, as shown in Figure 3.3. In this study, the sand of each size range was regarded as a representative of fine sand, coarse sand, and very coarse sand. The sieved sand was inspected visually for impurities and rinsed with tap water until no dust was noticeable, then soaked in 5% (W/W) nitric acid for 24 hours to digest organic matters. The acid was then rinsed with deionized water for 5 times. Afterwards, the sand was dried in the dry cabinet at 60 degrees Celsius for 96 hours. The processed sand is shown in Figure 3.3. Lastly, sample of each size range was collected for density measurement.



Figure 3.3 The sands (0.5-1.0, 1.0-2.0 and 2.0-4.0 mm respectively)

3.2.3 Microplastic

The microplastic, blue LDPE debris, as shown in Figure 3.4, was provided by Suntor Co., Ltd. The plastic was sieved with the meshes of size 0.25, 0.5, 1.0, and 2.0 mm and, afterwards, inspected for impurities. A sample of each size range was collected for density measurement.

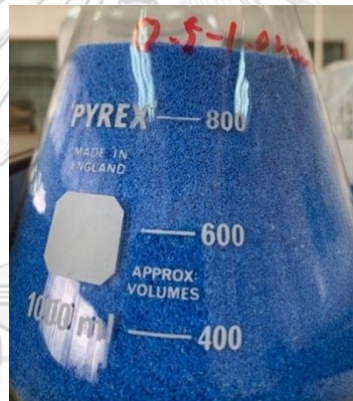


Figure 3.4 The microplastic provided by Suntor Co., Ltd.

3.2.4 Bulk density measurement

Each sample of sand and microplastic packed in a stainless-steel container of volume 100 cm³ and then weighed. The bulk density of each sample was calculated by Equation 3.1.

$$\rho_B = \frac{m}{V} \quad [3.1]$$

3.2.5 EC meter

Hanna Instruments two channel HI 3512 EC meter was used in the experiment. The meter was regularly calibrated with 1413 $\mu\text{S}/\text{cm}$ standard solution.

3.2.6 Tracer Solution

In each experiment, the tracer solution was prepared by dissolving 5 grams of sodium bromide (NaBr) (see Figure 3.5) in 5 liters of deionized water.



Figure 3.5 Sodium Bromide (NaBr)

3.2.7 Sand and MP mixtures

The sand and the plastic were mixed with various sand sizes and MP concentrations as shown in Table 3.1 and Figure 3.6.

Table 3.1 Combination of MP and sand

Particle size (mm)		Microplastic concentration (W/W)				
MP	Sand	0%	5%	10%	15%	20%
0.25-0.5	0.5-1.0	✓	✓	✓	✓	✓
0.5-1.0	0.5-1.0	✓	✓	✓	✓	✓
	1.0-2.0	✓	✓	-	✓	-
	2.0-4.0	✓	✓	-	✓	-



Figure 3.6 A mixture of 5% of 0.25-0.5 mm MP in 0.5-1.0 mm sand

3.2.8 Column packing

The first (bottom) 6-centimeter layer was packed pure sand of size 0.5-1.0 mm. Then the mixture was packed for 10 centimeters. And topped with another layer of 4-centimeter pure sand of size 0.5-1.0 mm. The packing was done by slowly putting little sand by a time and then carefully applying pure water to the sand to ensure the saturation, pressing, and slightly stirring might be required. The water amount should be appropriate as excessive water could lead to the floatation of MP. At the top of the sand, was a stainless-steel mesh placed, to prevent any erosion caused by water steam (see Figure 3.7). During the process of sand packing, water was regularly applied to ensure that the packed sand was saturated with water. Moreover, the total amount of water applied was recorded and regarded as the pore volume of the column.



Figure 3.7 Packed column

3.3 Column experiment procedure

3.3.1 EC measurement

Before each experiment was conducted, the deionized water and the tracer solution was measured with EC meter to obtain background EC of each environment

3.3.2 Column experiment

Firstly, deionized water was applied to the column, the pump adjusted to maintain ponding level constant. In this process, the flow rate of the column was measured and kept the flow time of 50 ml. Afterwards, the effluent was regularly measured for EC to keep the initial EC equal for each experiment. When the EC of effluent was approximately 50 $\mu\text{S}/\text{cm}$, the experiment was started pumping the tracer solution reservoir. At the same time, sample collection was started, the samples were collected in amount of 30 and 40 ml, depending on the periodical sampling collection. At a point the pump was moved back to deionized water reservoir (between No. 19 and No. 20 in Table 2), denoted by swap point, the flow continued until sample collection was completed. After the flow, measurement of each sample EC was done three times due to the fluctuation of the meter and the volume of each

sample was recorded.

The amount of collected effluent volume was adjusted after the pioneering column of 15% of 0.25-0.5 mm MP in 0.5-1.0 mm sand. The results suggested that the samples should be collected as follows.

Table 3.2 The volume of effluent solution samples to be collected in the experiment

No.	Volume (ml)	No.	Volume (ml)	No.	Volume (ml)	No.	Volume (ml)
1	40	11	30	21	40	31	30
2	40	12	30	22	40	32	30
3	40	13	30	23	40	33	30
4	40	14	30	24	40	34	30
5	30	15	40	25	30	35	40
6	30	16	40	26	30	36	40
7	30	17	40	27	30	37	40
8	30	18	40	28	30	38	40
9	30	19	40	29	30		
10	30	20	40	30	30		

Since the flow rate of each column might be different, the sample was collected with respect to volume instead of time interval. Moreover, the swap point, at which the pump was relocated back to deionized water reservoir, was simply between the sample number 19 and 20. After collected sampling, each sample was EC and volume measured (see Figure 3.8). The results were shown in APPENDIX.



Figure 3.8 EC measurement

3.3.3 Column section and sampling

For the sand column, after the experiment, no matter if there was sign of plastic particle movement to another layer of sand, the pure sand layers were inspected another time in the sectioning process. The mixing layer was sectioned in to three sublayers namely top, middle, and bottom, the process was done with estimation by sight, a sample from each sublayer was collected and prepared for density separation process as shown in Figure 3.9.



Figure 3.9 showing the sectioning column

3.3.4 Density separation

After collected from the column, the sample was kept dry at room temperature. In the process of density separation, pure water was added to the sample, stirring was applied until the plastic particle stayed afloat (see Figure 3.10), then the MP was gradually separated from the fluid by stainless-steel spatula. The spatula was regularly rinsed with pure water to recover the

sticking particles. The sand and plastic samples were kept in dry cabinet for 96 hours and weighed. Mass percentage of MP in each sample was calculated.

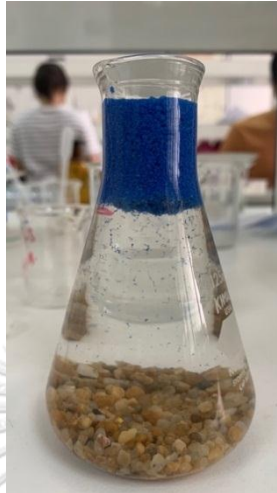


Figure 3.10 showing density separation

3.4 Data analysis

3.4.1 Hydraulic conductivity calculation

According to (Gefell, Larue, and Russell 2019), vertical hydraulic conductivity of a column could be calculated from Equation 2.3.

The hydraulic conductivity of the middle layer could be calculated from one of the entire column. As a column of stratified soil structure, the hydraulic conductivity of the column could be represented in Equation 3.2.

$$K = \frac{H}{\frac{H_1}{K_{V_1}} + \frac{H_2}{K_{V_2}} + \frac{H_3}{K_{V_3}}} \quad [3.2]$$

By taking $H = 20$ cm, $H_1 = 4$ cm, $H_2 = 10$ cm, $H_3 = 6$ cm, K is the hydraulic conductivity of the column, $K_{V_1} = K_{V_3}$ is the vertical hydraulic conductivity of the pure sand 0.5-1.0 mm, k_{V_2} could be represented in Equation 3.3.

$$K_{V_2} = \left(\frac{2}{K} - \frac{1}{K_{V_1}} \right)^{-1} \quad [3.3]$$

3.4.2 Breakthrough curve adjustment

To plot the normalized breakthrough curve of each column, it is necessary to convert the data in horizontal axis into the scale of pore volume with the formula in Equation 3.4.

$$v_k = \frac{(\sum_{i=0}^{k-1} x_i) + \frac{x_k}{2}}{PV} \quad 3.4$$

Where v_k stands for the middle point of the k^{th} interval on the horizontal axis in the unit of pore volume, $k = 1, 2, 3, \dots$

x_i stands for volume of the i^{th} sample, $i = 0, 1, 2, 3, \dots$ and $x_0 = 0$, and

PV stands for the pore volume of the column.

Meanwhile, the relative concentration was calculated from EC value by Equation 2.8. The scatterplot of adjusted volume (PV) and relative concentration would form the breakthrough curve.

3.4.3 Breakthrough curve fitting

The breakthrough curves were sectioned into two logs at the swap point, namely ascending, and descending. The ascending log and the descending log of each breakthrough curve were separately fitted to Equation 2.11 and Equation 2.12, respectively. The coefficient of determination (R^2) was used to determine the

The values of k and n of each log would be provided by the function solver of Microsoft Excel. The fitted breakthrough curve, one with highest R^2 value, would be used to determine the breakpoint of each breakthrough curve.

Moreover, HYDRUS-1D software was used to fit the curves as well, to obtain the value of longitudinal dispersivity and, consequently, coefficient of longitudinal dispersion.

3.4.4 Curve fitting with HYDRUS-1D

In the process of fitting breakthrough curves in HYDRUS-1D, the configuration was set as follows: Main Processes – simulate water flow and solute transport (standard solute transport), and enable inverse solution; Inverse solution – estimate soil hydraulic parameters, and solute transport parameters (from flux concentration); Soil Hydraulic Model – van Genuchten-Mualem with no hysteresis; Water Flow Boundary Conditions – constant pressure head for upper boundary condition and free drainage for lower boundary condition; Solute Transport – equilibrium model. In this case, some parameters of the sand and solute were to be input, namely residual water content (θ_r), saturated water content (θ_s), saturated hydraulic conductivity (K_s), longitudinal dispersivity (α_L), distribution coefficient (K_d), and van Genuchten parameters (α and n). The parameters θ_r , α , and n was provided by the software neural network prediction by inputting the bulk density of the sand due to the lack of data source and the fact that changes of those parameters have very little impact to the breakthrough curve, θ_s could be regarded as the porosity (ϕ), while α_L and K_d would be varied until the simulated breakthrough curve fit the experimental breakthrough curve ($R^2 > 0.95$).

CHAPTER 4 RESULTS AND DISCUSSION

The results of this study were divided into four main parts as follows: 1) Basic hydraulic properties, 2) Breakthrough curve analysis, 3) Microplastic migration, and 4) Additional results.

4.1 Basic hydraulic properties

This section consists of results and discussion on the following parameters, bulk density, pore volume, constant flow rate, and hydraulic conductivity.

4.1.1 Bulk density

The density of sand was measured without any obstruction, while one of microplastic could not be measured directly. As the plastic debris showed the characteristic of compressibility, i.e., the amount of to-be-weighed plastic was dependent on the tightness of particle packing in the container, resulting a considerable gap of density. So, the density of the plastic debris was assumed to be the same as of ordinary LDPE, which is 0.940 g/cm^3 (Source: <https://www.plasticseurope.org/en/about-plastics/what-are-plastics/large-family/polyolefins>). The result of the density is shown in Table 4.1.

Table 4.1 Density of the sands

Material	Density (g/cm^3)
Sand 0.5-1.0 mm	1.504
Sand 1.0-2.0 mm	1.764
Sand 2.0-4.0 mm	1.717

4.1.2 Pore volume and porosity

For pure sand columns (0% MP), it is noticeable that sand of size 0.5-1.0 mm has higher value of porosity than ones of size 1.0-2.0 and 2.0-4.0 mm, as shown in Figure 4.1. This could have explained the fact that sands of size 1.0-2.0 and 2.0-4.0 mm have higher bulk density than sand of size 0.5-1.0 mm.

It is reasonable that the porosity decreases while the MP percentage increases as plastic particles could have fulfilled the gap between sand particles. However, there were some columns having outlying pore volume. The fluctuations might have been a consequence of the abovementioned sponge-like behavior of the MP; slight change of packing tightness could have caused some change in porosity. The larger sands (sands of size 1.0-2.0 mm and 2.0-4.0 mm) having higher bulk densities (1.764 and 1.717 g/cm³) could compress the debris tighter, resulting greater decrease in pore volume than smaller sand (0.5-1.0).

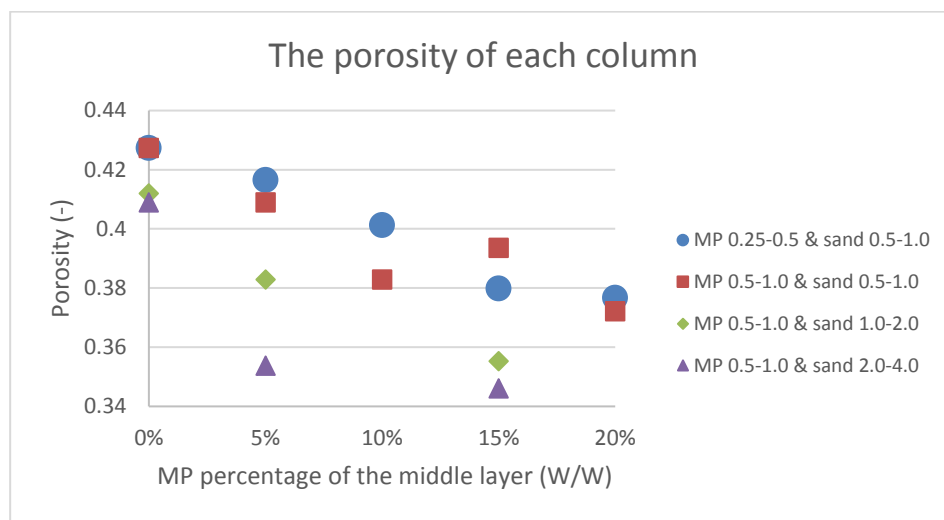


Figure 4.1 The porosity of the column over the mass percentage of MP in the middle layer

4.1.3 Porosity and bulk density

For each pair of sand and microplastic, positive correlation between bulk density and porosity of is noticeable, see Figure 4.2. This could have been caused by the fact that, in the column with more microplastic, the void between sand particles was fulfilled by the debris, causing lower porosity. Meanwhile, the bulk density would be lower as the plastic mass was lighter than the sand particle.

For ordinary sands, bulk density and porosity have negative correlation (Kakaire et al. 2015; Oleszczuk and Truba 2013), but the scatterplot above suggested that microplastic contaminated soil does not follow the trend of normal soil. Furthermore, the columns of 0.25-0.5 mm MP in 0.5-1.0 mm sand

and 0.5-1.0 mm MP in 2.0-4.0 mm sand have shown the manner in opposite way, having positive correlation.

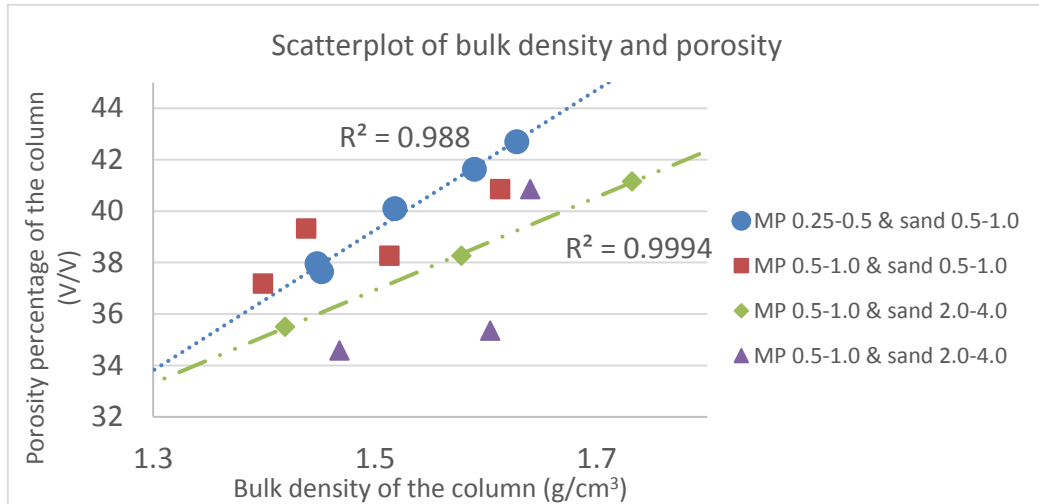


Figure 4.2 The scatterplot of bulk density and the porosity of the column

4.1.4 Constant flow rate

The constant flow rate of each column was measured and shown in Figure 4.3. It is noticeable that, firstly, columns of larger sand particles have higher constant flow rate than those of smaller sand particles, i.e., at the same percentage of MP. For example, the constant flow rate increases from 0.25-0.5 mm MP in 0.5-1.0 mm sand to 0.5-1.0 mm MP in 0.5-1.0 mm, 1.0-2.0 mm, and 2.0-4.0 mm sand respectively. This could have been caused by the bigger void space in each column which facilitates the water flow through the media.

Moreover, as MP amount increases, the MP particles, being smaller than sand particles, could fulfill the void between sand particles, causing lower flow rate. Secondly, the overall behavior of the constant flow rate is that it decreases and then increases at the end, such behavior shows up in every column experiments. This would be discussed later in section 4.1.7. Lastly, the constant flow rate of columns of 0.5-1.0 mm MP in 0.5-1.0 sand appeared to be steady. While ones of the other columns (MP smaller than sand) appeared to be decreasing. This could lead to a conclusion that relative size between MP and sand has affected the constant flow rate. That is the lower the average particle size, the lower the constant flow rate.

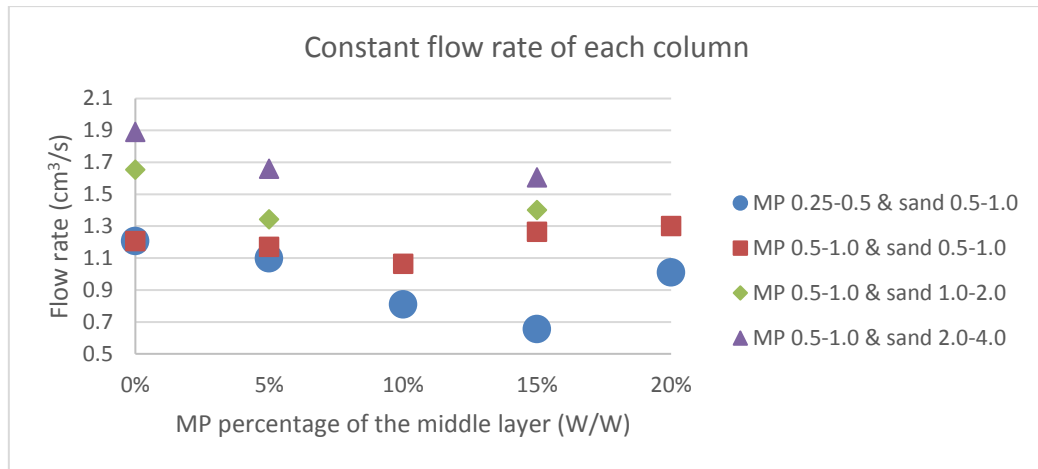


Figure 4.3 The constant flow rate of the column over the mass percentage of MP in the middle layer

4.1.5 Constant flow rate and bulk density

The scatterplot of bulk density and pore volume in Figure 4.4 showed no visible correlation between the parameters despite considering separately by groups of sand and microplastic. This could lead to a conclusion that the constant flow rate and bulk density of the column with microplastic-contaminated sand have no direct relationship, that is microplastic contamination did not introduce any correlation between the two parameters.

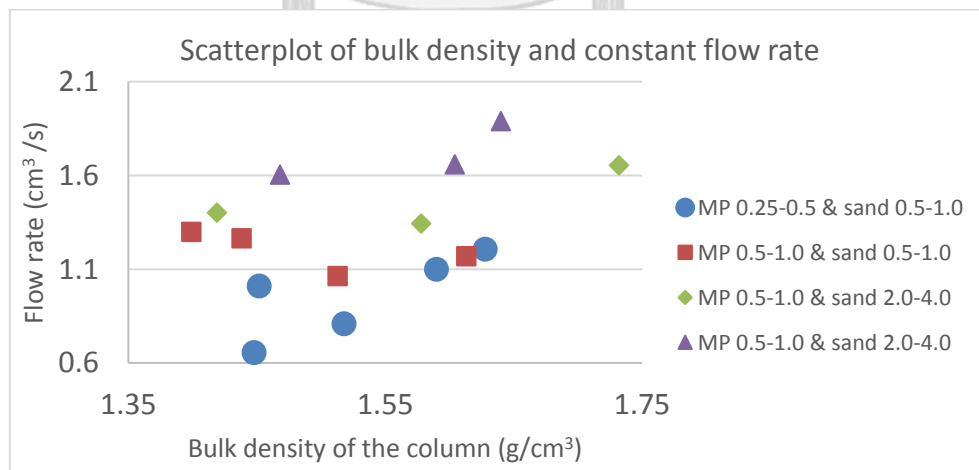


Figure 4.4 The scatterplot of the bulk density and the constant flow rate of the column

4.1.6 Constant flow rate and pore volume

Like one of bulk density and the constant flow rate of the column, the scatterplot of pore volume and flow rate in Figure 4.5 showed no direct relationship between the pore volume and the flow rate in this experiment. Therefore, a conclusion could be drawn in the same manner that microplastic did not introduce any correlation between the parameters.

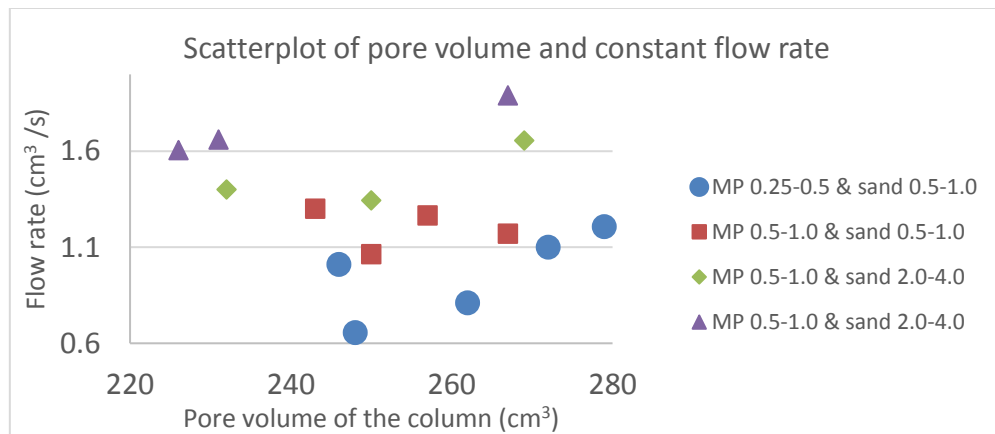


Figure 4.5 The scatterplot of the pore volume and the constant flow rate of the column

4.1.7 Hydraulic conductivity of the column

Hydraulic conductivity of the column could be calculated by Equation 2.3 and shown as follows in Figure 4.6.

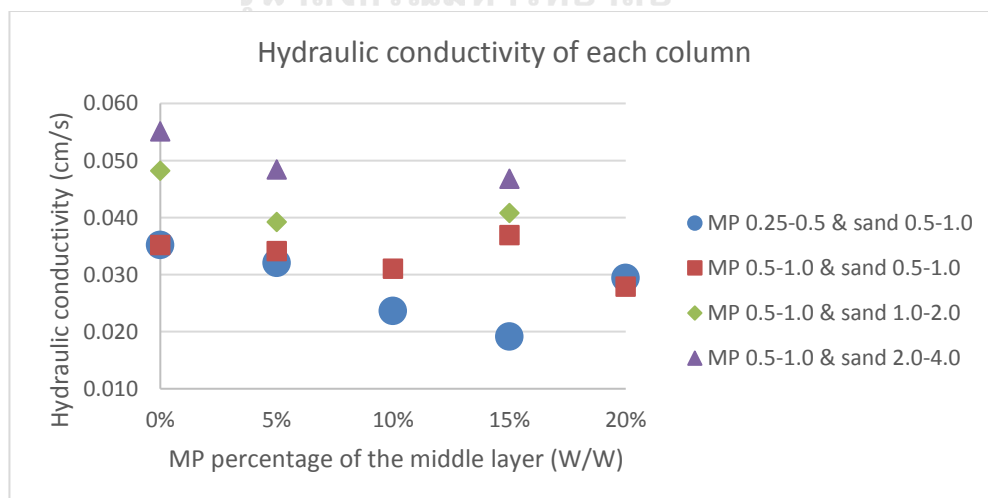


Figure 4.6 Hydraulic conductivity of the column over the mass percentage of MP in the middle layer

4.1.8 Hydraulic conductivity of the middle layer

The hydraulic conductivity of the middle layer of each column could be calculated from the ones of the whole column and of 0.5-1.0 mm sand with Equation 2.4 and represented in Figure 4.7. The hydraulic conductivity of pure sand of size 0.5-1.0 mm stayed unchanged for the hydraulic conductivity is depth-independent, while ones of the other columns would vary due to the media difference. The result of calculation showed that the hydraulic conductivities of the middle layers lie in the range of 0.01-0.04 cm/s (0.5-1.0 mm sand), 0.04-0.08 cm/s (1.0-2.0 mm sand) and 0.06-0.13 cm/s (2.0-4.0 mm sand). These values coincide the hydraulic conductivity of fine sand, medium sand, and coarse sand respectively (Source: https://structx.com/Soil_Properties_007.html), confirming that the three sizes of sand were good representatives of sands.

Moreover, to investigate the ‘turning point’ of the trendlines, the unit of horizontal axis was changed into ‘volume percentage of microplastic in the middle layer’. All the trendlines were generated to fit with polynomial of degree 2 (see 4.1.9). For columns of 0.25-0.5 mm MP in 0.5-1.0 mm sand and, the turning point, the point where the hydraulic conductivity reaches the minimum value, appeared to lie between 15-20% of MP (V/V) while ones of the columns of 0.5-1.0 mm MP in all sizes of sands (0.5-1.0, 1.0-2.0 and 2.0-4.0 mm) appeared to lie between 10-15% of MP (V/V). This could be concluded that the turning point is determined only by the MP size, the smaller the MP, the further the turning point. Interestingly, if the MP is smaller, the turning point would lie closer to 100%, making the curve continually decreasing with no turning up.

The manner of ‘turning’ of hydraulic conductivity is similar to one proposed by (Woessner and Poeter 2020) (see Figure 4.8). That is normally the hydraulic conductivity would decrease to a point and slightly increase. Such behavior was described as “The larger grains of coarse sand occupy some of the pore space available for water flow in the 100% fine-sand sample.”

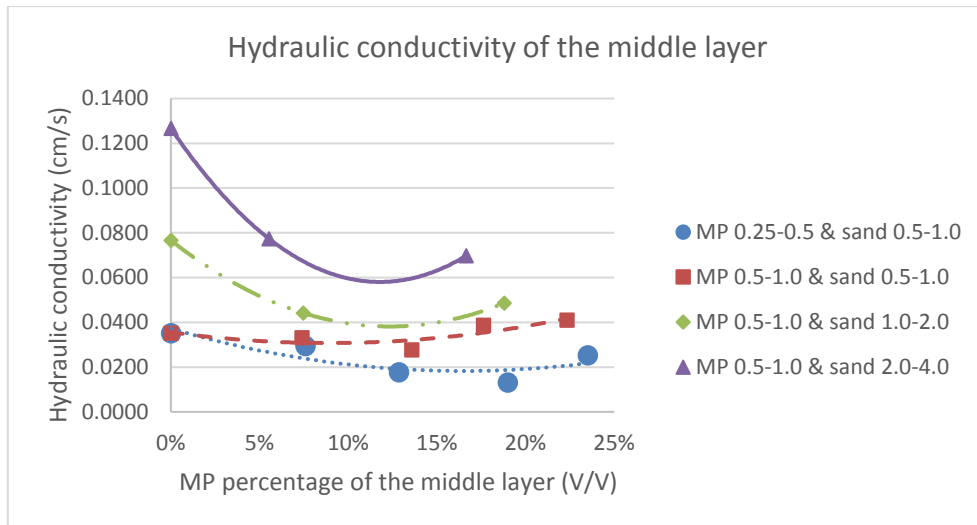


Figure 4.7 Hydraulic conductivity of the middle layer over the volume percentage of MP in the middle layer

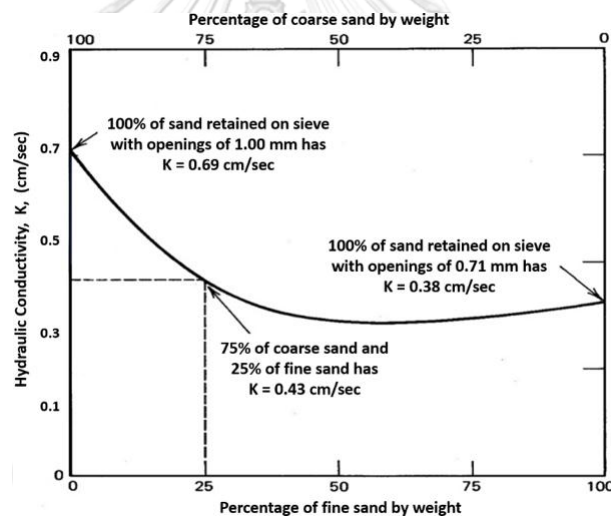


Figure 4.8 Hydraulic conductivity of sand at various percentage of fine-coarse sand

(Woessner and Poeter 2020)

4.1.9 Hydraulic conductivity and grain size

According (Hazen 1983), empirical relationship between the hydraulic conductivity and particle grain size could be described by Equation 4.1.

$$K = A(d_{10})^2 \quad [4.1]$$

Where K stands for the hydraulic conductivity (cm/s).

A is a constant (1/cm·s), and

d_{10} is a grain size of which 10% of the particles are finer (cm).

Later, (Krumbein and Monk 1943) had proposed Equation 4.2 which could predict and describe the hydraulic conductivity more precisely.

$$K = 760(d_w)^2 \exp(-1.31\sigma_\psi) \quad [4.2]$$

Where d_w stands for geometric mean diameter by weight (mm), and

σ_ψ stands for standard deviation of the ψ distribution function (-).

However, Equation 4.2 was complicated and hard to calculate, so (Kozeny 1927) had proposed an equation, later modified by (Carman 1956). Known as Kozeny-Carman Model, Equation 4.3 has been well-known and widely used.

$$K = \left(\frac{\rho_w g}{\mu} \right) \frac{\phi^3}{(1 - \phi)^2} \frac{(d_m)^2}{180} \quad [4.3]$$

Where ρ_w stands for the density of the fluid (g/cm^3)

μ stands for the viscosity of the fluid ($\text{N}\cdot\text{s/m}^2$)

ϕ stands for the porosity (-), and

d_m stands for representative grain size (mm).

It is empirical that hydraulic conductivity is proportional to the square of representative grain size of sand, by weight, that is the relationship between hydraulic conductivity and grain size could be fitted with polynomial of degree 2. This could be another explanation that the middle layer of pure sand larger than 1.0 mm has lower hydraulic conductivity than the whole column. As the top and bottom layers of 0.5-1.0 mm sand was excluded, the average grain size was higher, resulting higher hydraulic conductivity.

Theoretically, if MP behaves in the same manner as sand particles the trendlines of hydraulic conductivity should be decreasing, except the line of 0.5-1.0 mm MP in 0.5-1.0 mm sand which should be invariant, while the percentage of MP increases, i.e., the average particle size being dominated by MP particle size. Moreover, the lines would intersect only at the point of 100% MP, for the same variation of MP. Yet, all the trendlines have a manner of ‘turning’ after passing the turning point. This could lead to a conclusion that the equations were not able to precisely model the hydraulic conductivity of MP-contaminated sand.

Although none of the equations could thoroughly describe the hydraulic conductivity of MP-contaminated sand, they could be used to approximate the hydraulic conductivity of sands when the contamination is lower than the turning point. Because the hydraulic conductivities behave in the same manner as the equations describe; ones of columns of MP smaller than sand (0.25-0.5 mm MP in 0.5-1.0 mm sand, 0.5-1.0 mm MP in 1.0-2.0- and 2.0-4.0-mm sand) were decreasing, while ones of columns of 0.5-1.0 mm MP in 0.5-1.0 mm sand were steady.

4.2 Breakthrough curve analysis

To analyze results from breakthrough curves, the curves were fitted. In this study, two approaches of curve fitting (Spreadsheet and HYDRUS-1D) were used as described in 3.4.

4.2.1 Breakthrough curve fitting using spreadsheet software(Excel)

The ascending and descending logs of breakthrough curve from column of 10% MP 0.25-0.5 in sand 0.5-1.0, experimental ones, exp, and fitted ones, fit, are shown in Figure 4.9 and Figure 4.10 as follows. The values of best fitted k , n and R^2 are shown underneath.

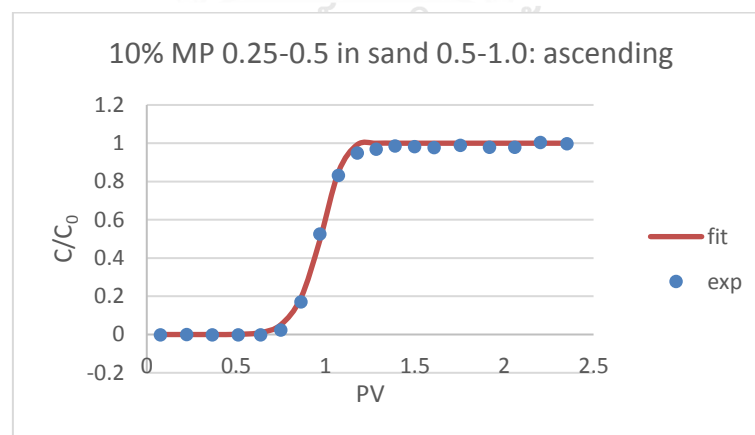


Figure 4.9 The ascending log of breakthrough curve derived from the column of 10% MP 0.25-0.5 mm in sand 0.5-1.0 mm
($k = 0.396$, $n = 10.392$, $R^2 = 0.988$)

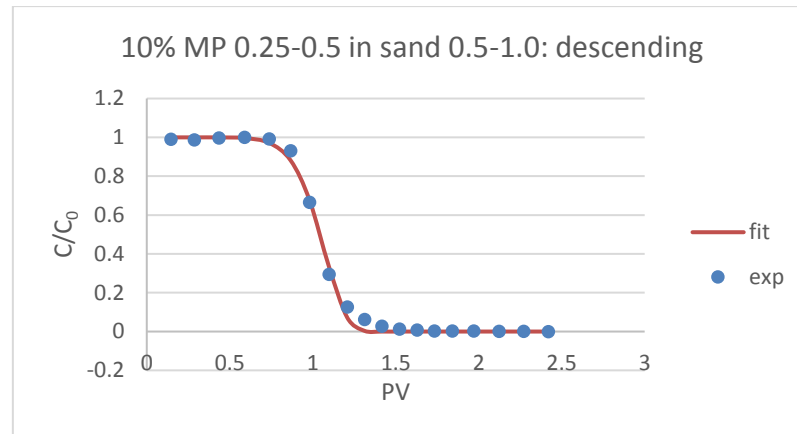


Figure 4.10 The descending log of breakthrough curve derived from the column of 10% MP 0.25-0.5 mm in sand 0.5-1.0 mm ($k = 0.206$, $n = 10.064$, $R^2 = 0.992$)

(i) The parameters of breakthrough curve fitting

To investigate the behavior of k and n from each log scatterplot of each parameter was plotted over different amount of MP as shown in Figure 4.11 and Figure 4.12. Note that the data from column of pure 0.5-1.0 mm sand was outlying, therefore excluded. For both logs, the overall decreasing trend of k is noticeable, linear correlation is clear for the columns of 0.5-1.0 mm. Additionally, it is notable that the value of k of ascending log is higher than one of descending log of each column. Meanwhile, the parameter n showed fluctuation on both logs. However, the scattering patterns of n of the two logs were quite similar.

Moreover, to investigate the relationship between k and n scatterplot of the two parameters of each log was plotted and represented in Figure 4.13. Although no relationship between k and n has yet been discovered from the scatterplot, it will not be concluded that there is no relationship between the two parameters. As it could be discovered by future study.

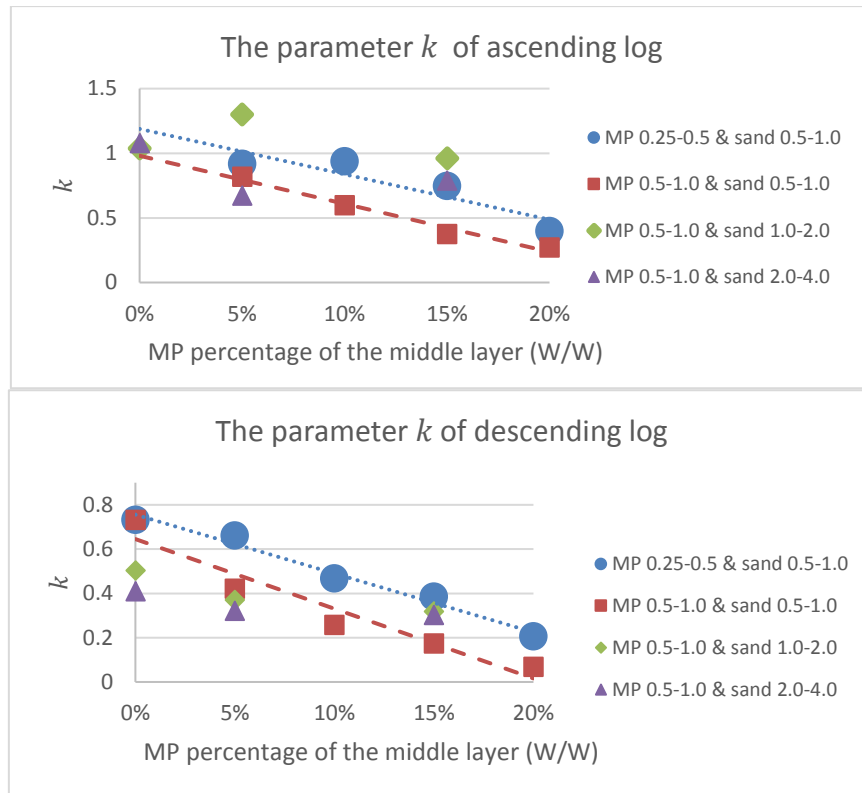


Figure 4.11 The scatterplot of k over the mass percentage of MP in the middle layer

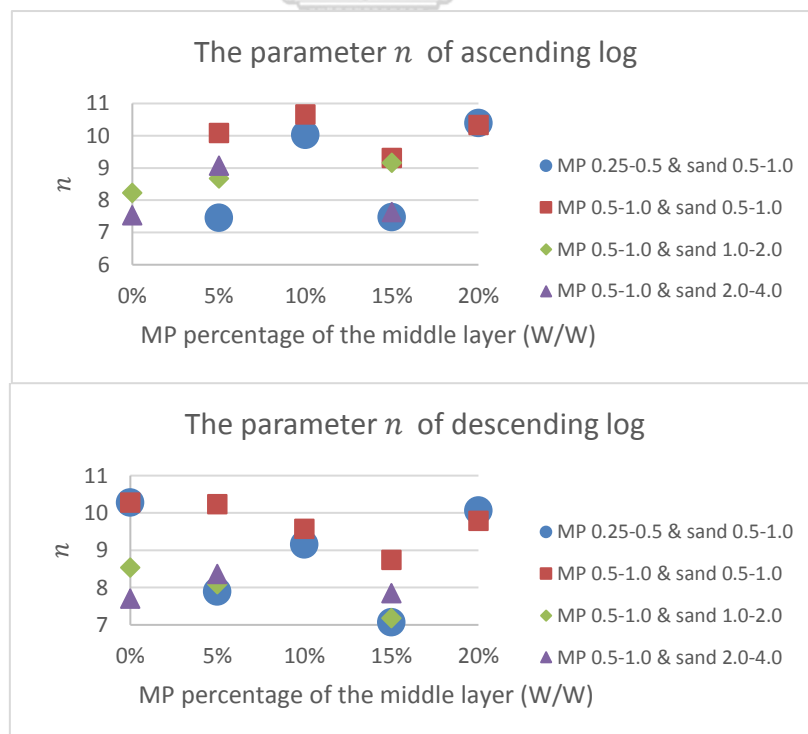


Figure 4.12 The scatterplot of n over the mass percentage of MP in the middle layer

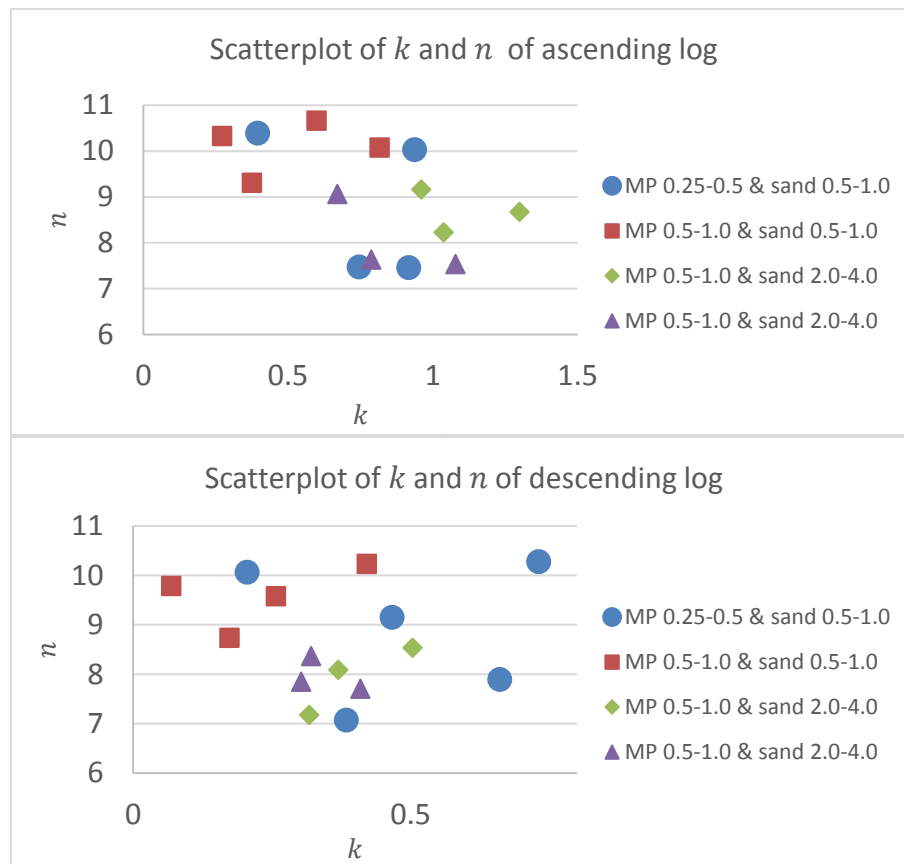


Figure 4.13 The scatterplot of the parameters k and n from ascending logs of breakthrough curve fitting

(ii) Usable capacity, total capacity, and usable fraction

After fitting, the formula of breakthrough curve could be used to calculate the breakpoint, total capacity and consequently, usable fraction by Equation 2.8 and Equation 2.9. The results were shown in Figure 4.14, Figure 4.15, and Figure 4.16 respectively. Note that only ascending log of each breakthrough curve was in consideration in this section.

The graphs showed that breakpoint and total capacity have overall positive correlation to the amount of MP contaminant, especially in the column of 0.5-1.0 mm MP in 0.5-1.0 mm sand. While the usable fraction expressed fluctuation, especially in the column of 0.25-0.5 mm MP in 0.5-1.0 mm sand. The correlation of breakpoint and total capacity could be

confirmation of normalizing breakthrough curve into dimensionless one, the one with horizontal axis of unit relative to PV.

The increasing of total capacity, in the other word higher area over the breakthrough curve, is associated with the shift of breakthrough curve to the right, which means it took the solute longer to pass the sand column. That is the column has higher sorption capacity. However, the increase is noticeable in the column of 0.5-1.0 mm sand only. The sand particle compaction might have been the cause of such incident, i.e., the sand of smaller size could compress the MP debris better than sand of larger size, especially when the MP and sand are of the same size (0.5-1.0 mm). While the amount of MP is higher in the column, the bulk density becomes less, causing less compression to the MP debris. So, they could adsorb the solute more causing the increase in total capacity. Such increase is smaller in larger sands (1.0-2.0 and 2.0-4.0 mm) for the void between the sand particles are larger, causing less compression to the MP.

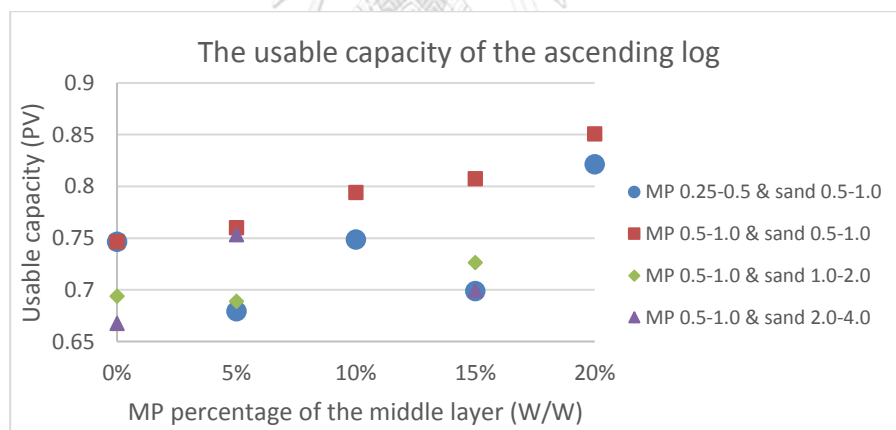


Figure 4.14 The usable capacity of the ascending log over the mass percentage of MP in the middle layer

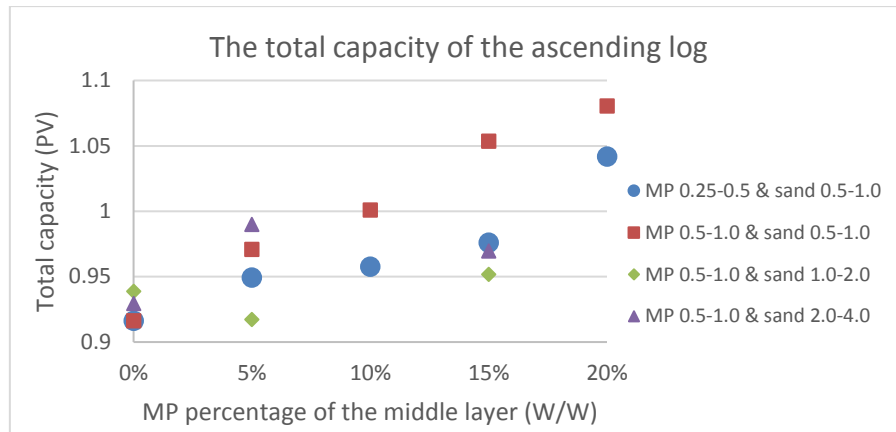


Figure 4.15 The total capacity of the ascending log over the mass percentage of MP in the middle layer

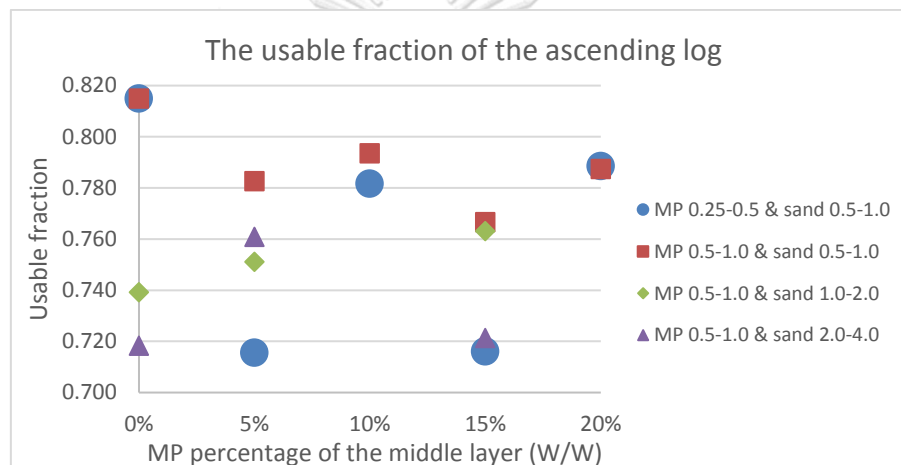


Figure 4.16 The usable fraction of the ascending log over the mass percentage of MP in the middle layer

CHULALONGKORN UNIVERSITY

4.2.2 Breakthrough curve fitting (HYDRUS-1D)

Each breakthrough curve was also fitted with HYDRUS-1D. An example of this fitting approach is shown in Figure 4.17. The results of distribution coefficient, longitudinal dispersivity, and consequently, dispersion coefficient derived from breakthrough curve fitting are shown in Table 4.2, Table 4.3, and Table 4.4 respectively.

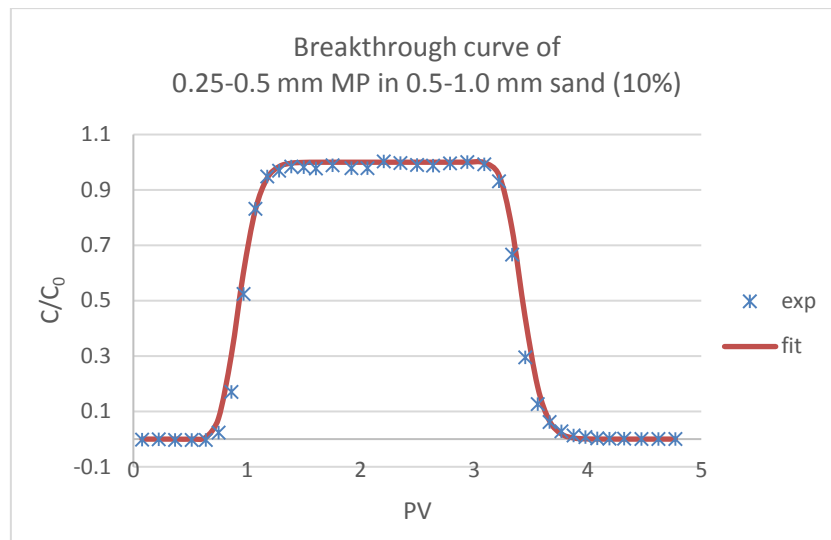


Figure 4.17 The result of curve fitting with HYDRUS-1D for the breakthrough curve of 10% MP 0.25-0.5 mm in sand 0.5-1.0 mm ($R^2 = 0.9917$)

Table 4.2 Distribution coefficient of the column experiments

Distribution coefficient (L/kg)						
Particle size (mm)		MP concentration (W/W)				
MP	Sand	0%	5%	10%	15%	20%
0.25-0.5	0.5-1.0	0.080	0.085	0.090	0.090	0.100
0.5-1.0	0.5-1.0	0.080	0.080	0.090	0.110	0.120
	1.0-2.0	0.085	0.090	-	0.090	-
	2.0-4.0	0.085	0.085	-	0.085	-

Although NaBr is normally regarded as a nonreactive tracer, still it has some sorption to the soil particles, in this case, sand and microplastic particles. However, the amount of adsorption is relatively low, compared to another solute, such as Cu^{2+} ($K_d = 3.58-9.41$ L/kg, $C_0 = 10$ mg/L) and Pb^{2+} ($K_d = 3.07-7.47$ L/kg, $C_0 = 10$ mg/L) (Masipan, Chotpantararat, and Boonkaewwan 2016), therefore the adsorption of NaBr could be omitted. Moreover, as the initial concentration of NaBr used in this study was quite high (1000 mg/L), the distribution coefficient could also be high according to (Naranjo et al. 2013). The increase of sorption, which is associated to the distribution coefficient, was previously discussed in (ii).

Table 4.3 Longitudinal dispersivity of the column experiments

Longitudinal dispersivity (cm)						
Particle size (mm)		MP concentration (W/W)				
MP	Sand	0%	5%	10%	15%	20%
0.25-0.5	0.5-1.0	0.18	0.22	0.23	0.24	0.25
0.5-1.0	0.5-1.0	0.18	0.19	0.20	0.21	0.22
	1.0-2.0	0.18	0.20	-	0.20	-
	2.0-4.0	0.20	0.21	-	0.21	-

As it is noticeable that dispersion coefficient and longitudinal dispersivity of the column have some common manner, increasing in the columns of 0.25-0.5 mm MP in 0.5-1.0 mm sand, slightly increasing in ones of 0.5-1.0 mm MP in 0.5-1.0 mm sand, and quite stable in ones of 0.5-1.0 mm MP in 1.0-2.0 mm and 2.0-4.0 mm sand. The scatterplot between the two parameters was then plotted to investigate the correlation as shown in Figure 4.18.

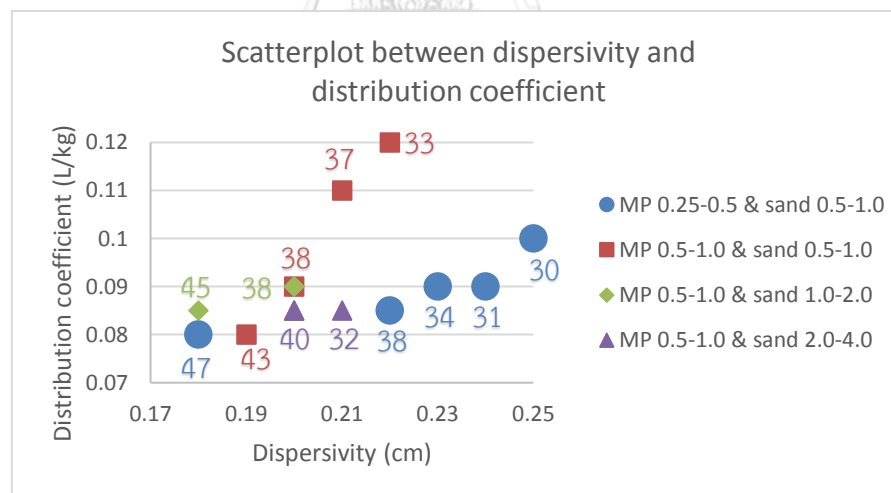


Figure 4.18 The scatterplot between dispersivity and dispersion coefficient; the number of each datapoint representing the Pelet number of individual column

The scatterplot showed that the slope of increasing was quite high in the columns of 0.5-1.0 mm MP in 0.5-1.0 mm sand, while one of the other columns was quite low. Interestingly, the data of those columns has aligned in the same line. The direction of data could be determined by the Pelet

number (shown in figure), higher on the left. That is when advection predominates dispersion, as well as sorption, the distribution coefficient and dispersivity have lower value. Especially in columns of larger sands (1.0-2.0 and 2.0-4.0 mm), the advection rate is higher, resulting higher Peclet number and small change in the two parameters. Moreover, the direction coincides with the amount of MP contaminant in the column, lower on the left. Therefore, this relationship might be induced by MP contamination. Furthermore, it could be concluded that in the columns of MP and sand of same size, the correlation between dispersivity and distribution coefficient is stronger than one in the columns of MP smaller than sand. However, it is still unclear if the MP is the cause of such incident, therefore, more information on this topic is required for more precise conclusion.

Table 4.4 Longitudinal dispersion coefficient of the column experiments

Longitudinal dispersion coefficient (cm ² /s)						
Particle size (mm)		MP concentration (W/W)				
MP	Sand	0%	5%	10%	15%	20%
0.25-0.5	0.5-1.0	0.0156	0.0176	0.0142	0.0127	0.0201
0.5-1.0	0.5-1.0	0.0156	0.0166	0.0170	0.0207	0.0235
	1.0-2.0	0.0221	0.0215	-	0.0242	-
	2.0-4.0	0.0283	0.0302	-	0.0299	-

It is noticeable that the trend of dispersion coefficient over the amount of MP contaminant is not linear, decreasing at first and increasing at higher amount of MP. This is similar to the behavior of hydraulic conductivity of the column, therefore the relationship between dispersion coefficient and hydraulic conductivity was in focus. Moreover the factors affecting the dispersion coefficient include the parameters of the medium, namely porosity and permeability; characteristic of fluid; and the characteristic of displacement (Fried 1975). Therefore, in addition, relationship between dispersivity, dispersion coefficient and the mentioned parameters were to be observed to find empirical relationship. Three relationships were discovered

and shown as follows. Note that the following relationships were discovered in no prior study and possibly also behavior of typical sand, therefore further study and data are required for more precise conclusion.

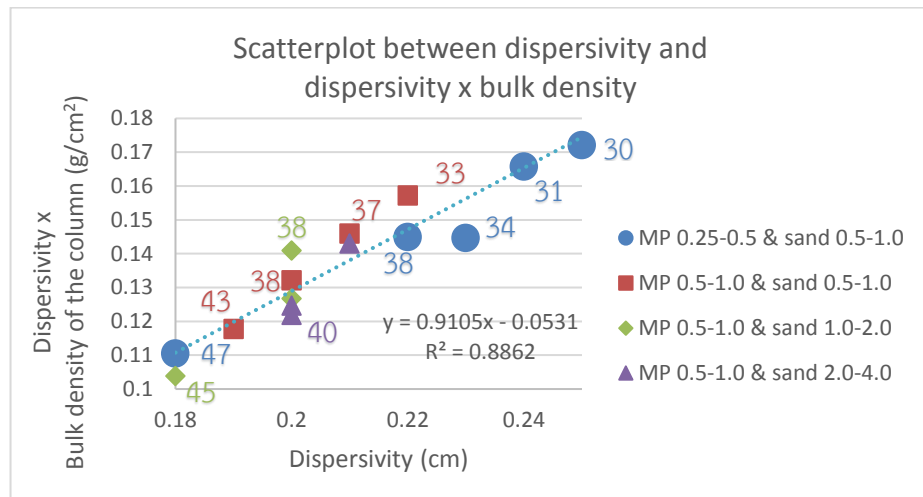


Figure 4.19 The scatterplot between dispersivity and dispersivity x bulk density of the column; the number of each datapoint representing the Pelet number of individual column

Direct scatterplot between dispersivity and bulk density of the column did not represent any empirical correlation, yet one between dispersivity and the product of bulk density and dispersivity coefficient has shown a clearer trend, as shown in Figure 4.19. For each batch of experiment, especially in the columns of 0.25-0.5 mm and 0.5-1.0 mm MP in 0.5-1.0 sand, the data of columns with lower MP contamination lies on the left and move to the right when MP contamination increases. Moreover, the direction coincides with the Pelet number of each column (shown in figure), higher on the left. Therefore, it might be concluded that the relationship could describe overall behavior of the sand-MP mixture with respect to the amount of MP contaminant. The relationship between bulk density and dispersivity could be represented in Equation 4.4 with R^2 of 0.8862 as follows.

$$\alpha_L \rho_B = 0.9105 \alpha_L - 0.0531 \quad [4.4]$$

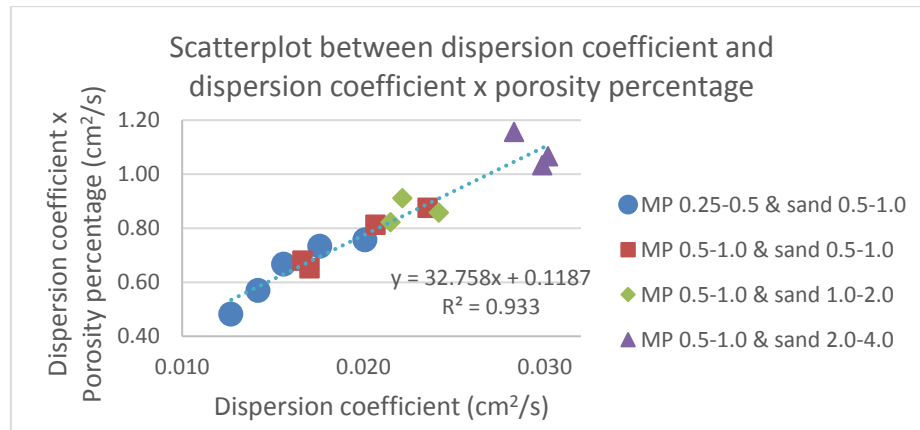


Figure *Error! No text of specified style in document..1* The scatterplot between dispersion coefficient and dispersion coefficient x porosity percentage of the column

Like bulk density, the relation between dispersion coefficient and porosity could be obtained from the scatterplot between porosity itself and the product with dispersion coefficient as shown in Figure 4.20.

It is noticeable that the data of each combination has clustered together, data from batch of smaller grain size on the left, and vice versa, implying that the direction of trendline is associated to the representative grain size. But the amount of MP contamination in each batch is not associated with the direction of the trendline as the dispersion coefficient has a non-monotone behavior. That is this relationship might determine behavior of typical porous media despite the MP contamination. In addition, the cluster of data from columns of 0.5-1.0 mm MP in 2.0-4.0 sand could have been excluded from the whole data set due to outlying as a result of high flow rate, providing more compact clustering of the data. The relationship between porosity percentage and dispersion coefficient could be represented in Equation 4.5 with R^2 of 0.933 as follows.

$$D_L \phi = 32.758 D_L + 0.1187 \quad [4.5]$$

As permeability and hydraulic conductivity are linearly proportional, it is reasonable to investigate the relationship between dispersion coefficient

and hydraulic conductivity instead. The relationship was discovered by the same manner as the previous ones and shown in Figure 4.21 as follows.

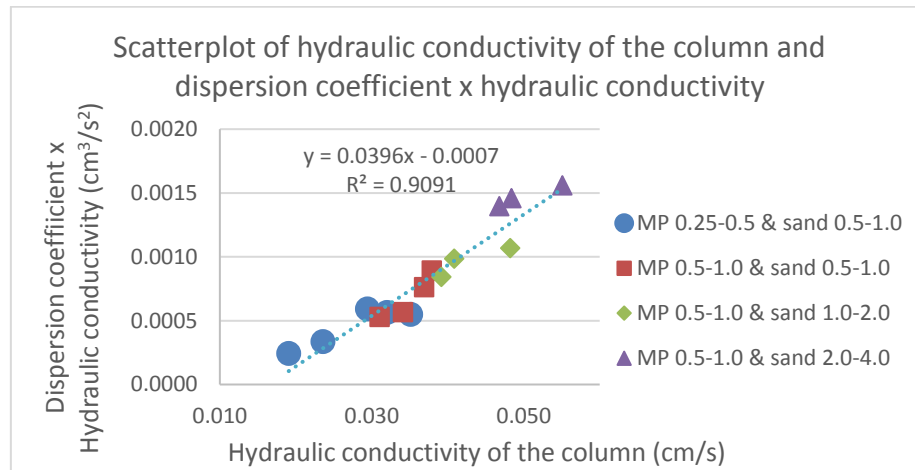


Figure 4.21 The scatterplot between hydraulic conductivity and hydraulic conductivity x dispersion coefficient of the column

Like the previous scatterplot, clustering of data from each combination was noticeable, and the direction is associated to the average particle size but the MP contamination amount. That is the following relationship could have described behavior of typical sand, regardless of MP contamination. The relationship between hydraulic conductivity of the column and the dispersion coefficient could be shown in Equation 4.6 as follows with R^2 of 0.9091.

$$D_L K_V = 0.0396 K_V - 0.0007 \quad [4.6]$$

4.2.3 The connection between two curve fitting methods (Excel and HYDRUS-1D)

Although each curve fitting method has different approach, the result of each could be compared for some possible relationships. Sorption is one common link between two methods, associating both total capacity (of unit PV), and distribution coefficient (K_d). The two parameters, unlike other parameters, have represented quite good and simple correlation as follows (see Figure 4.22). This is another confirmation of normalizing the breakthrough curve into dimensionless one.

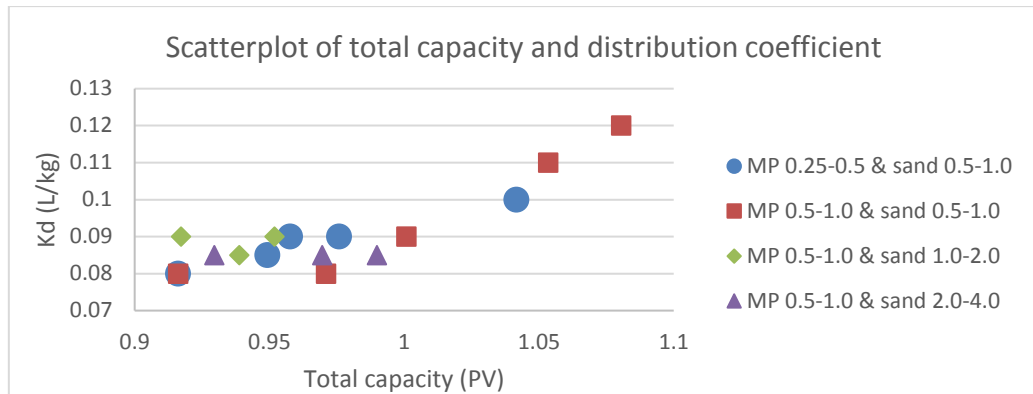


Figure 4.22 The scatterplot between total capacity and the distribution coefficient of the column

The scatterplot shows that the distribution coefficient of columns of 0.5-1.0 mm sand has slight increasing trend along with the total capacity, while one of columns of larger sands (1.0-2.0 and 2.0-4.0 mm) has quite steady distribution coefficient, associated to lower total capacity. The increase of distribution coefficient is apparent only when the total capacity is higher than 1 PV. However, there are only a few columns with such high total capacities, therefore the increasing manner might have been valid to all the columns. Scattering of data from each batch shows that columns with sand of size 0.5-1.0 mm have been affected more than columns with larger sand size. This could lead to a conclusion that one major factor causing the change is the sand particle size. Sand of smaller size provides smaller void, resulting higher pressure to the debris. Together with sponge-like behavior of the MP, this could have affected the sorption capacity of the column.

Even though the scatterplot did not show direct relationship between the curve fitting parameters, k , n and K_d , this could have been a foundational link between the two fitting methods. The link could lead to better comprehension and interpretation of breakthrough curves.

4.3 Microplastic migration

The observation during the experiment and on the pure sand layers suggested that there was neither visible movement nor intrusion of MP. Therefore, only the middle layer was sectioned and sampled.

The result from sand column sectioning and density separation could be shown as follows.

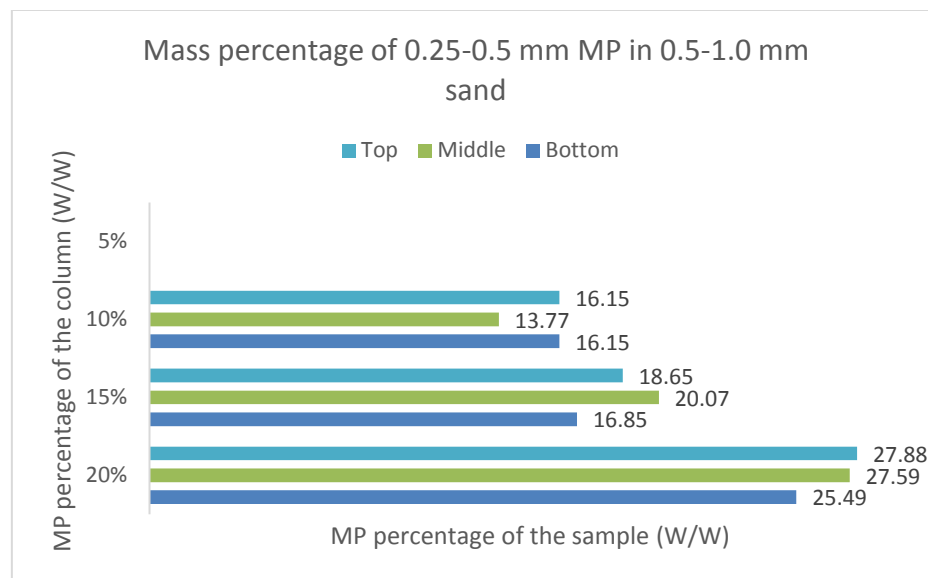


Figure 4.23 Results from the columns of 0.25-0.5 mm MP and 0.5-1.0 mm sand
S.D. = 1.056 (10%), 1.318 (15%), 1.065 (20%)

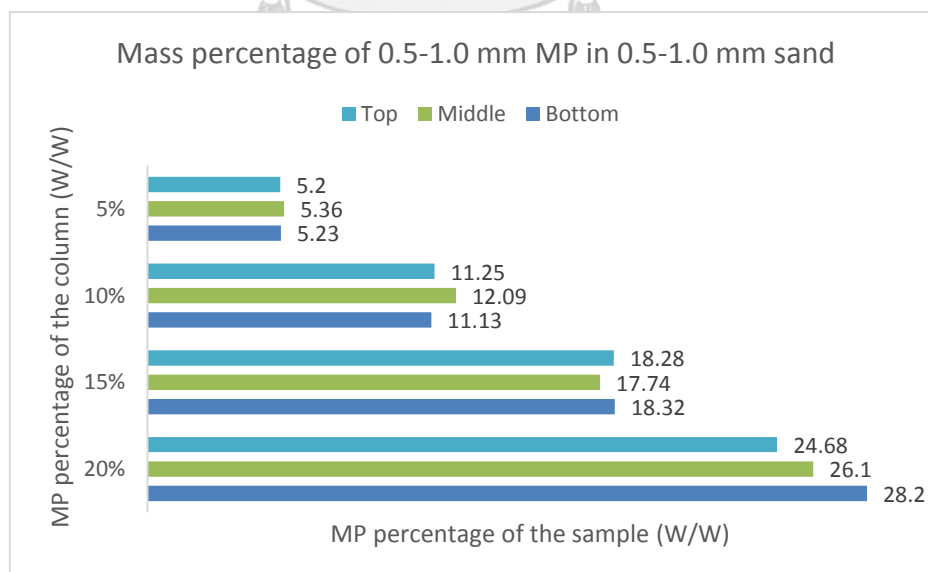


Figure 4.24 Results from the columns of 0.5-1.0 mm MP and 0.5-1.0 mm sand
S.D. = 0.069 (5%), 0.427 (10%), 0.264 (15%), 1.446 (20%)

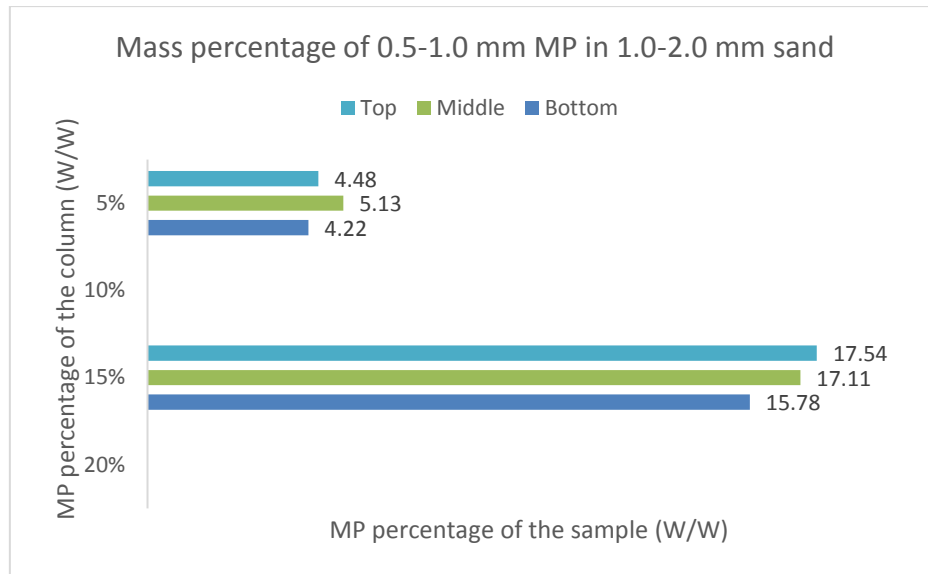


Figure 4.25 Results from the columns of 0.5-1.0 mm MP and 1. 0-2.0 mm sand
S.D. = 0.383 (5%), 0.749 (15%)

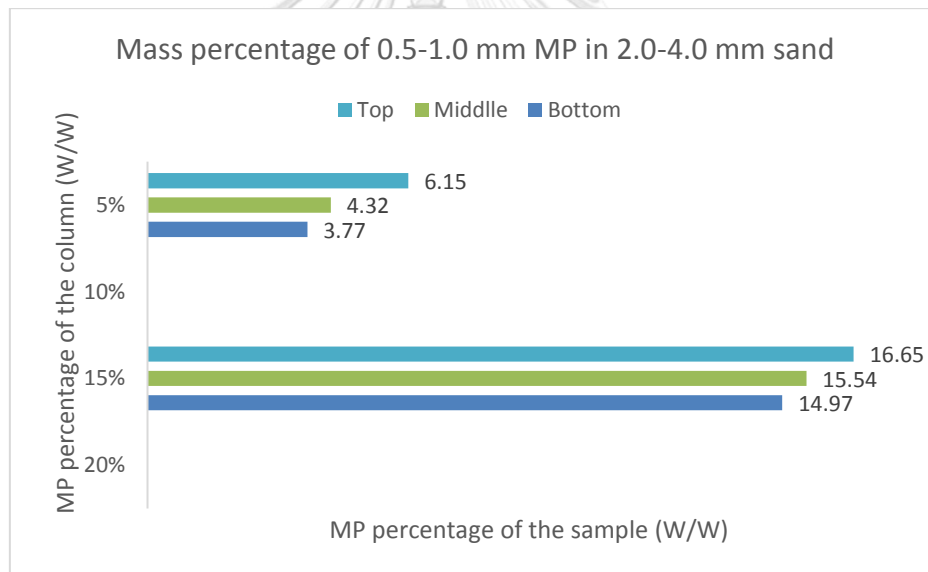


Figure 4.26 Results from the columns of 0.5-1.0 mm MP and 2.0-4.0 mm sand
S.D. = 1.017 (5%), 0.698 (15%)

In the sectioning process of column of 5% 0.25-0.5 mm MP in 0.5-1.0 mm sand, there was an accident causing the data lost that could not be recovered. So, the data was left blank. Moreover, the MP of such size was insufficient for any replication.

The result from the samples showed no certain direction of gradient of MP percentage over the depth among the columns. Therefore the conclusion should be drawn that the plastic particles did not intrude the layers of pure sand, but

should be inconclusive that there were, any or none, migration within the mixing layer. As there might have been some unnoticed one.

4.4 Additional results

In the process of mixing MP and sand together, it was noticeable that the plastic particle in sand of larger particle sizes (1.0-2.0 and 2.0-4.0 mm) had more tendency to sink into the bottom of mixing container (see Figure 4.27). In order to avoid non-uniform distribution of microplastic that might be caused by such incident, the mixture was stirred from the bottom up every time before being packed into the column.



Figure 4.27 The mixture of 15% MP 0.5-1.0 mm in sand 2.0-4.0 mm

In the density separation process, after pure water was added to some samples, it appeared that the dry mixture had formed bubble trap in the water (see Figure 4.28), suspending plastic and sand particles. The swelling behavior suggested that it might take MP some time to be wet with the water. This issue was coped by stirring until the air bubble perished.

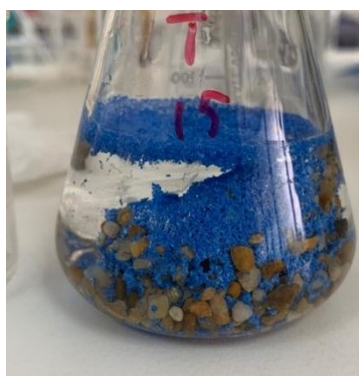


Figure 4.28 The bubbling in the process of density separation

CHAPTER 5 CONCLUSIONS AND RECOMMENDATION

5.1 Conclusions

It is noticeable that MP contamination have some effects on the hydraulic properties of sand, as the hypothesis was set. Porosity was decreased by the MP occupation of void space between the sand particles. Consequently, the relationship between bulk density and porosity of MP-contaminated sand was of opposite direction to one of normal sand due to lower density of MP. For constant flow rate, and hydraulic conductivity, behavior of decreasing and turning up at some point was discovered. Such behavior is similar to one of sand with various percentage of fine sand. Therefore, in the aspect of water flow, it can be concluded that MP behaved as a low-density fine sand. In terms of contaminant transport, breakthrough curve analysis had provided information about sorption capacity (usable capacity, and total capacity), distribution coefficient, dispersivity and consequently, dispersion coefficient. The data showed that sorption capacity, distribution coefficient and dispersivity increase when the percentage of MP is higher. Meanwhile the dispersion coefficient decreases and turns up. This suggest that in some columns, MP contamination could induce more sorption of bromide tracer. However, the amount of such sorption is relatively low, compared to any other pollutants. Some relationships were discovered, such as, distribution coefficient-dispersivity, dispersion coefficient-bulk density, dispersion coefficient-porosity and distribution coefficient-total capacity. The first two have showed coincident direction to the percentage of MP and Peclet number, therefore, are expected to be MP-induced relationships.

For the migration of MP, it can be concluded that the MP intruded to neither layer of pure sand. The dynamic of MP in the mixing layer was still inconclusive as the gradient of MP percentage of samples might have been a result of column packing.

The result of this study could also be applied to some real situations of pollutant transport. In MP-contaminated sands, both colloid and dispersive ones could migrate with more difficulty, as the MP lower both advection and

dispersion rate of the contaminant through the media. Moreover, the sorption could deal more capacity. Therefore, the contaminant is more likely to stay accumulate in a small area.

5.2 Recommendations

For further research, it is suggested that the range of concentrations of MP should be wider, up to 40%, in order to obtain clearer trend of each parameter. Moreover, the column could have more monitoring points to obtain more detailed data. The flow could have been more various, higher flow rate or even upward mode. The discovered relationship should also be tested to in MP-free sand columns to ensure if the behavior was induced by MP contamination or not. The variation of microplastic type, size as well as the sand, or soil should be considered to verify the theory. Lastly, to study and analyze factors increasing sorption capacity, the variations in pH and ionic conditions should be in consideration.

APPENDIX A

Data of bulk density

Here follow the tables of bulk density of each column in the experiment. Furthermore, percentage of MP, by weight, in the entire column and percentage of MP, by volume, in the middle layer were calculated and included.

Table A-1 The bulk density of columns of MP 0.25-0.5 mm and sand 0.5-1.0 mm

		MP concentration of the middle layer (W/W)					
		Layer	0%	5%	10%	15%	20%
Mass (g)	Top	-	292	235	215	235	
	Middle	-	466	395	389	361	
	Bottom	-	281	362	342	353	
Bulk mass (g)			1064	1039	992	946	949
Bulk density (g/cm ³)			1.628	1.590	1.518	1.448	1.452
%MP of the middle layer (W/W)			0	7.77	15.09	22.01	28.57
%MP of the column (V/V)			0	2.24	3.98	6.17	7.61

Table A-2 The bulk density of columns of MP 0.5-1.0 mm and sand 0.5-1.0 mm

		MP concentration of the middle layer (W/W)					
		Layer	0%	5%	10%	15%	20%
Mass (g)	Top	-	262	216	245	232	
	Middle	-	454	417	361	343	
	Bottom	-	388	356	334	339	
Bulk mass (g)			1064	1054	989	940	914
Bulk density (g/cm ³)			1.628	1.613	1.513	1.438	1.399
%MP of the middle layer (W/W)			0	7.77	15.09	22.01	28.57
%MP of the column (V/V)			0	2.15	4.22	5.76	7.51

Table A-3 The bulk density of columns of MP 0.5-1.0 mm and sand 1.0-2.0 mm

		MP concentration of the middle layer (W/W)				
		Layer	0%	5%	10%	15%
Mass (g)	Top	243	212	-	201	-

	Middle	547	459	-	385	-
	Bottom	342	360	-	341	-
Bulk mass (g)		1132	1031	-	927	-
Bulk density (g/cm ³)		1.732	1.578	-	1.419	-
%MP of the middle layer (W/W)		0	8.99	-	24.88	-
%MP of the column (V/V)		0	2.23	-	6.23	-

Table A-4 The bulk density of columns of MP 0.5-1.0 mm and sand 2.0-4.0 mm

		MP concentration of the middle layer (W/W)				
Layer		0%	5%	10%	15%	20%
Mass (g)	Top	206	201	-	223	-
	Middle	527	507	-	395	-
	Bottom	339	340	-	341	-
Bulk mass (g)		1072	1048	-	959	-
Bulk density (g/cm ³)		1.640	1.604	-	1.468	-
%MP of the middle layer (W/W)		0	8.77	-	24.37	-
%MP of the column (V/V)		0	2.42	-	6.18	-

Data of pore volume

Table A-5 The pore volume of each column

Pore volume (cm ³)						
Particle size (mm)		MP concentration (W/W)				
MP	Sand	0%	5%	10%	15%	20%
0.25-0.5	0.5-1.0	279	272	262	248	246
0.5-1.0	0.5-1.0	279	267	250	257	243
	1.0-2.0	269	250	-	232	-
	2.0-4.0	267	231	-	226	-

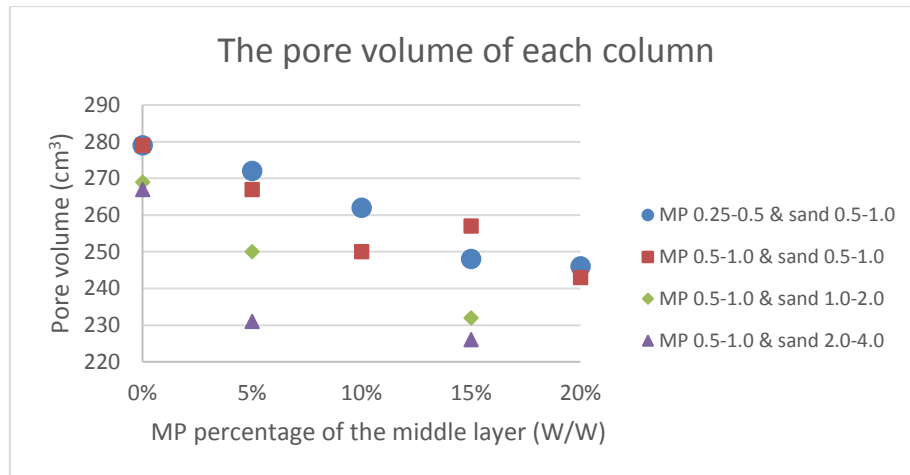


Figure A-1 The pore volume of the column over the mass percentage of MP in the middle layer

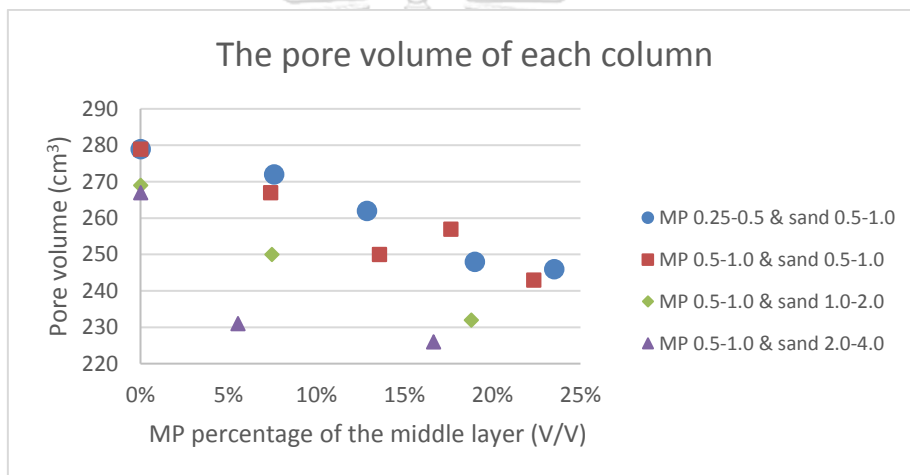


Figure A-2 The pore volume of the column over the volume percentage of MP in the middle layer

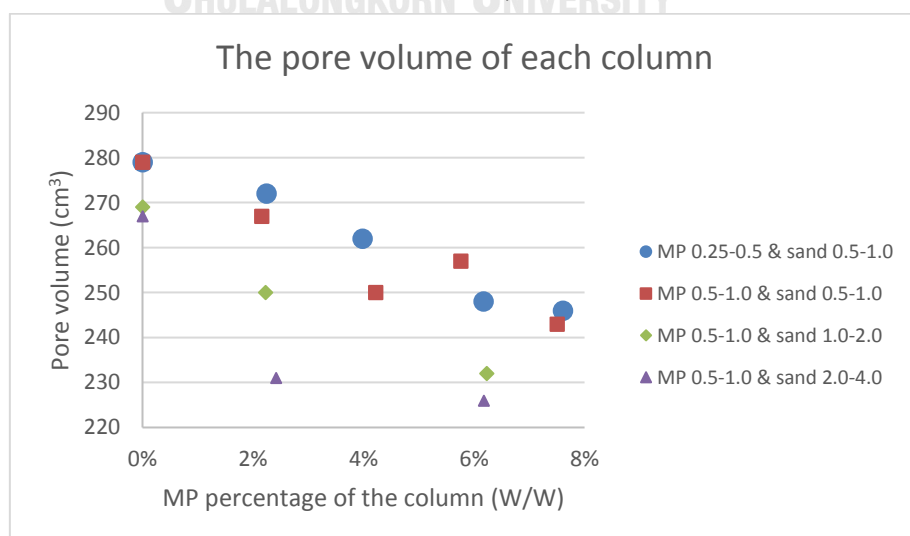


Figure A-3 The pore volume of the column over the mass percentage of MP in the column

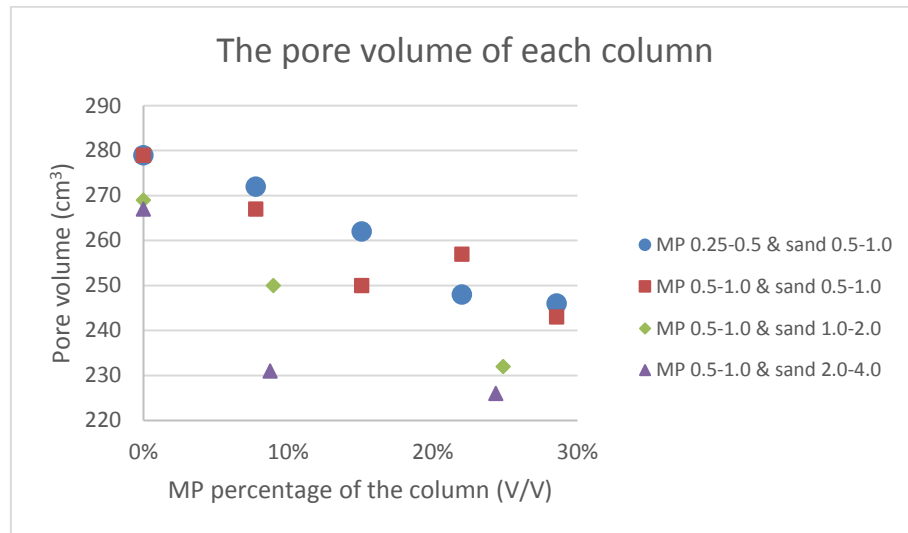


Figure A-4 The pore volume of the column over the weight percentage of MP in the column

Table A-6 The porosity of each column

Particle size (mm)		Porosity percentage (V/V)				
MP	Sand	MP concentration (W/W)				
		0%	5%	10%	15%	20%
0.25-0.5	0.5-1.0	42.69	41.62	40.09	37.95	37.64
0.5-1.0	0.5-1.0	42.69	40.86	38.26	39.33	37.18
	1.0-2.0	41.16	38.26	-	35.50	-
	2.0-4.0	40.86	35.35	-	34.58	-

Data of constant flow rate

Table A-7 Constant flow measurement of columns of MP 0.25-0.5 mm in sand 0.5-1.0 mm

Record	MP concentration (W/W)				
	0%	5%	10%	15%	20%
1	41.27	45.70	61.69	76.68	50.62
2	41.54	45.93	62.02	76.08	50.22
3	41.56	45.89	61.79	76.69	50.59

	Time of 50 cm ³ flow (s)				
Mean time (s)	41.46	54.84	61.83	76.48	50.48
Flow rate (cm ³ /s)	1.206	1.099	0.809	0.654	1.010

Table A-8 Constant flow measurement of columns of MP 0.5-1.0 mm in sand 0.5-1.0 mm

	MP concentration (W/W)				
Record	0%	5%	10%	15%	20%
1	41.27	42.79	46.68	39.66	38.54
2	41.54	42.52	47.38	39.85	38.42
3	41.56	42.93	46.90	39.07	38.43
	Time of 50 cm ³ flow (s)				
Mean time (s)	41.46	42.75	46.99	39.53	38.46
Flow rate (cm ³ /s)	1.206	1.170	1.064	1.265	1.300

Table A-9 Constant flow measurement of columns of MP 0.5-1.0 mm in sand 1.0-2.0 mm

	MP concentration (W/W)				
Record	0%	5%	10%	15%	20%
1	30.45	37.00	-	35.78	-
2	30.13	37.23	-	35.75	-
3	30.06	37.37	-	35.53	-
	Time of 50 cm ³ flow (s)				
Mean time (s)	30.21	37.20	-	35.69	-
Flow rate (cm ³ /s)	1.655	1.344	-	1.401	-

Table A-10 Constant flow measurement of columns of MP 0.5-1.0 mm in sand 2.0-4.0 mm

	MP concentration (W/W)				
Record	0%	5%	10%	15%	20%
1	26.34	30.14	-	31.16	-
2	26.40	30.05	-	31.11	-
3	26.61	30.18	-	31.05	-

	Time of 50 cm ³ flow (s)				
Mean time (s)	26.45	30.12	-	31.16	-
Flow rate (cm ³ /s)	1.890	1.660	-	1.605	-

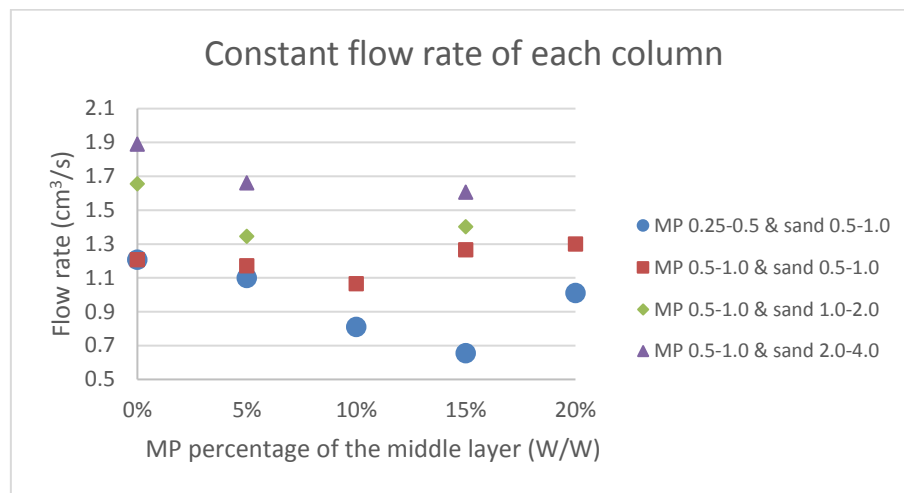


Figure A-5 The constant flow rate of the column over the mass percentage of MP in the middle layer

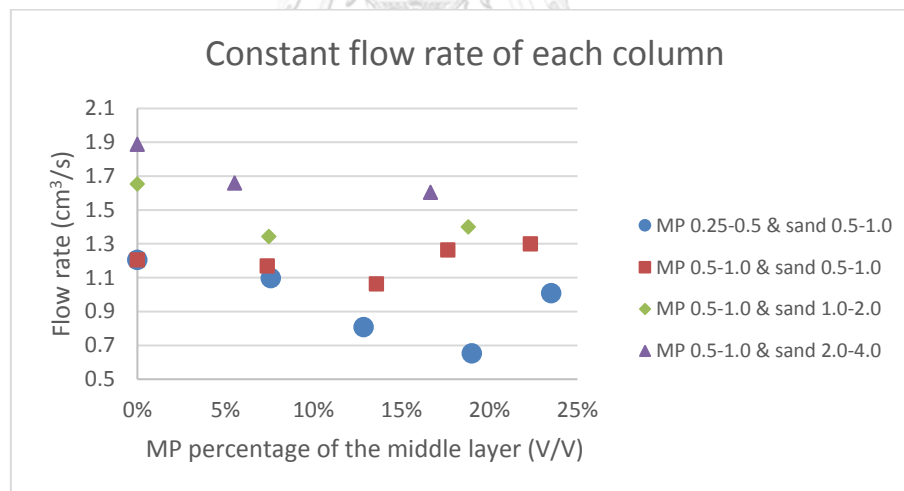


Figure A-6 The constant flow rate of the column over the volume percentage of MP in the middle layer

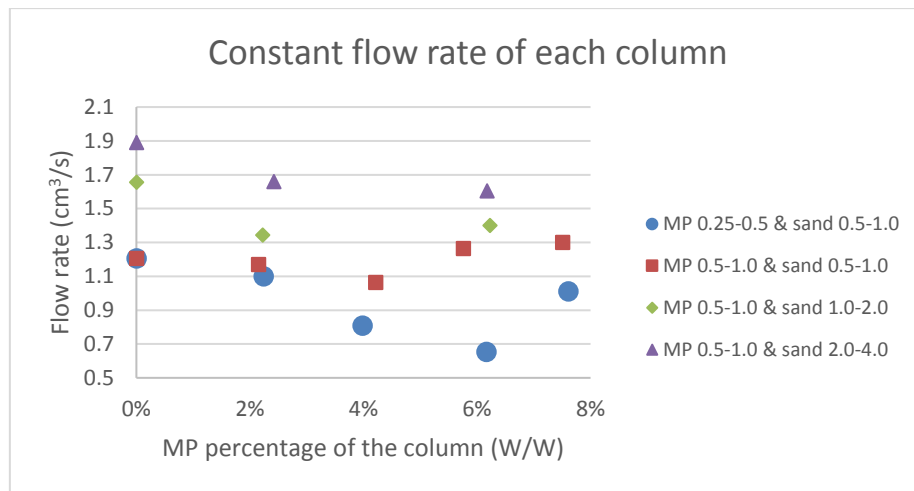


Figure A-7 The constant flow rate of the column over the mass percentage of MP in the column

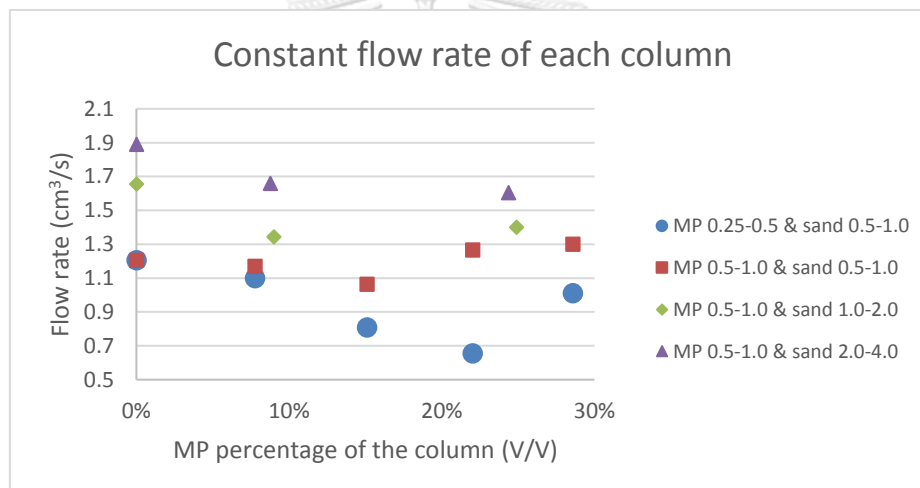


Figure A-8 The constant flow rate of the column over the weight percentage of MP in the column

Data of hydraulic conductivity of the column

Table A-11 The hydraulic conductivity of the column

Particle size (mm)		MP concentration (W/W)				
MP	Sand	0%	5%	10%	15%	20%
0.25-0.5	0.5-1.0	0.0351	0.0320	0.0236	0.0191	0.0294
0.5-1.0	0.5-1.0	0.0351	0.0341	0.0310	0.0369	0.0379
	1.0-2.0	0.0482	0.0392	-	0.0408	-
	2.0-4.0	0.0551	0.0484	-	0.0468	-
Vertical hydraulic conductivity of the column (cm/s)						

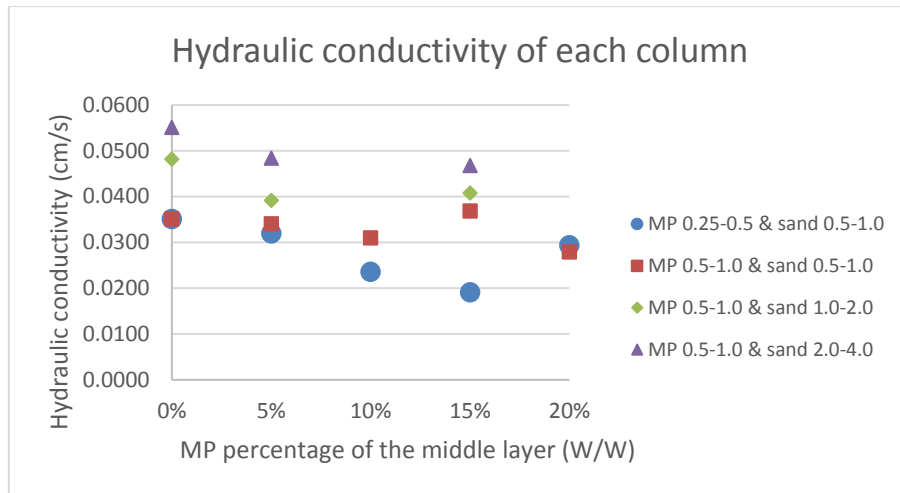


Figure A-9 Hydraulic conductivity of the column over the mass percentage of MP in the middle layer

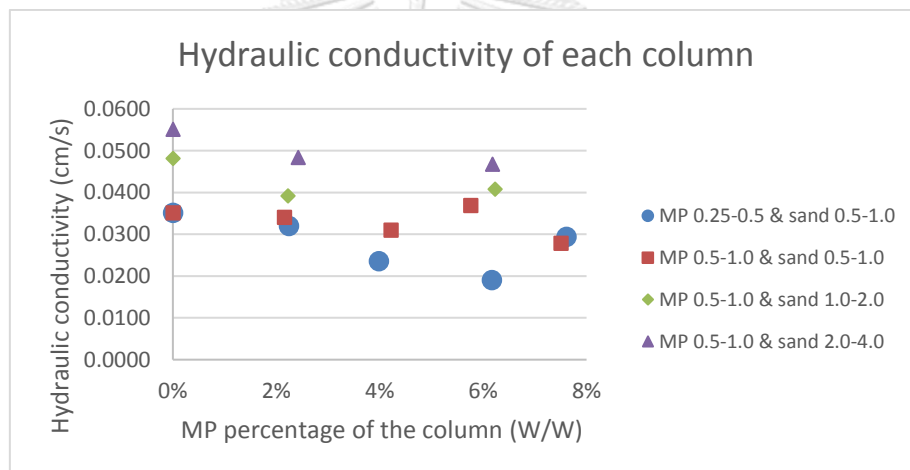


Figure A-10 Hydraulic conductivity of the column over the volume percentage of MP in the middle layer

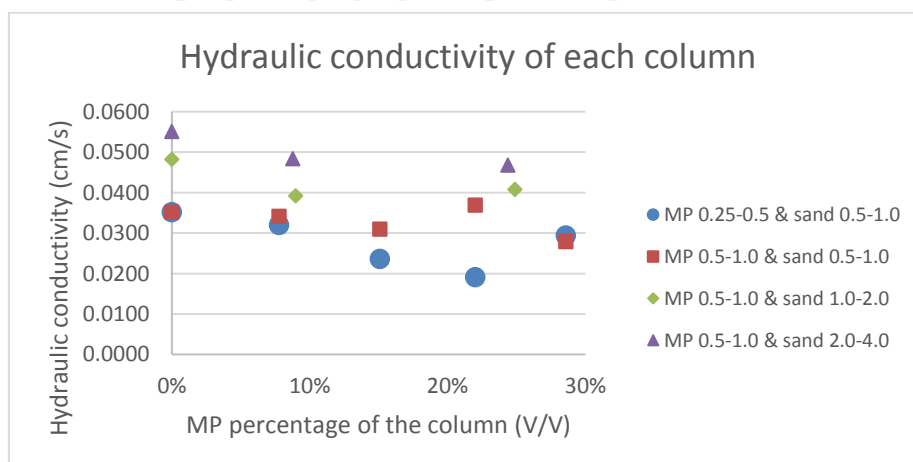


Figure A-11 Hydraulic conductivity of the column over the mass percentage of MP in the column

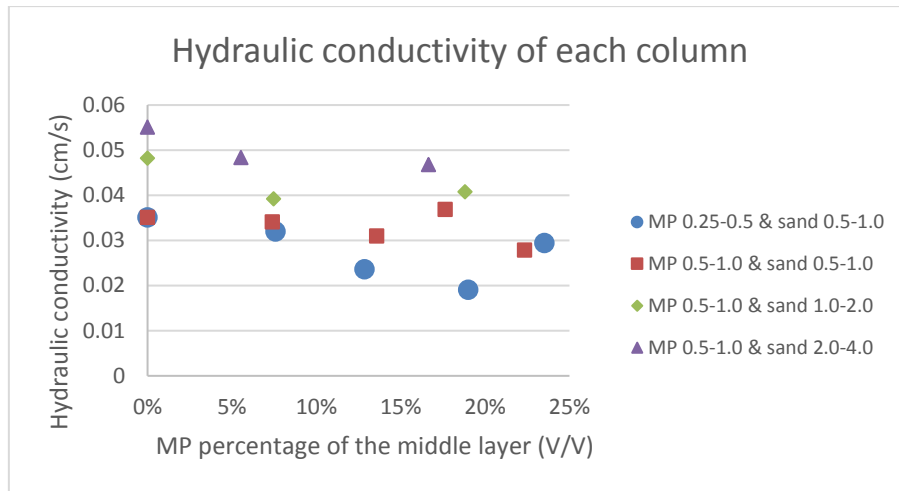


Figure A-12 Hydraulic conductivity of the column over the volume percentage of MP in the column

Data of hydraulic conductivity of the middle layer

Table A-12 The hydraulic conductivity of the middle layer of each column

Particle size (mm)		MP concentration (W/W)				
MP	Sand	0%	5%	10%	15%	20%
0.25-0.5	0.5-1.0	0.0351	0.0294	0.0177	0.0131	0.0253
0.5-1.0	0.5-1.0	0.0351	0.0331	0.0277	0.0390	0.0410
	1.0-2.0	0.0766	0.0442	-	0.0486	-
	2.0-4.0	0.1266	0.0774	-	0.0697	-

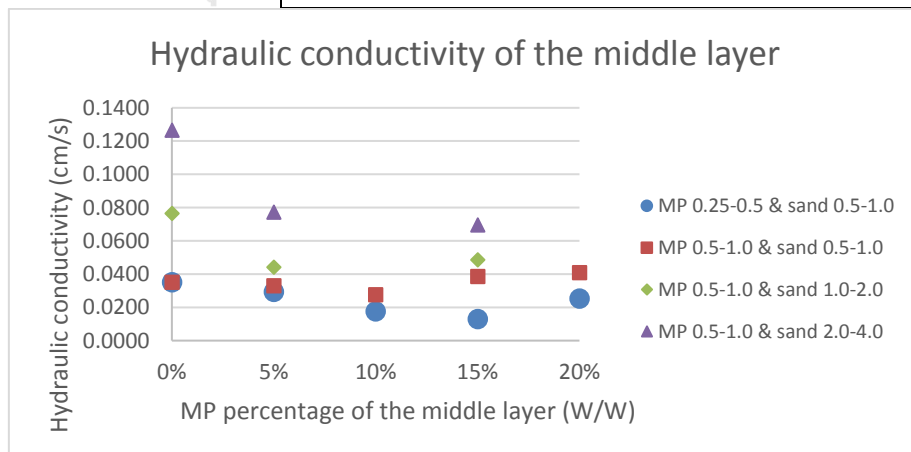


Figure A-13 Hydraulic conductivity of the middle layer over the mass percentage of MP in the middle layer

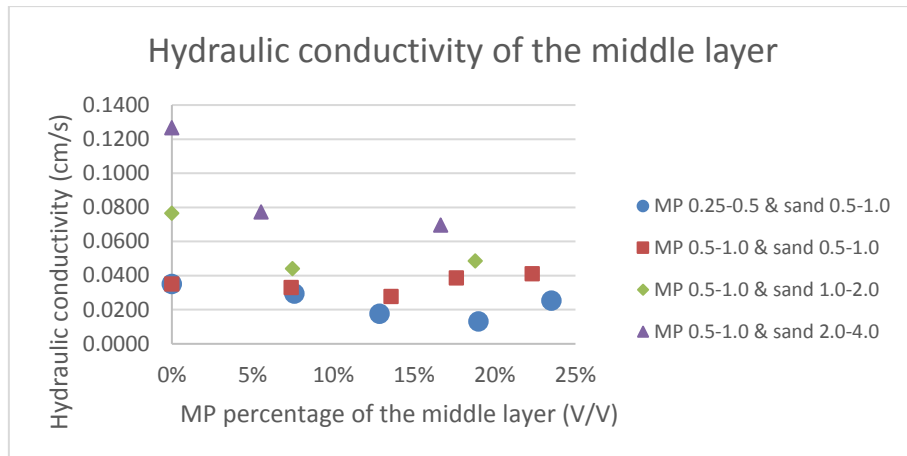


Figure A-14 Hydraulic conductivity of the middle layer over the volume percentage of MP in the middle layer



APPENDIX B

Data from column section

Table B-1 Data from the columns of MP 0.25-0.5 mm in sand 0.5-1.0 mm

Location	Material	MP concentration of the column (W/W)			
		5%	10%	15%	20%
Top	MP mass (g)	-	2.589	3.556	3.831
	Sand mass (g)	-	18.384	19.062	13.739
	%MP (W/W)	-	14.08	18.65	27.88
Middle	MP mass (g)	-	3.290	3.310	5.735
	Sand mass (g)	-	23.891	16.489	20.787
	%MP (W/W)	-	13.77	20.07	27.59
Bottom	MP mass (g)	-	3.516	2.711	3.209
	Sand mass (g)	-	21.767	16.092	12.590
	%MP (W/W)	-	16.15	16.85	25.49
S.D. of %MP		-	1.056	1.318	1.065

Table B-2 Data from the columns of MP 0.5-1.0 mm in sand 0.5-1.0 mm

Location	Material	MP concentration of the column (W/W)			
		5%	10%	15%	20%
Top	MP mass (g)	1.095	1.981	2.894	2.739
	Sand mass (g)	21.062	17.613	15.829	11.099
	%MP (W/W)	5.20	11.25	18.28	24.68
Middle	MP mass (g)	1.200	1.950	2.969	3.060
	Sand mass (g)	22.370	16.132	16.738	11.723
	%MP (W/W)	5.36	12.09	17.74	26.10
Bottom	MP mass (g)	0.969	2.139	2.135	2.591
	Sand mass (g)	18.516	19.224	11.655	9.187

	%MP (W/W)	5.23	11.13	18.32	28.20
S.D. of %MP		0.069	0.427	0.264	1.446

Table B-3 Data from the columns of MP 0.5-1.0 mm in sand 1.0-2.0 mm

		MP concentration of the column (W/W)			
Location	Material	5%	10%	15%	20%
Top	MP mass (g)	1.278	-	3.583	-
	Sand mass (g)	28.518	-	20.425	-
	%MP (W/W)	4.48	-	17.54	-
Middle	MP mass (g)	1.524	-	3.175	-
	Sand mass (g)	29.726	-	18.555	-
	%MP (W/W)	5.13	-	17.11	-
Bottom	MP mass (g)	1.306	-	2.606	-
	Sand mass (g)	30.932	-	16.519	-
	%MP (W/W)	4.22	-	15.78	-
S.D. of %MP		0.383	-	0.749	-

Table B-4 Data from the columns of MP 0.5-1.0 mm in sand 2.0-4.0 mm

		MP concentration of the column (W/W)			
Location	Material	5%	10%	15%	20%
Top	MP mass (g)	1.867	-	2.789	-
	Sand mass (g)	30.348	-	16.729	-
	%MP (W/W)	6.15	-	16.65	-
Middle	MP mass (g)	1.455	-	3.180	-
	Sand mass (g)	33.712	-	20.466	-
	%MP (W/W)	4.32	-	15.54	-
Bottom	MP mass (g)	1.105	-	3.357	-
	Sand mass (g)	29.282	-	22.430	-
	%MP (W/W)	3.77	-	14.97	-
S.D. of %MP		1.017	-	0.698	-

APPENDIX C

Data for breakthrough curve

Column of 0.5-1.0 mm sand

Table C-1 Data from the column of 0.5-1.0 mm sand

No.	Volume (cm ³)	EC (μS/cm)	No.	Volume (cm ³)	EC (μS/cm)
1	40	45.48	21	37	1064
2	38	44.97	22	39	1061
3	37	43.67	23	30	1056
4	38	42.37	24	27	1033
5	26	41.35	25	27	1026
6	27	41.3	26	26	1005
7	27	103.5	27	26	855.4
8	31	428.3	28	27	437.6
9	32	892.8	29	27	202
10	29	1017	30	28	132.6
11	33	1036	31	29	92.71
12	32	1040	32	26	72.8
13	28	1047	33	36	62.46
14	33	1050	34	37	53.68
15	31	1054	35	39	49.94
16	27	1063	36	38	47.99
17	37	1067	37	35	45.48
18	38	1056	38	36	44.97
19	37	1063		Background	44.24
20	38	1059		Tracer	1074

Table C-2 Adjusted data from the column of 0.5-1.0 mm sand

No.	PV	C/C ₀	No.	PV	C/C ₀
1	0.07168459	0.00120416	21	2.42831541	0.990289
2	0.21146953	0.0007089	22	2.56451613	0.9873757
3	0.34587814	-0.0005535	23	2.68817204	0.9825202
4	0.48028674	-0.001816	24	2.79032258	0.9601849
5	0.59498208	-0.0028065	25	2.88709677	0.9533872
6	0.68996416	-0.002855	26	2.98207885	0.9329941
7	0.78673835	0.05754739	27	3.07526882	0.78771753
8	0.890681	0.37296069	28	3.1702509	0.38199192
9	1.00358423	-0.82403667	29	3.26702509	0.15320075
10	1.11290323	0.9446473	30	3.3655914	0.0858064
11	1.22401434	0.9630982	31	3.46774194	0.04706922
12	1.34050179	0.9669826	32	3.56630824	0.02773462
13	1.44802867	0.9737803	33	3.67741935	0.01769344
14	1.55734767	0.9766936	34	3.80824373	0.00916718
15	1.67204301	0.980578	35	3.94444444	0.00553527
16	1.77598566	0.9893179	36	4.08243728	0.00364163
17	1.890681	0.9932023	37	4.21326165	0.00120416
18	2.02508961	0.9825202	38	4.34050179	0.0007089
19	2.15949821	0.9893179			
20	2.29390681	0.9854335			

Columns of 0.25-0.5 mm MP in 0.5-1.0 mm sand

Table C-3 Data from the column of MP 0.25-0.5 mm and sand 0.5-1.0 mm (5%)

No.	Volume (cm ³)	EC (μS/cm)	No.	Volume (cm ³)	EC (μS/cm)
1	36	40.04	21	39	1095
2	36	42	22	41	1087
3	38	44.28	23	40	1079
4	37	43.4	24	38	1071
5	30	42.61	25	29	1002

6	28	44.56	26	28	724.2
7	28	158.8	27	31	395
8	27	505.5	28	27	207.5
9	30	767.4	29	29	129
10	27	917	30	27	92.71
11	26	1010	31	27	73.61
12	28	1055	32	28	64.2
13	28	1067	33	30	58.64
14	28	1089	34	28	54.98
15	38	1064	35	40	53.86
16	40	1076	36	38	52.47
17	38	1079	37	38	51.08
18	40	1091	38	38	50.04
19	38	1094		Background	50.27
20	37	1105		Tracer	1105

Table C-4 Adjusted data from the column of MP 0.25-0.5 mm and sand 0.5-1.0 mm (5%)

No.	PV	C/C ₀	No.	PV	C/C ₀
1	0.06617647	-0.0096992	21	2.49080882	0.9905189
2	0.19852941	-0.0078409	22	2.63786765	0.98293402
3	0.33455882	-0.0056792	23	2.78676471	0.97534914
4	0.47242647	-0.0065135	24	2.93014706	0.96776426
5	0.59558824	-0.0072625	25	3.05330882	0.90234468
6	0.70220588	-0.0054137	26	3.15808824	0.63895973
7	0.80514706	0.10289837	27	3.26654412	0.32684194
8	0.90625	0.43160809	28	3.37316176	0.14907133
9	1.01102941	0.67991808	29	3.47610294	0.0746447
10	1.11580882	0.82175533	30	3.57904412	0.04023779
11	1.21323529	0.90992956	31	3.67830882	0.02212889
12	1.3125	0.9525945	32	3.77941176	0.01320717

13	1.41544118	0.96397182	33	3.88602941	0.00793568
14	1.51838235	0.98483024	34	3.99264706	0.0044656
15	1.63970588	0.96112749	35	4.11764706	0.00340371
16	1.78308824	0.97250481	36	4.26102941	0.00208584
17	1.92647059	0.97534914	37	4.40073529	0.00076797
18	2.06985294	0.98672646	38	4.54044118	-0.0002181
19	2.21323529	0.98957079			
20	2.35110294	1			

Table C-5 Data from the column of MP 0.25-0.5 mm and sand 0.5-1.0 mm (10%)

No.	Volume (cm ³)	EC (μS/cm)	No.	Volume (cm ³)	EC (μS/cm)
1	40	52.57	21	38	1079
2	37	53.26	22	40	1088
3	38	51.63	23	40	1092
4	38	51.41	24	38	1084
5	28	51.41	25	30	1020
6	31	78.78	26	30	745.4
7	28	230.6	27	31	360.1
8	27	598.6	28	27	185.5
9	28	917.5	29	27	118.2
10	27	1039	30	28	83.35
11	28	1060	31	28	67.58
12	28	1076	32	27	62.07
13	29	1073	33	28	57.44
14	28	1068	34	28	56.5
15	49	1080	35	40	56.51
16	37	1070	36	40	55.22
17	37	1070	37	38	54.88
18	38	1095	38	40	54.13
19	40	1089		Background	54.31
20	36	1082		Tracer	1092

Table C-6 Adjusted data from the column of MP 0.25-0.5 mm and sand 0.5-1.0 mm (10%)

No.	PV	C/C ₀	No.	PV	C/C ₀
1	0.07633588	-0.0016768	21	2.63740458	0.98747217
2	0.22328244	-0.0010119	22	2.78625954	0.99614528
3	0.36641221	-0.0025827	23	2.9389313	1
4	0.51145038	-0.0027947	24	3.08778626	0.99229057
5	0.63740458	-0.0027947	25	3.21755725	0.93061512
6	0.75	0.02358122	26	3.33206107	0.66598888
7	0.86259542	0.16988696	27	3.44847328	0.29468338
8	0.96755725	-0.52452081	28	3.55916031	0.12642504
9	1.07251908	0.83183802	29	3.66221374	0.06156945
10	1.17748092	0.94892502	30	3.76717557	0.02798524
11	1.28244275	0.96916227	31	3.8740458	0.01278802
12	1.38931298	0.98458114	32	3.97900763	0.00747815
13	1.4980916	0.9816901	33	4.08396947	0.00301632
14	1.60687023	0.97687171	34	4.19083969	0.00211046
15	1.75381679	0.98843585	35	4.32061069	0.00212009
16	1.91793893	0.97879906	36	4.47328244	0.00087695
17	2.05916031	0.97879906	37	4.6221374	0.0005493
18	2.20229008	1.00289104	38	4.77099237	-0.0001735
19	2.35114504	0.99710896			
20	2.49618321	0.99036321			

Table C-7 Data from the column of MP 0.25-0.5 mm and sand 0.5-1.0 mm (15%)

No.	Volume (cm ³)	EC (μS/cm)	No.	Volume (cm ³)	EC (μS/cm)
1	37	41.33	24	36	1107
2	36	40.6	25	37	1111
3	37	42.7	26	39	1117
4	40	43.68	27	40	1102
5	30	46.04	28	37	1116

6	30	116	29	40	1117
7	30	382.8	30	40	1104
8	28	711.6	31	28	947.8
9	28	940.4	32	28	665.2
10	28	1045	33	27	394.6
11	28	1073	34	28	226.9
12	27	1094	35	30	134.1
13	28	1111	36	29	87.56
14	28	1109	37	27	69.18
15	37	1109	38	28	60.75
16	40	1104	39	28	57.15
17	37	1108	40	27	53.77
18	39	1112	41	40	53.62
19	37	1111	42	40	51.06
20	36	1109	43	38	50.07
21	39	1111	44	40	50.08
22	36	1115		Background	41.31
23	37	1108		Tracer	1116

Table C-8 Adjusted data from the column of MP 0.25-0.5 mm and sand 0.5-1.0 mm (15%)

No.	PV	C/C ₀	No.	PV	C/C ₀
1	0.07459677	-9.30527E-06	24	3.18951613	0.991625258
2	0.22177419	-0.00068859	25	3.33669355	0.995347366
3	0.36895161	0.001265517	26	3.48991935	1.000930527
4	0.52419355	0.002177433	27	3.64919355	0.986972624
5	0.66532258	0.004373476	28	3.80443548	1
6	0.78629032	0.069473136	29	3.95967742	1.000930527
7	0.90725806	0.317737703	30	4.12096774	0.988833678
8	1.02419355	0.623694936	31	4.25806452	0.843485381
9	1.13709677	0.836599483	32	4.37096774	0.58051849

10	1.25	0.933932593	33	4.48185484	0.32871792
11	1.36290323	0.959987345	34	4.59274194	0.172668565
12	1.47379032	0.979528409	35	4.70967742	0.086315672
13	1.58467742	0.995347366	36	4.82862903	0.043008952
14	1.69758065	0.993486312	37	4.94153226	0.025905868
15	1.82862903	0.993486312	38	5.05241935	0.018061526
16	1.98387097	0.988833678	39	5.16532258	0.014711163
17	2.1391129	0.992555785	40	5.27620968	0.011566449
18	2.29233871	0.996277893	41	5.41129032	0.01142687
19	2.44556452	0.995347366	42	5.57258065	0.009044721
20	2.59274194	0.993486312	43	5.72983871	0.0081235
21	2.74395161	0.995347366	44	5.88709677	0.008132805
22	2.89516129	0.999069473			
23	3.04233871	0.992555785			

Table C-9 Data from the column of MP 0.25-0.5 mm and sand 0.5-1.0 mm (20%)

No.	Volume (cm ³)	EC (μS/cm)	No.	Volume (cm ³)	EC (μS/cm)
1	36	51.45	21	37	1109
2	37	52.3	22	38	1102
3	38	51.37	23	40	1108
4	36	50.75	24	42	1102
5	28	62.81	25	28	1041
6	25	86.71	26	31	741.3
7	32	224.7	27	28	335.9
8	31	586.3	28	32	166.2
9	31	974.4	29	31	106.8
10	29	1052	30	28	77.3
11	28	1071	31	28	63.79
12	28	1089	32	28	56.36
13	28	1088	33	27	53.28
14	29	1095	34	27	51.81

15	41	1105	35	38	49.67
16	37	1095	36	37	48.93
17	40	1109	37	38	48.56
18	38	1099	38	41	48.38
19	38	1104		Background	51.48
20	36	1109		Tracer	1111

Table C-10 Adjusted data from the column of MP 0.25-0.5 mm and sand 0.5-1.0 mm (20%)

No.	PV	C/C ₀	No.	PV	C/C ₀
1	0.07317073	-2.831E-05	21	2.78252033	0.99811235
2	0.22154472	0.00077394	22	2.93495935	0.99150559
3	0.37398374	-0.0001038	23	3.09349593	0.99716853
4	0.52439024	-0.000689	24	3.2601626	0.99150559
5	0.65447154	0.01069352	25	3.40243902	0.93393235
6	0.76219512	0.03325091	26	3.52235772	0.65106841
7	0.87804878	0.16348913	27	3.64227642	0.26844231
8	1.00609756	0.50477575	28	3.76422764	0.10827545
9	1.13211382	0.87107369	29	3.89227642	0.05221232
10	1.25406504	0.94431441	30	4.01219512	0.02436953
11	1.3699187	0.96224706	31	4.12601626	0.01161847
12	1.48373984	0.97923588	32	4.2398374	0.00460586
13	1.59756098	0.97829206	33	4.35162602	0.00169888
14	1.71341463	0.98489882	34	4.46138211	0.00031146
15	1.85569106	0.99433706	35	4.59349593	-0.0017083
16	2.01422764	0.98489882	36	4.74593496	-0.0024068
17	2.17073171	0.99811235	37	4.89837398	-0.002756
18	2.32926829	0.98867412	38	5.05894309	-0.0029259
19	2.48373984	0.99339323			
20	2.63414634	0.99811235			

Data from columns of 0.5-1.0 mm MP in 0.5-1.0 mm sand

Table C-11 Data from the column of MP 0.5-10 mm and sand 0.5-1.0 mm (5%)

No.	Volume (cm ³)	EC (μ S/cm)	No.	Volume (cm ³)	EC (μ S/cm)
1	41	52.49	21	38	1047
2	41	52.23	22	40	1052
3	41	51.69	23	38	1040
4	38	50.52	24	37	1041
5	30	53.26	25	31	1021
6	28	83.48	26	28	883.7
7	27	213	27	28	359.1
8	30	569.5	28	28	255
9	28	894.4	29	28	139.9
10	28	1004	30	28	89.92
11	29	1042	31	29	69.66
12	28	1044	32	31	59.99
13	31	1041	33	29	55
14	29	1038	34	29	52.45
15	38	1045	35	40	50.97
16	38	1041	36	38	49.48
17	39	1044	37	37	48.4
18	40	1049	38	38	48.12
19	38	1050		Background	52.08
20	41	1049		Tracer	1063

Table C-12 Adjusted data from the column of MP 0.5-10 mm and sand 0.5-1.0 mm (5%)

No.	PV	C/C ₀	No.	PV	C/C ₀
1	0.07677903	0.00040557	21	2.62921348	0.98417283
2	0.23033708	0.00014838	22	2.7752809	0.98911882
3	0.38389513	-0.0003858	23	2.92134831	0.97724845
4	0.53183521	-0.0015431	24	3.06179775	0.97823764

5	0.65917603	0.00116725	25	3.18913858	0.95845369
6	0.76779026	0.03106082	26	3.29962547	0.82263681
7	0.87078652	0.15918174	27	3.40449438	0.30370356
8	0.97752809	0.51183081	28	3.5093633	0.20072805
9	1.08614232	0.83322122	29	3.61423221	0.08687136
10	1.19101124	0.94163732	30	3.71910112	0.03743125
11	1.29775281	0.97922684	31	3.8258427	0.0173901
12	1.40449438	0.98120524	32	3.93820225	0.00782456
13	1.51498127	0.97823764	33	4.0505618	0.00288846
14	1.62734082	0.97527005	34	4.15917603	0.000366
15	1.75280899	0.98219444	35	4.28838951	-0.001098
16	1.89513109	0.97823764	36	4.43445693	-0.0025719
17	2.03932584	0.98120524	37	4.57490637	-0.0036402
18	2.18726592	0.98615123	38	4.71535581	-0.0039172
19	2.33333333	0.98714043			
20	2.48127341	0.98615123			

Table C-13 Data from the column of MP 0.5-10 mm and sand 0.5-1.0 mm (10%)

No.	Volume (cm ³)	EC (μS/cm)	No.	Volume (cm ³)	EC (μS/cm)
1	38	51.03	21	37	1113
2	38	51.03	22	38	1115
3	41	51.13	23	41	1119
4	39	51.1	24	41	1119
5	31	52.36	25	29	1038
6	28	78.89	26	28	807.7
7	27	249.6	27	29	409.8
8	31	699.7	28	28	182.6
9	28	1008	29	28	106
10	29	1065	30	28	75.98
11	30	1105	31	30	66.7
12	27	1103	32	29	61.3

13	27	1105	33	29	58.21
14	29	1107	34	28	56.65
15	40	1116	35	39	55.27
16	40	1110	36	41	54.06
17	37	1112	37	38	53.78
18	38	1115	38	38	53.08
19	41	1120		Background	51.34
20	39	1110		Tracer	1133

Table C-14 Adjusted data from the column of MP 0.5.-10 mm and sand 0.5-1.0 mm (10%)

No.	PV	C/C ₀	No.	PV	C/C ₀
1	0.076	-0.0002866	21	2.786	0.9815099
2	0.228	-0.0002866	22	2.936	0.98335891
3	0.386	-0.0001941	23	3.094	0.98705693
4	0.546	-0.0002219	24	3.258	0.98705693
5	0.686	0.000943	25	3.398	0.91217203
6	0.804	0.02547011	26	3.512	0.69925855
7	0.914	0.18329235	27	3.626	0.33139804
8	1.03	0.59941201	28	3.74	0.12135052
9	1.148	0.88443688	29	3.852	0.05053344
10	1.262	0.93713366	30	3.964	0.0227798
11	1.38	0.97411386	31	4.08	0.0142004
12	1.494	0.97226485	32	4.198	0.00920807
13	1.602	0.97411386	33	4.314	0.00635135
14	1.714	0.97596287	34	4.428	0.00490912
15	1.852	0.98428342	35	4.562	0.0036333
16	2.012	0.97873639	36	4.722	0.00251465
17	2.166	0.9805854	37	4.88	0.00225579
18	2.316	0.98335891	38	5.032	0.00160864
19	2.474	0.98798144			

20	2.634	0.97873639			
----	-------	------------	--	--	--

Table C-15 Data from the column of MP 0.5.-10 mm and sand 0.5-1.0 mm (15%)

No.	Volume (cm ³)	EC (μS/cm)	No.	Volume (cm ³)	EC (μS/cm)
1	40	44.48	21	40	1093
2	38	44.58	22	40	1097
3	38	44.26	23	38	1092
4	38	43.77	24	40	1081
5	31	44.73	25	28	1048
6	29	61.46	26	28	967.6
7	28	141.4	27	29	705.9
8	28	365.2	28	28	372.4
9	28	719.9	29	28	203.1
10	28	962.2	30	29	112.9
11	29	1059	31	30	72.8
12	28	1071	32	28	59.58
13	31	1084	33	28	53.52
14	29	1090	34	30	50.35
15	38	1090	35	40	48.19
16	37	1091	36	37	46.96
17	41	1097	37	38	45.24
18	38	1098	38	40	44.91
19	40	1094		Background	43.51
20	38	1091		Tracer	1098

Table C-16 Adjusted data from the column of MP 0.5.-10 mm and sand 0.5-1.0 mm (15%)

No.	PV	C/C ₀	No.	PV	C/C ₀
1	0.07782101	0.00091988	21	2.70428016	0.99525837
2	0.22957198	0.00101471	22	2.85992218	0.99905167
3	0.37743191	0.00071124	23	3.01167315	0.99431005
4	0.52529183	0.00024656	24	3.16342412	0.98387846

5	0.65953307	0.00115696	25	3.29571984	0.95258371
6	0.77626459	0.01702245	26	3.40466926	0.87633832
7	0.88715953	0.09283161	27	3.5155642	0.62816148
8	0.99610895	0.3050669	28	3.62645914	0.31189485
9	1.10505837	0.64143804	29	3.73540856	0.1513433
10	1.21400778	0.87121737	30	3.8463035	0.06580432
11	1.32490272	0.9630153	31	3.96108949	0.02777646
12	1.43579767	0.97439521	32	4.07392996	0.01523959
13	1.55058366	0.98672344	33	4.18287938	0.00949274
14	1.66731518	0.99241339	34	4.29571984	0.00648655
15	1.79766537	0.99241339	35	4.43190661	0.00443816
16	1.94357977	0.99336172	36	4.58171206	0.00327172
17	2.09533074	0.99905167	37	4.72762646	0.0016406
18	2.24902724	1	38	4.87937743	0.00132766
19	2.40077821	0.9962067			
20	2.55252918	0.99336172			

Table C-17 Data from the column of MP 0.5-10 mm and sand 0.5-1.0 mm (20%)

No.	Volume (cm ³)	EC (μS/cm)	No.	Volume (cm ³)	EC (μS/cm)
1	38	51.18	21	37	1098
2	39	51.24	22	40	1096
3	41	50.37	23	38	1094
4	42	49.89	24	40	1097
5	29	49.67	25	31	1070
6	31	78.3	26	29	1017
7	31	231.4	27	28	778.8
8	28	580	28	28	437
9	27	933.8	29	29	203.6
10	28	1067	30	27	113
11	27	1082	31	28	76.08
12	28	1085	32	31	62.12

13	28	1088	33	28	56.68
14	27	1090	34	28	53.97
15	37	1091	35	37	52.17
16	38	1093	36	38	51.18
17	41	1097	37	39	50.72
18	40	1098	38	40	50.44
19	41	1095		Background	50.96
20	39	1094		Tracer	1106

Table C-18 Adjusted data from the column of MP 0.5.-10 mm and sand 0.5-1.0 mm (20%)

No.	PV	C/C ₀	No.	PV	C/C ₀
1	0.0781893	0.00020852	21	2.8744856	0.99241735
2	0.23662551	0.00026539	22	3.03292181	0.99052169
3	0.40123457	-0.0005592	23	3.19341564	0.98862602
4	0.57201646	-0.0010142	24	3.35390947	0.99146952
5	0.718107	-0.0012227	25	3.5	0.96587807
6	0.84156379	0.02591371	26	3.62345679	0.91564301
7	0.9691358	0.17102669	27	3.74074074	0.68986958
8	1.09053498	0.5014407	28	3.85596708	0.36590082
9	1.2037037	0.83678344	29	3.97325103	0.14467698
10	1.31687243	0.96303458	30	4.08847737	0.05880346
11	1.43004115	0.97725205	31	4.20164609	0.02380952
12	1.54320988	0.98009554	32	4.32304527	0.0105778
13	1.65843621	0.98293904	33	4.44444444	0.0054216
14	1.77160494	0.9848347	34	4.55967078	0.00285297
15	1.90329218	0.98578253	35	4.69341564	0.00114688
16	2.05761317	0.98767819	36	4.84773663	0.00020852
17	2.22016461	0.99146952	37	5.00617284	-0.0002275
18	2.38683128	0.99241735	38	5.16872428	-0.0004929
19	2.55349794	0.98957386			

20	2.718107	0.98862602			
----	----------	------------	--	--	--

Data from column of 1.0-2.0 mm sand

Table C-19 Data from the column of sand 1.0-2.0 mm

No.	Volume (cm ³)	EC (μS/cm)	No.	Volume (cm ³)	EC (μS/cm)
1	39	46.21	21	41	1101
2	42	46.97	22	41	1103
3	40	47.02	23	38	1101
4	41	47.25	24	40	1096
5	29	49.74	25	32	1000
6	31	117.1	26	29	681.3
7	28	369.4	27	29	357.4
8	28	712.3	28	29	184.7
9	29	939.4	29	32	119.5
10	30	1039	30	32	90.16
11	29	1078	31	29	78.44
12	32	1091	32	28	70.75
13	28	1096	33	29	66.67
14	29	1092	34	29	62.59
15	38	1096	35	41	59.82
16	38	1093	36	39	56.58
17	37	1096	37	38	54.3
18	41	1101	38	40	52.87
19	42	1099		Background	46.69
20	39	1096		Tracer	1106

Table C-20 Adjusted data from the column of sand 1.0-2.0 mm

No.	PV	C/C ₀	No.	PV	C/C ₀
1	0.07249071	-0.0004531	21	2.64126394	0.99527995
2	0.22304833	0.00026432	22	2.7936803	0.99716797
3	0.37546468	0.00031152	23	2.94052045	0.99527995
4	0.5260223	0.00052865	24	3.08550186	0.99055989

5	0.65613383	0.00287923	25	3.21933086	0.89993486
6	0.76765799	0.0664678	26	3.33271375	0.59907865
7	0.87732342	0.3046417	27	3.44052045	0.29331357
8	0.98141264	0.62834298	28	3.54832714	0.13028292
9	1.08736059	0.84272781	29	3.66171004	0.06873342
10	1.19702602	0.93675128	30	3.78066914	0.04103615
11	1.30669145	0.9735677	31	3.89405204	0.02997234
12	1.42007435	0.98583984	32	4	0.0227129
13	1.53159851	0.99055989	33	4.10594796	0.01886133
14	1.63754647	0.98678385	34	4.21375465	0.01500977
15	1.76208178	0.99055989	35	4.34386617	0.01239486
16	1.90334572	0.98772786	36	4.49256506	0.00933627
17	2.04275093	0.99055989	37	4.63568773	0.00718392
18	2.18773234	0.99527995	38	4.78066914	0.00583399
19	2.34200743	0.99339192			
20	2.49256506	0.99055989			

Data from columns of 0.5-1.0 mm MP in 1.0-2.0 mm sand

Table C-21 Data from the column of MP 0.5-10 mm and sand 1.0-2.0 mm (5%)

No.	Volume (cm ³)	EC (μS/cm)	No.	Volume (cm ³)	EC (μS/cm)
1	39	52.07	21	38	1101
2	40	52.31	22	38	1099
3	41	52.92	23	38	1098
4	38	54.06	24	39	1095
5	31	58.85	25	29	1031
6	29	225.3	26	29	647
7	29	636.2	27	34	366.6
8	29	922.3	28	30	182.1
9	29	1022	29	29	120.4
10	29	1055	30	30	94.88
11	30	1086	31	28	78.69

12	31	1096	32	28	69.79
13	29	1095	33	28	63.62
14	31	1092	34	28	60.23
15	38	1094	35	41	57.48
16	39	1094	36	37	55.87
17	41	1097	37	41	53.52
18	40	1099	38	41	52.82
19	40	1103		Background	53.93
20	40	1099		Tracer	1105

Table C-22 Adjusted data from the column of MP 0.5.-10 mm and sand 1.0-2.0 mm (5%)

No.	PV	C/C ₀	No.	PV	C/C ₀
1	0.078	-0.0017696	21	2.848	0.99619435
2	0.236	-0.0015413	22	3	0.99429153
3	0.398	-0.0009609	23	3.152	0.99334012
4	0.556	0.00012368	24	3.306	0.99048589
5	0.694	0.00468094	25	3.442	0.92959556
6	0.814	0.16304337	26	3.558	0.56425357
7	0.93	0.55397833	27	3.684	0.29747781
8	1.046	0.82617713	28	3.812	0.1219424
9	1.162	0.92103285	29	3.93	0.06324032
10	1.278	0.95242943	30	4.048	0.0389603
11	1.396	0.98192318	31	4.164	0.02355695
12	1.518	0.9914373	32	4.276	0.01508939
13	1.638	0.99048589	33	4.388	0.00921918
14	1.758	0.98763165	34	4.5	0.00599389
15	1.896	0.98953447	35	4.638	0.00337751
16	2.05	0.98953447	36	4.794	0.00184574
17	2.21	0.99238871	37	4.95	-0.0003901
18	2.372	0.99429153	38	5.114	-0.0010561

19	2.532	0.99809718			
20	2.692	0.99429153			

Table C-23 Data from the column of MP 0.5.-10 mm and sand 1.0-2.0 mm (15%)

No.	Volume (cm ³)	EC (μS/cm)	No.	Volume (cm ³)	EC (μS/cm)
1	44	52.74	21	41	1077
2	39	52.21	22	39	1079
3	39	52.2	23	40	1057
4	38	52.32	24	39	1034
5	29	74.12	25	33	810.7
6	29	301.4	26	39	397.3
7	29	744.5	27	27	205.2
8	31	966.2	28	29	132.3
9	28	1015	29	29	98.86
10	28	1057	30	28	79.61
11	28	1062	31	29	69.12
12	31	1071	32	29	62.57
13	31	1072	33	28	58.43
14	31	1073	34	32	56.04
15	37	1073	35	37	54.22
16	40	1076	36	38	52.8
17	40	1076	37	40	52.02
18	38	1078	38	40	51.13
19	41	1077		Background	53.03
20	38	1074		Tracer	1088

Table C-24 Adjusted data from the column of MP 0.5.-10 mm and sand 1.0-2.0 mm (15%)

No.	PV	C/C ₀	No.	PV	C/C ₀
1	0.09482759	-0.0002802	21	3.05818966	0.98937167
2	0.2737069	-0.0007923	22	3.23060345	0.9913041
3	0.44181034	-0.000802	23	3.40086207	0.97004744

4	0.60775862	-0.000686	24	3.57112069	0.94782457
5	0.75215517	0.0203774	25	3.7262931	0.73206953
6	0.87715517	0.23997797	26	3.88146552	0.33263766
7	1.00215517	0.66810632	27	4.0237069	0.14702842
8	1.13146552	0.88231543	28	4.14439655	0.07659159
9	1.25862069	0.92946655	29	4.26939655	0.04428148
10	1.37931034	0.97004744	30	4.39224138	0.0256819
11	1.5	0.9748785	31	4.51508621	0.01554634
12	1.62715517	0.9835744	32	4.64008621	0.00921766
13	1.76077586	0.98454061	33	4.76293103	0.00521754
14	1.89439655	0.98550683	34	4.89224138	0.0029083
15	2.04094828	0.98550683	35	5.04094828	0.00114979
16	2.20689655	0.98840546	36	5.20258621	-0.0002222
17	2.37931034	0.98840546	37	5.37068966	-0.0009759
18	2.54741379	0.99033788	38	5.54310345	-0.0018358
19	2.71767241	0.98937167			
20	2.88793103	0.98647304			

Data from column of 2.0-4.0 mm sand

Table C-25 Data from the column of sand 2.0-4.0 mm

No.	Volume (cm ³)	EC (μ S/cm)	No.	Volume (cm ³)	EC (μ S/cm)
1	42	54.66	21	38	1102
2	42	54.09	22	38	1104
3	39	54.08	23	39	1106
4	40	54.26	24	41	1089
5	30	62.99	25	32	1030
6	30	167.8	26	29	747.9
7	31	476.5	27	32	446.4
8	30	793.1	28	30	239.8
9	29	964	29	32	141.2
10	29	1063	30	30	98.1

11	29	1084	31	29	78.25
12	30	1096	32	29	68.98
13	29	1098	33	28	63.96
14	29	1097	34	31	61.2
15	38	1101	35	41	58.99
16	38	1100	36	38	57.2
17	42	1106	37	39	56.85
18	39	1105	38	40	56.14
19	39	1108		Background	54.60
20	42	1104		Tracer	1101

Table C-26 Adjusted data from the column of sand 2.0-4.0 mm

No.	PV	C/C ₀	No.	PV	C/C ₀
1	0.07865169	5.7339E-05	21	2.68164794	1.00095566
2	0.23595506	-0.0004874	22	2.82397004	1.00286697
3	0.38764045	-0.0004969	23	2.96816479	1.00477829
4	0.53558052	-0.0003249	24	3.11797753	0.98853211
5	0.66666667	0.00801797	25	3.25468165	0.93214832
6	0.77902622	0.10818043	26	3.36891386	0.66255734
7	0.89325843	0.4031919	27	3.48314607	0.37442661
8	1.00749064	0.70575306	28	3.59925094	0.17698777
9	1.11797753	0.86907492	29	3.71535581	0.08275994
10	1.22659176	0.96368502	30	3.83146067	0.0415711
11	1.33520599	0.98375382	31	3.94194757	0.0226013
12	1.44569288	0.99522171	32	4.0505618	0.01374235
13	1.55617978	0.99713303	33	4.15730337	0.00894495
14	1.66479401	0.99617737	34	4.26779026	0.00630734
15	1.79026217	1	35	4.40262172	0.00419534
16	1.93258427	0.99904434	36	4.5505618	0.00248471
17	2.082397	1.00477829	37	4.69475655	0.00215023
18	2.2340824	1.00382263	38	4.84269663	0.00147171

19	2.38014981	1.0066896			
20	2.53183521	1.00286697			

Data from columns of 0.5-1.0 mm MP in 2.0-4.0 mm sand

Table C-27 Data from the column of MP 0.5.-10 mm and sand 2.0-4.0 mm (5%)

No.	Volume (cm ³)	EC (μS/cm)	No.	Volume (cm ³)	EC (μS/cm)
1	43	52.29	21	42	1090
2	39	52.04	22	39	1088
3	39	51.46	23	46	1091
4	39	51.31	24	37	1023
5	32	66.84	25	29	659.4
6	30	271.6	26	29	334.4
7	30	682.3	27	28	168.1
8	31	974.4	28	29	106.1
9	31	1051	29	29	78.21
10	31	1061	30	29	67.01
11	29	1071	31	32	60.39
12	32	1083	32	29	56.44
13	30	1083	33	29	54.12
14	39	1081	34	29	52.69
15	38	1084	35	38	51.16
16	43	1086	36	41	50.46
17	41	1083	37	38	49.11
18	41	1089	38	40	48.39
19	42	1083		Background	52.85
20	43	1088		Tracer	1095

Table C-28 Adjusted data from the column of MP 0.5.-10 mm and sand 2.0-4.0 mm (5%)

No.	PV	C/C ₀	No.	PV	C/C ₀
1	0.09307359	-0.0005374	21	3.22077922	0.99520223
2	0.27056277	-0.0007772	22	3.3961039	0.99328312

3	0.43939394	-0.0013338	23	3.58008658	0.99616178
4	0.60822511	-0.0014777	24	3.75974026	0.93091206
5	0.76190476	0.01342417	25	3.9025974	0.58201794
6	0.8961039	0.20990261	26	4.02813853	0.27016264
7	1.02597403	0.60399175	27	4.15151515	0.11058869
8	1.15800866	0.8842777	28	4.27489177	0.05109629
9	1.29220779	0.95777959	29	4.4004329	0.02433431
10	1.42640693	0.96737514	30	4.52597403	0.0135873
11	1.55627706	0.97697069	31	4.65800866	0.00723504
12	1.68831169	0.98848534	32	4.79004329	0.0034448
13	1.82251082	0.98848534	33	4.91558442	0.00121863
14	1.97186147	0.98656623	34	5.04112554	-0.0001535
15	2.13852814	0.9894449	35	5.18614719	-0.0016216
16	2.31385281	0.99136401	36	5.35714286	-0.0022933
17	2.495671	0.98848534	37	5.52813853	-0.0035887
18	2.67316017	0.99424267	38	5.6969697	-0.0042796
19	2.85281385	0.98848534			
20	3.03679654	0.99328312			

Table C-29 Data from the column of MP 0.5.-10 mm and sand 2.0-4.0 mm (15%)

No.	Volume (cm ³)	EC (μ S/cm)	No.	Volume (cm ³)	EC (μ S/cm)
1	39	54.01	21	42	1090
2	39	54.38	22	41	1090
3	39	54.21	23	38	1080
4	39	54.59	24	39	1024
5	20	66.57	25	32	737.7
6	31	245.1	26	29	371.3
7	28	612.3	27	29	186.9
8	34	892.7	28	29	112.6
9	29	1031	29	29	81.49
10	31	1069	30	32	67.91

11	29	1074	31	29	61.45
12	28	1078	32	29	58.08
13	28	1081	33	29	56.52
14	29	1080	34	29	55.1
15	29	1078	35	41	54.47
16	38	1083	36	42	53.88
17	40	1088	37	41	53.52
18	38	1089	38	41	53.19
19	40	1089		Background	54.25
20	39	1090		Tracer	1092

Table C-30 Adjusted data from the column of MP 0.5.-10 mm and sand 2.0-4.0 mm (15%)

No.	PV	C/C ₀	No.	PV	C/C ₀
1	0.08628319	-0.0002313	21	3.04424779	0.99807275
2	0.25884956	0.00012527	22	3.22787611	0.99807275
3	0.43141593	-3.854E-05	23	3.40265487	0.98843652
4	0.6039823	0.00032763	24	3.57300885	0.93447362
5	0.73451327	0.01187184	25	3.7300885	0.65858829
6	0.84734513	0.18390749	26	3.86504425	0.30551674
7	0.97787611	0.53774994	27	3.99336283	0.12782462
8	1.11504425	0.80794989	28	4.12168142	0.05622742
9	1.25442478	0.94121898	29	4.25	0.0262491
10	1.38716814	0.97783667	30	4.38495575	0.01316309
11	1.5199115	0.98265478	31	4.5199115	0.00693809
12	1.6460177	0.98650927	32	4.64823009	0.00369068
13	1.7699115	0.98940014	33	4.77654867	0.00218742
14	1.8960177	0.98843652	34	4.90486726	0.00081908
15	2.02433628	0.98650927	35	5.05973451	0.000212
16	2.17256637	0.99132739	36	5.24336283	-0.0003565
17	2.34513274	0.99614551	37	5.42699115	-0.0007034

18	2.51769912	0.99710913	38	5.60840708	-0.0010214
19	2.69026549	0.99710913			
20	2.86504425	0.99807275			



APPENDIX D

Breakthrough curve fitting (Excel)

The curve

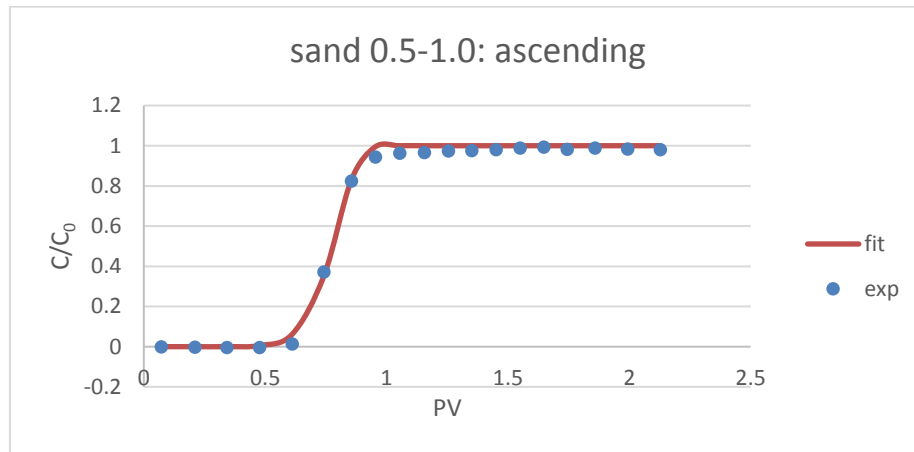


Figure D-1 The ascending log of breakthrough curve derived from the column of sand 0.5-1.0 mm

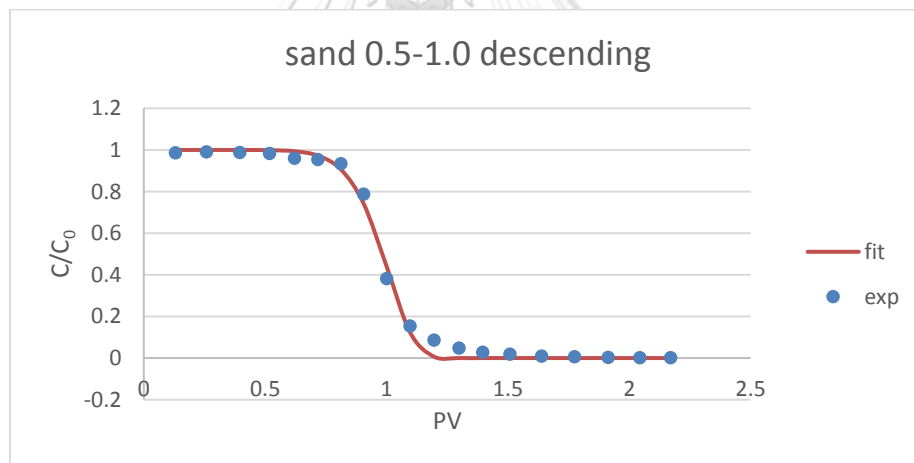


Figure D-2 The descending log of breakthrough curve derived from the column of sand 0.5-1.0 mm

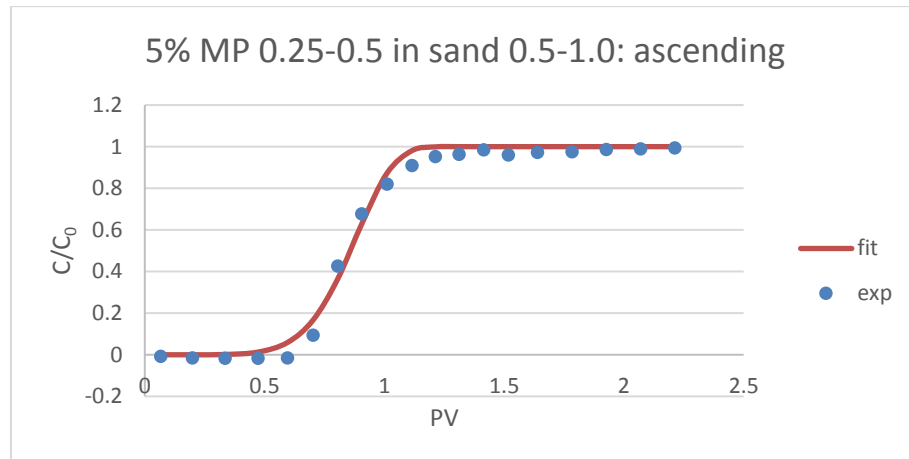


Figure D-3 The ascending log of breakthrough curve derived from the column of 5% MP 0.25-0.5 mm in sand 0.5-1.0 mm

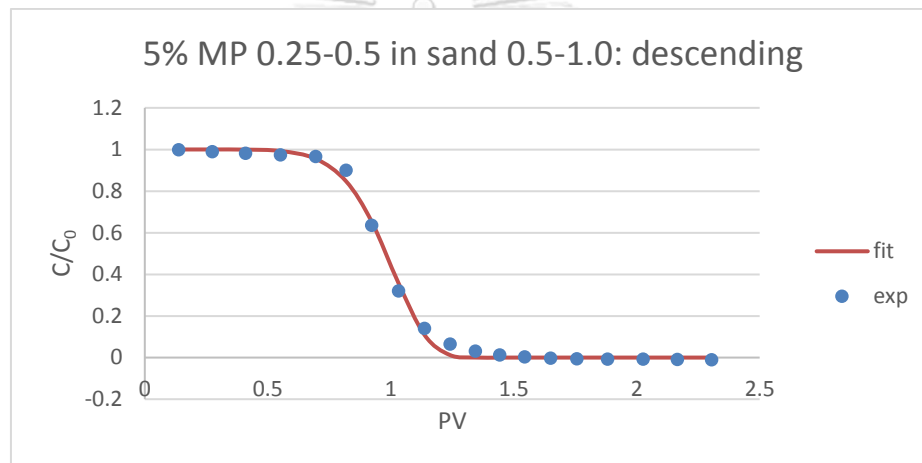


Figure D-4 The descending log of breakthrough curve derived from the column of 5% MP 0.25-0.5 mm in sand 0.5-1.0 mm

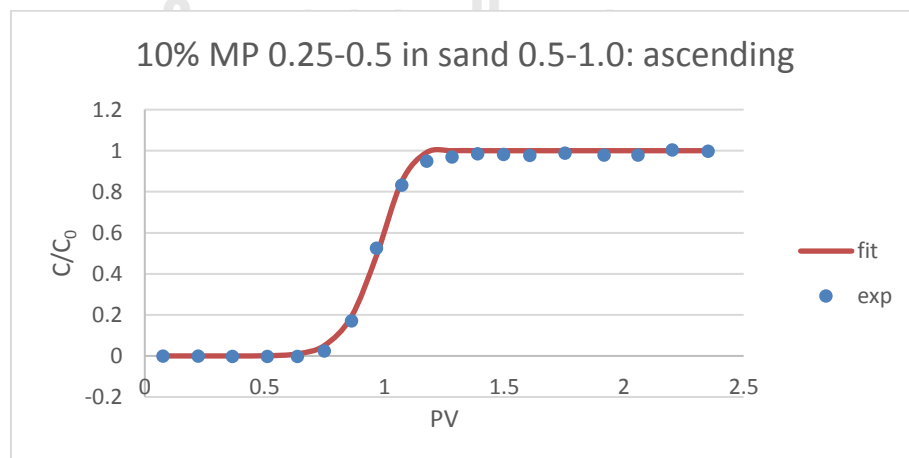


Figure D-5 The ascending log of breakthrough curve derived from the column of 10% MP 0.25-0.5 mm in sand 0.5-1.0 mm

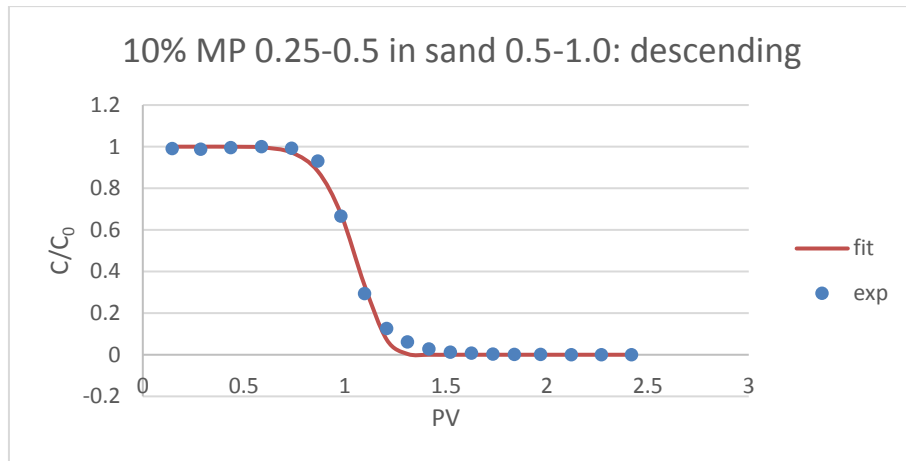


Figure D-6 The descending log of breakthrough curve derived from the column of 10% MP 0.25-0.5 mm in sand 0.5-1.0 mm

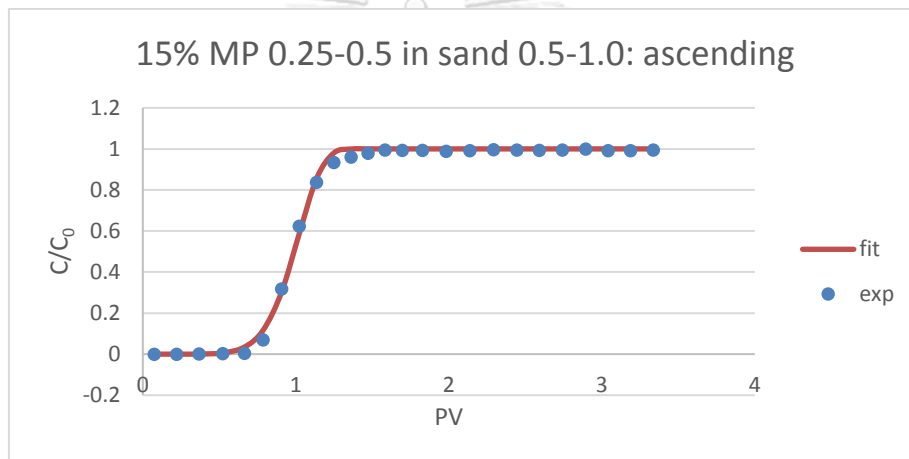


Figure D-7 The ascending log of breakthrough curve derived from the column of 15% MP 0.25-0.5 mm in sand 0.5-1.0 mm

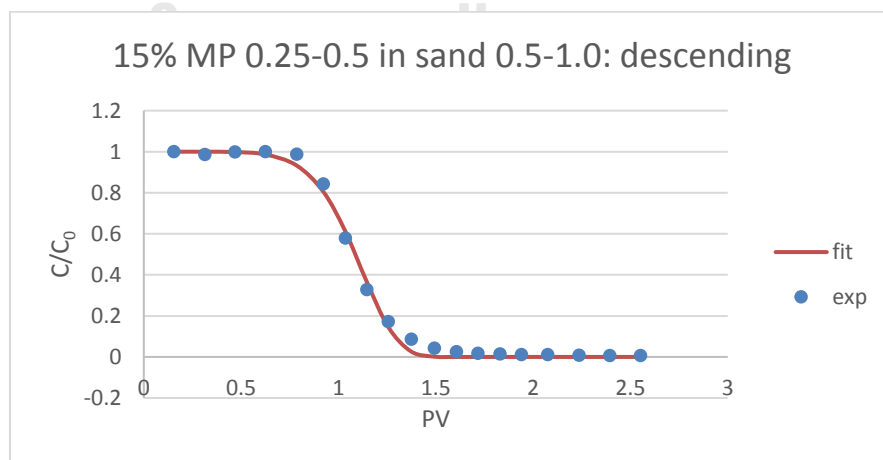


Figure D-8 The descending log of breakthrough curve derived from the column of 15% MP 0.25-0.5 mm in sand 0.5-1.0 mm

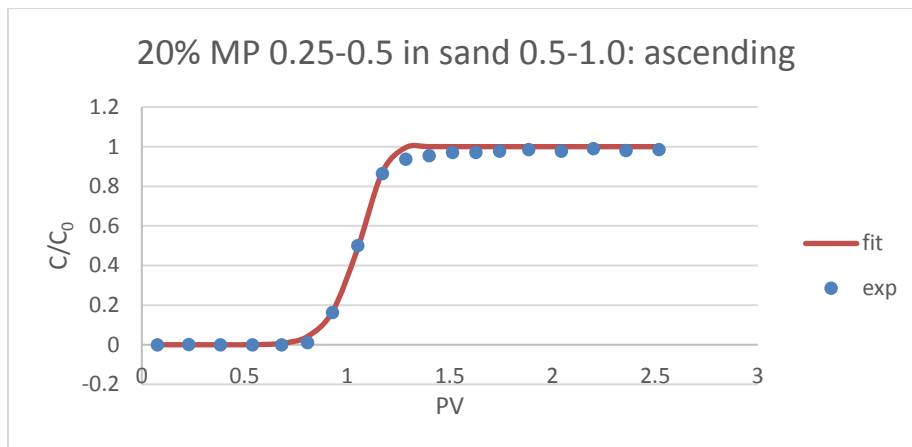


Figure D-9 The ascending log of breakthrough curve derived from the column of 20% MP 0.25-0.5 mm in sand 0.5-1.0 mm

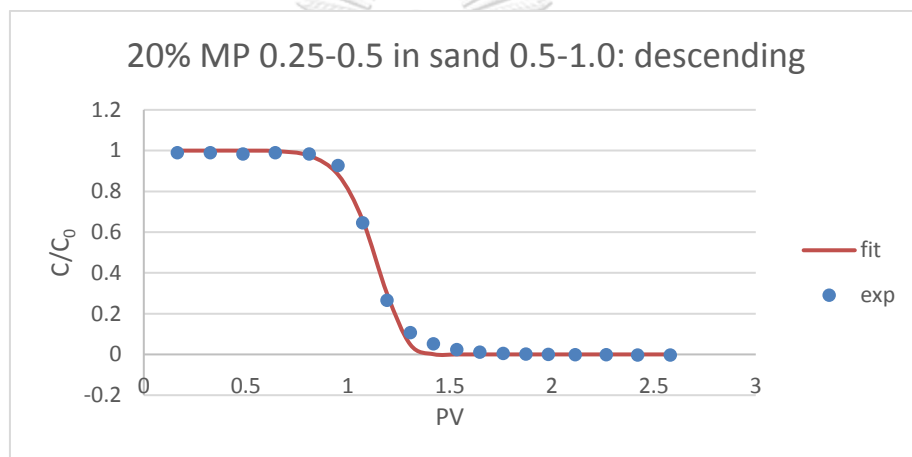


Figure D-10 The descending log of breakthrough curve derived from the column of 20% MP 0.25-0.5 mm in sand 0.5-1.0 mm

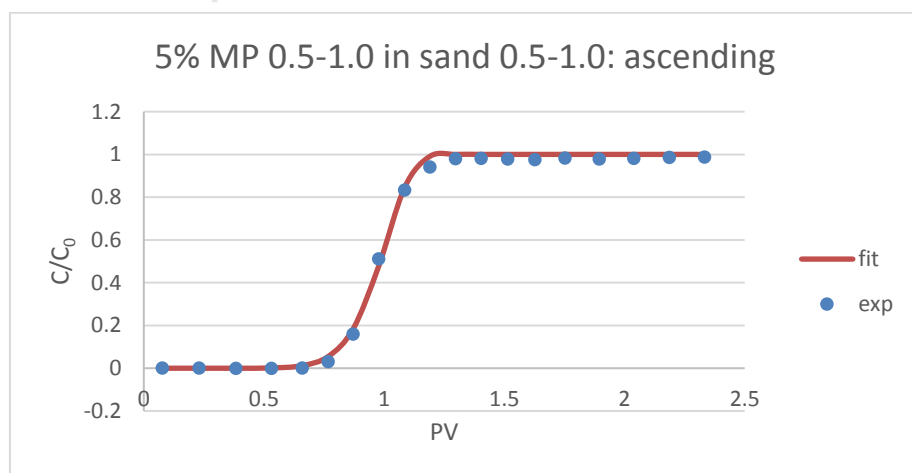


Figure D-11 The ascending log of breakthrough curve derived from the column of 5% MP 0.5-1.0 mm in sand 0.5-1.0 mm

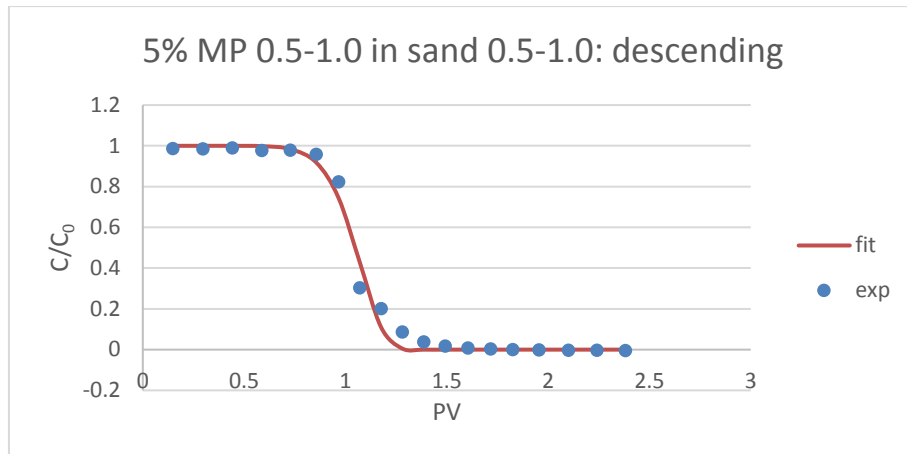


Figure D-12 The descending log of breakthrough curve derived from the column of 5% MP 0.5-1.0 mm in sand 0.5-1.0 mm

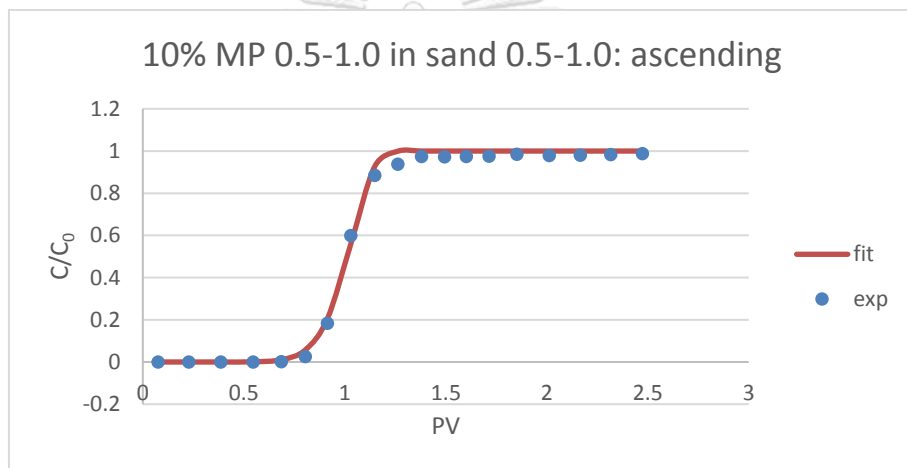


Figure D-13 The ascending log of breakthrough curve derived from the column of 10% MP 0.5-1.0 mm in sand 0.5-1.0 mm

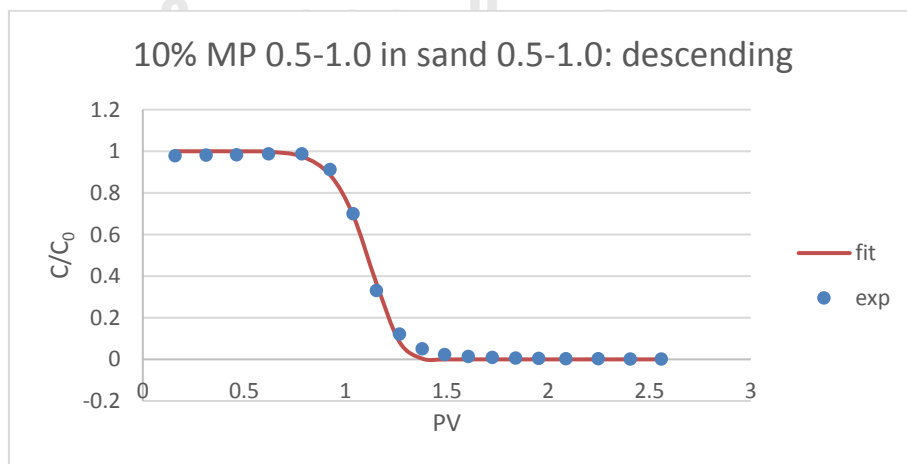


Figure D-14 The descending log of breakthrough curve derived from the column of 10% MP 0.5-1.0 mm in sand 0.5-1.0 mm

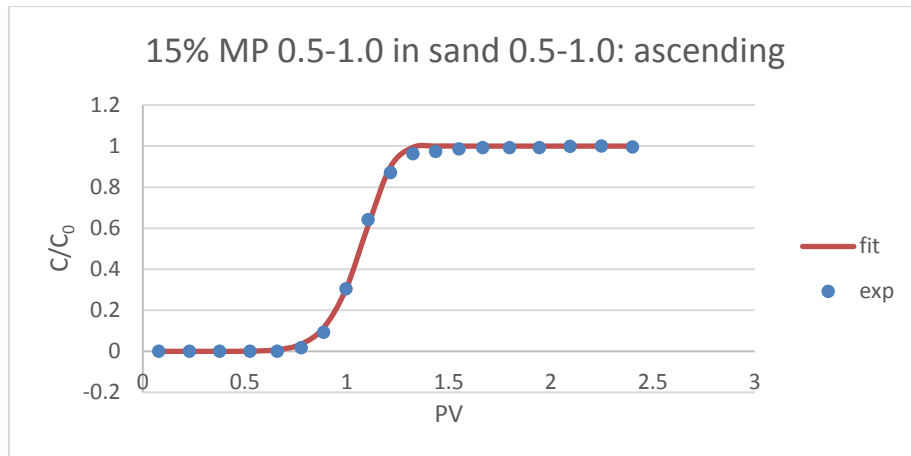


Figure D-15 The ascending log of breakthrough curve derived from the column of 15% MP 0.5-1.0 mm in sand 0.5-1.0 mm

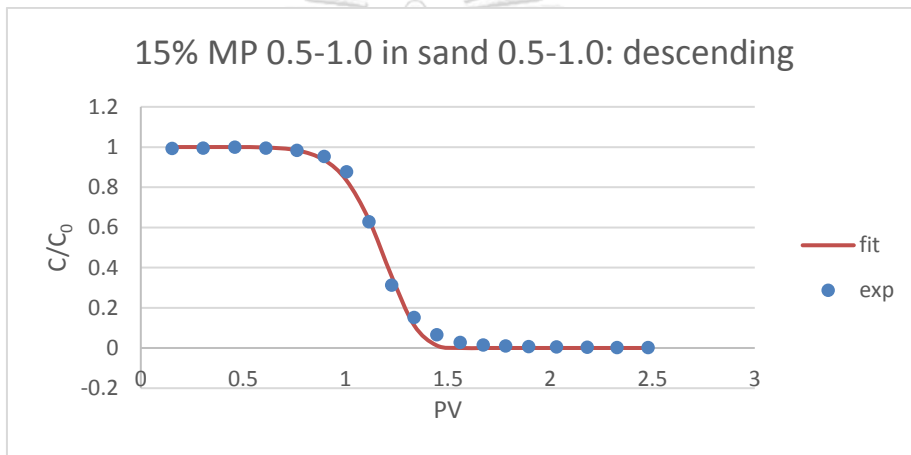


Figure D-16 The descending log of breakthrough curve derived from the column of 15% MP 0.5-1.0 mm in sand 0.5-1.0 mm

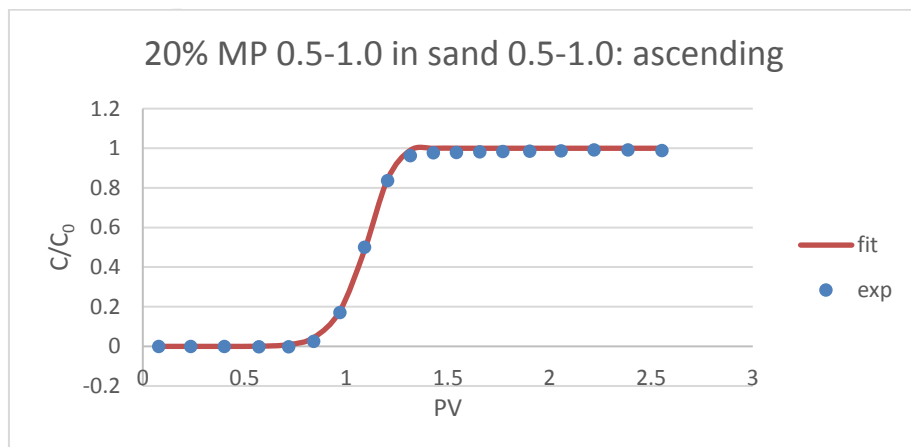


Figure D-17 The ascending log of breakthrough curve derived from the column of 20% MP 0.5-1.0 mm in sand 0.5-1.0 mm

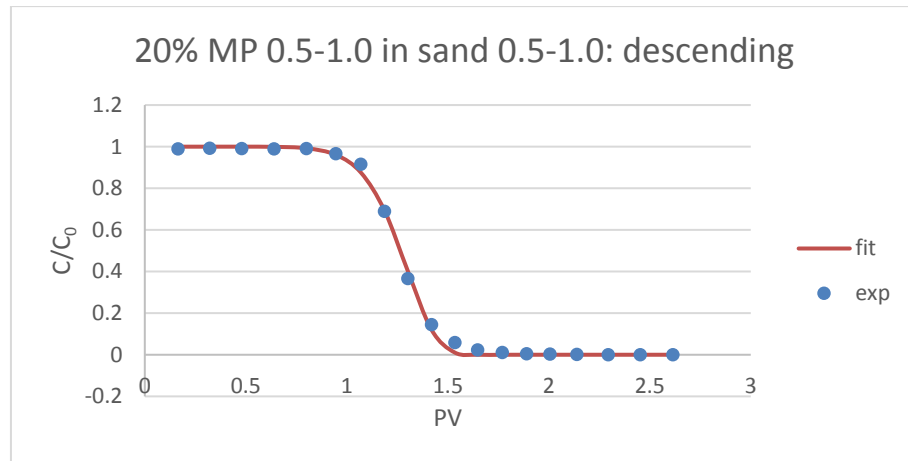


Figure D-18 The descending log of breakthrough curve derived from the column of 20% MP 0.5-1.0 mm in sand 0.5-1.0 mm

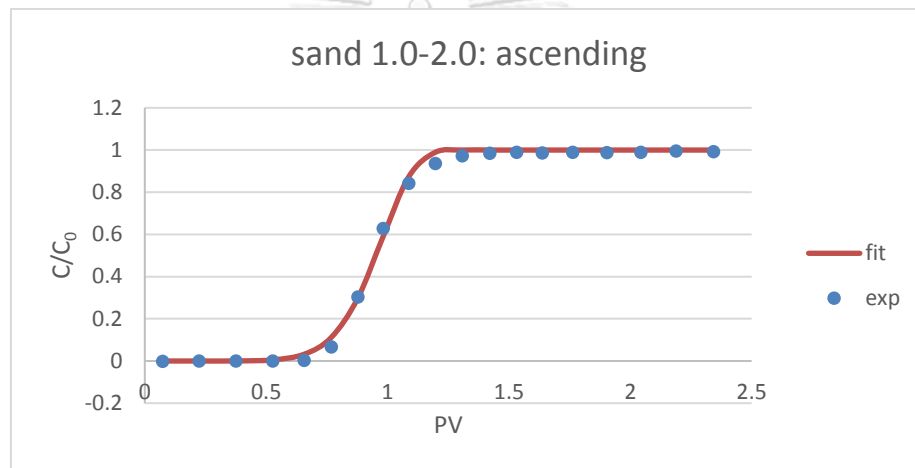


Figure D-19 The ascending log of breakthrough curve derived from the column of sand 1.0-2.0 mm

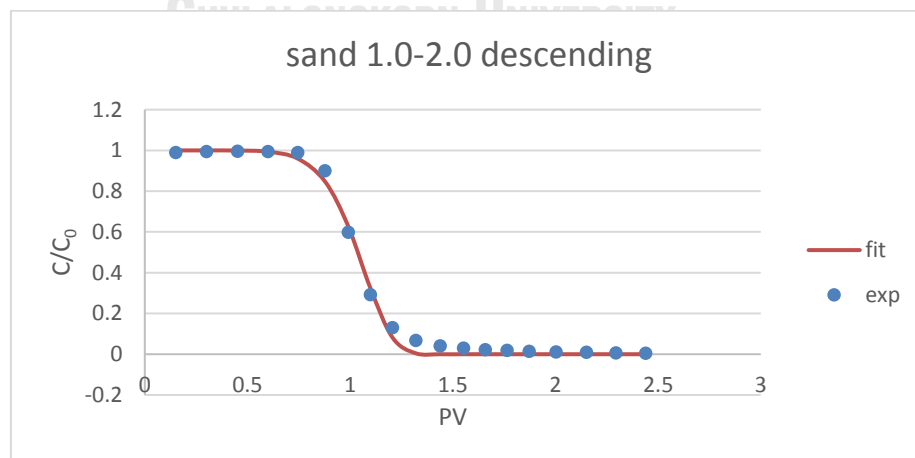


Figure D-20 The descending log of breakthrough curve derived from the column of sand 1.0-2.0 mm

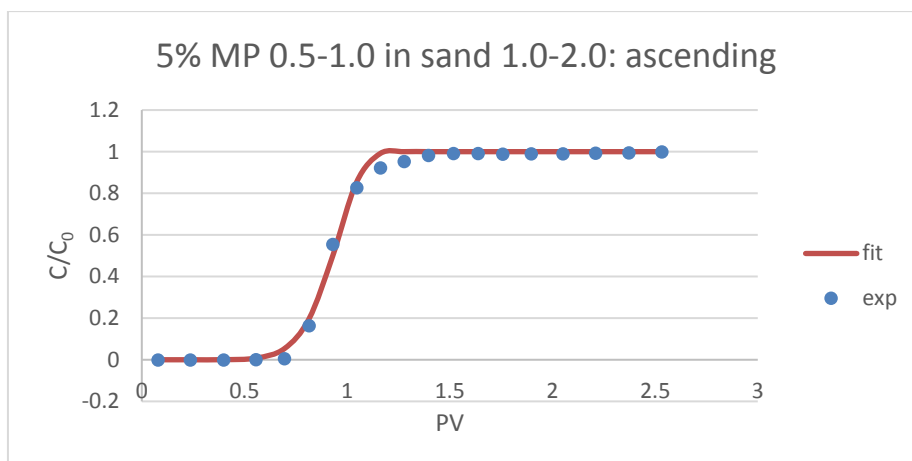


Figure D-21 The ascending log of breakthrough curve derived from the column of 5% MP 0.5-1.0 mm in sand 1.0-2.0 mm

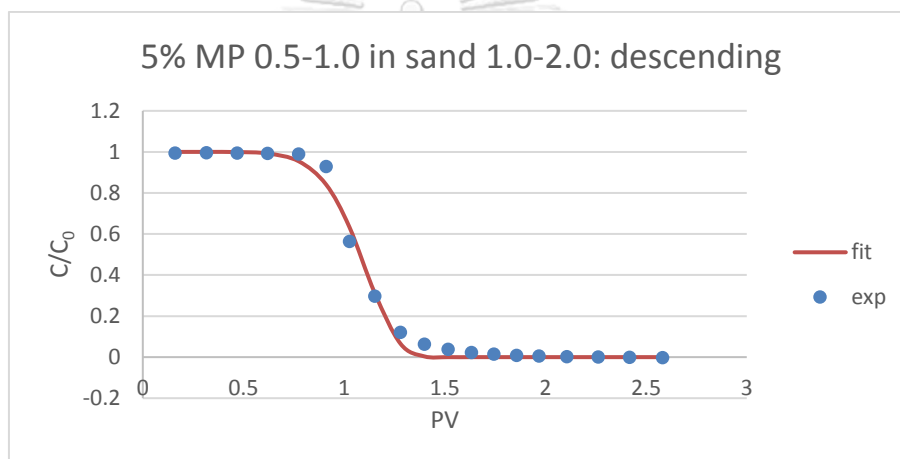


Figure D-22 The descending log of breakthrough curve derived from the column of 5% MP 0.5-1.0 mm in sand 1.0-2.0 mm

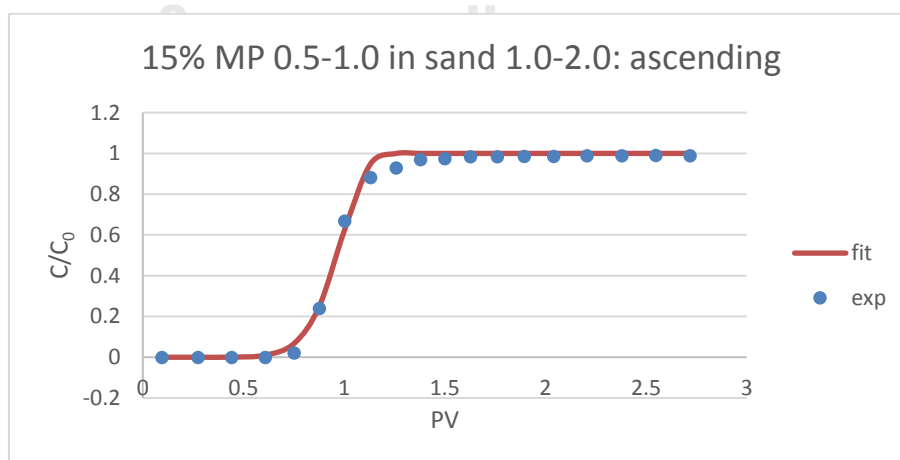


Figure D-23 The ascending log of breakthrough curve derived from the column of 15% MP 0.5-1.0 mm in sand 1.0-2.0 mm

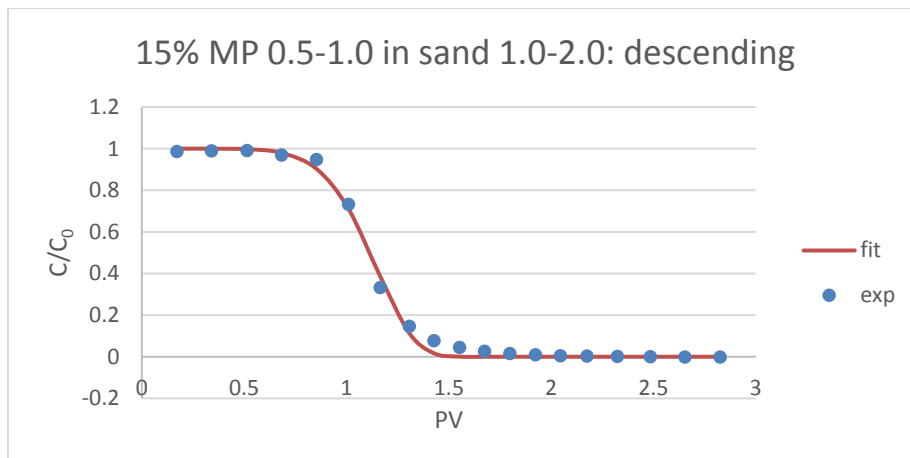


Figure D-24 The descending log of breakthrough curve derived from the column of 15% MP 0.5-1.0 mm in sand 1.0-2.0 mm

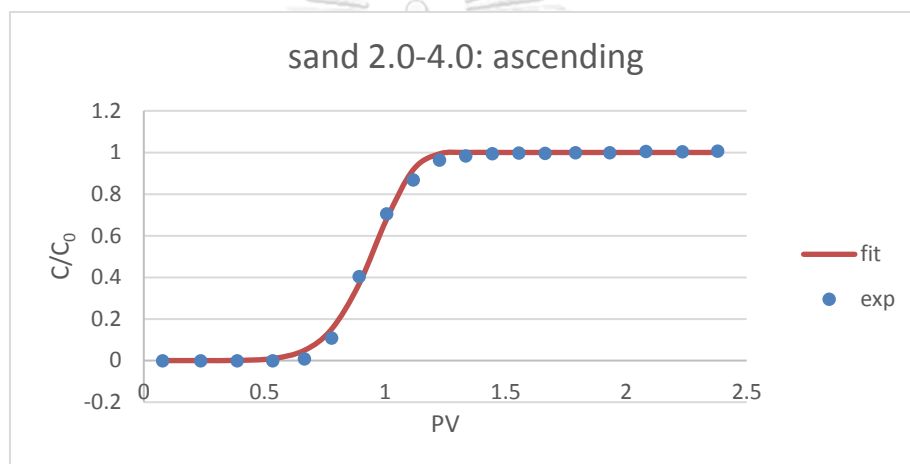


Figure D-25 The ascending log of breakthrough curve derived from the column of sand 2.0-4.0 mm

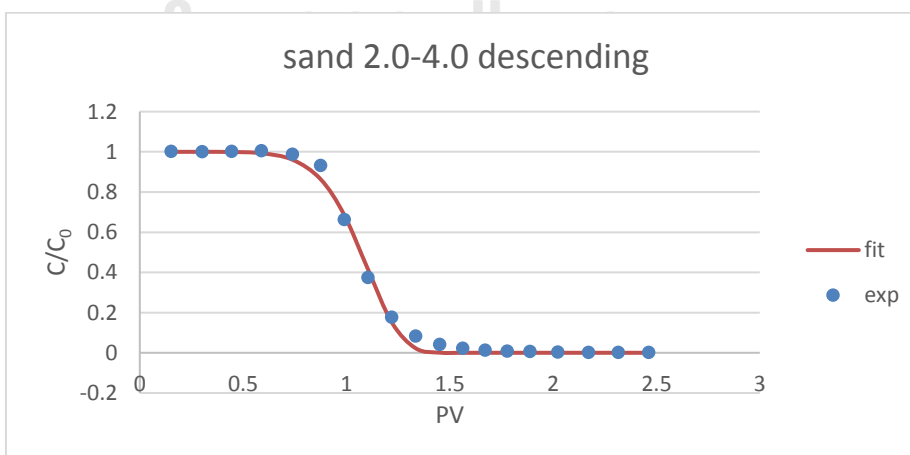


Figure D-26 The descending log of breakthrough curve derived from the column of sand 2.0-4.0 mm

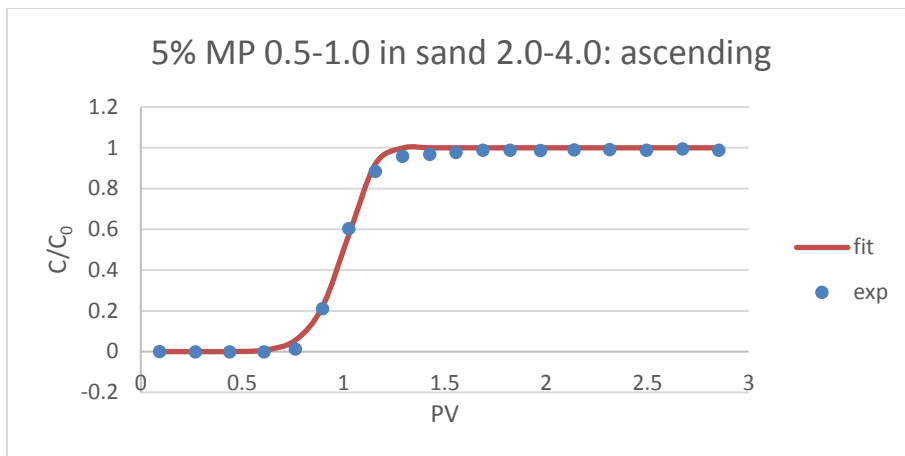


Figure D-27 The ascending log of breakthrough curve derived from the column of 5% MP 0.5-1.0 mm in sand 2.0-4.0 mm

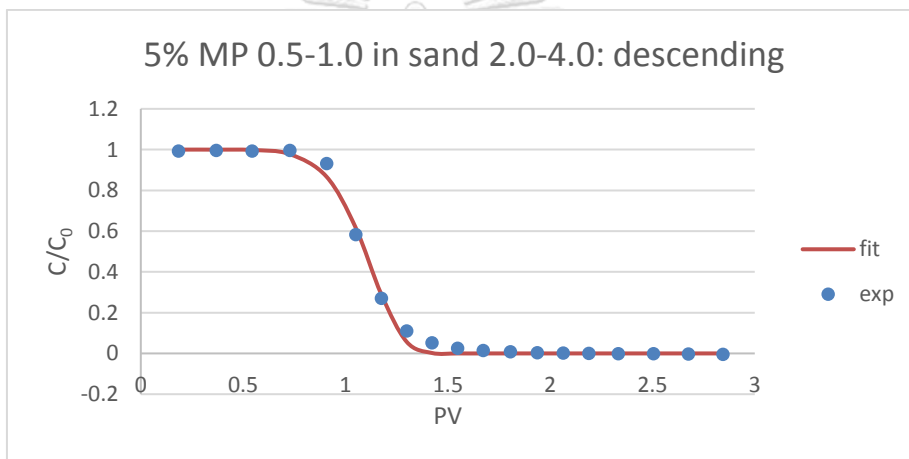


Figure D-28 The descending log of breakthrough curve derived from the column of 5% MP 0.5-1.0 mm in sand 2.0-4.0 mm

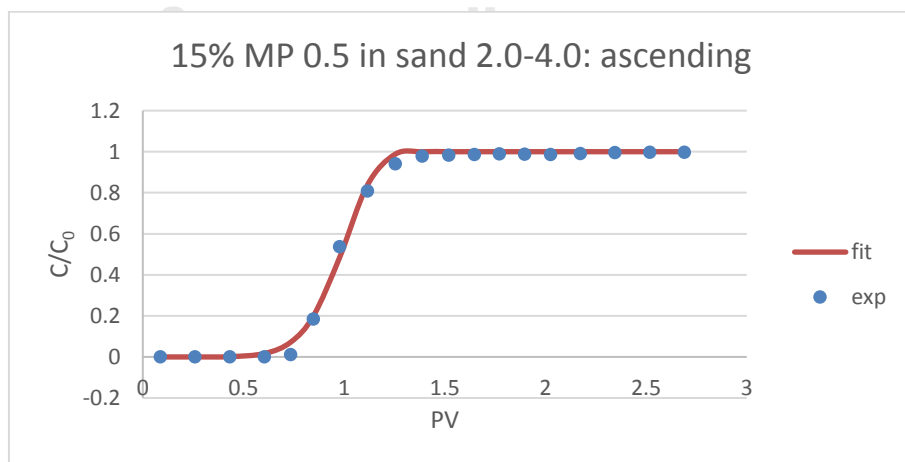


Figure D-29 The ascending log of breakthrough curve derived from the column of 15% MP 0.5-1.0 mm in sand 2.0-4.0 mm

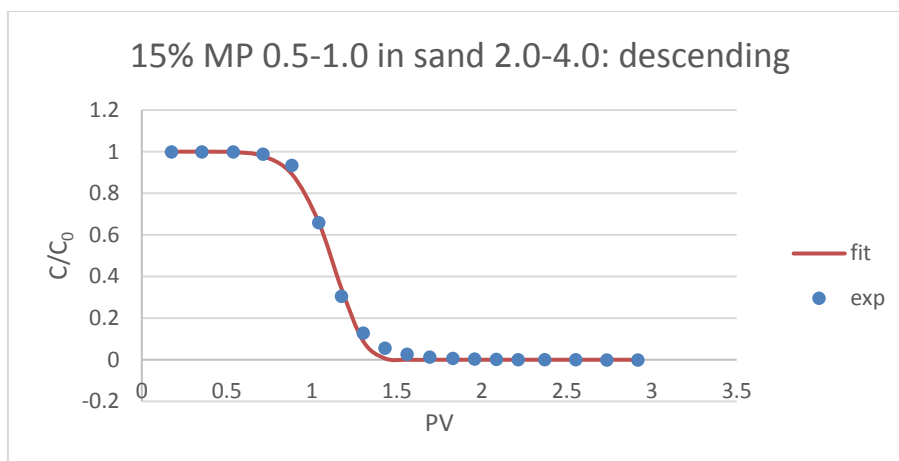


Figure D-30 The descending log of breakthrough curve derived from the column of 15% MP 0.5-1.0 mm in sand 2.0-4.0 mm

The parameters from ascending logs

Table D-1 The parameters of ascending section of the breakthrough curves

MP size (mm)	Sand size (mm)	%MP	k	n	R ²
0.25-0.5	0.5-1.0	0	8.35665361	9.9078761	0.99678583
		5	1.915402	6.65740707	0.98994571
		10	0.93722777	10.0281246	0.99776032
		15	0.74693127	7.47576425	0.99777321
		20	0.39626591	10.3916744	0.99695423
0.5-1.0	0.5-1.0	5	0.817152223	10.0839276	0.99756649
		10	0.599001018	10.6669671	0.99630661
		15	0.375509439	9.3123297	0.99876544
		20	0.272203429	10.3354219	0.9989933
	1.0-2.0	0	1.03733142	8.23061033	0.99714245
		5	1.29964652	8.67566143	0.99541658
		15	0.96082139	9.16458755	0.99490935
	2.0-4.0	0	1.07859159	7.53986285	0.9973234
		5	0.67109776	9.0724602	0.99743991
		15	0.78747731	7.63669236	0.99659738

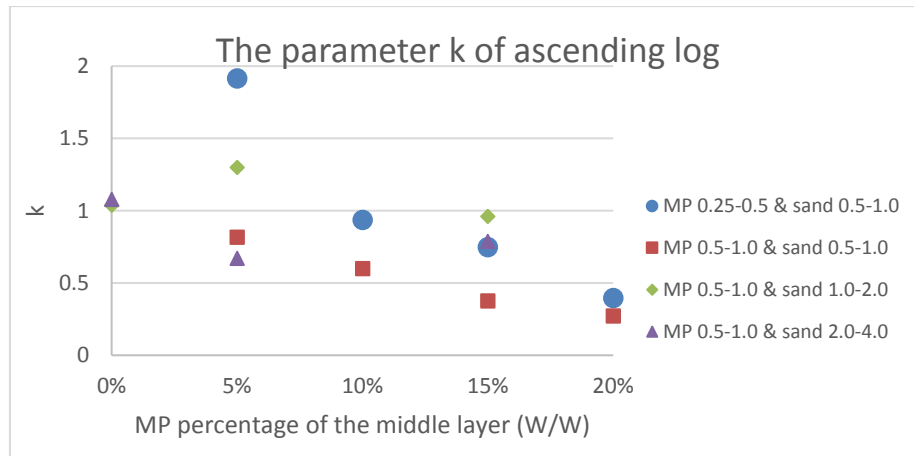


Figure D-31 The scatterplot of k (ascending) over the mass percentage of MP in the middle layer

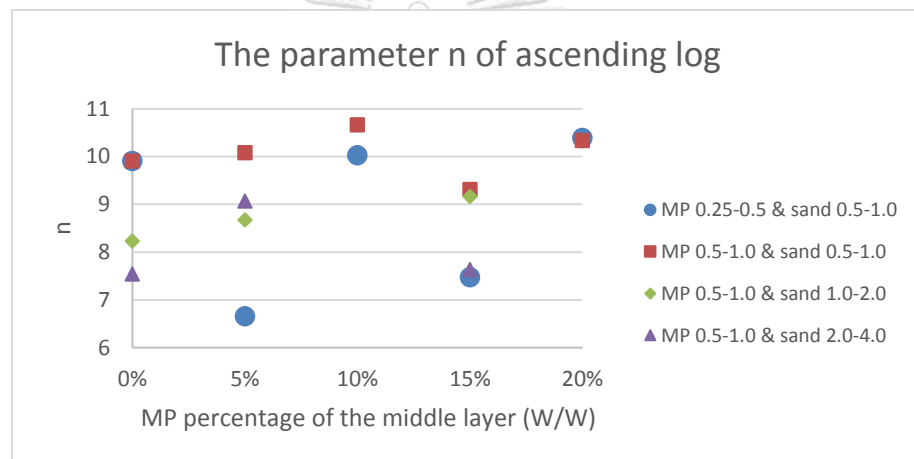


Figure D-32 The scatterplot of n (ascending) over the mass percentage of MP in the middle layer

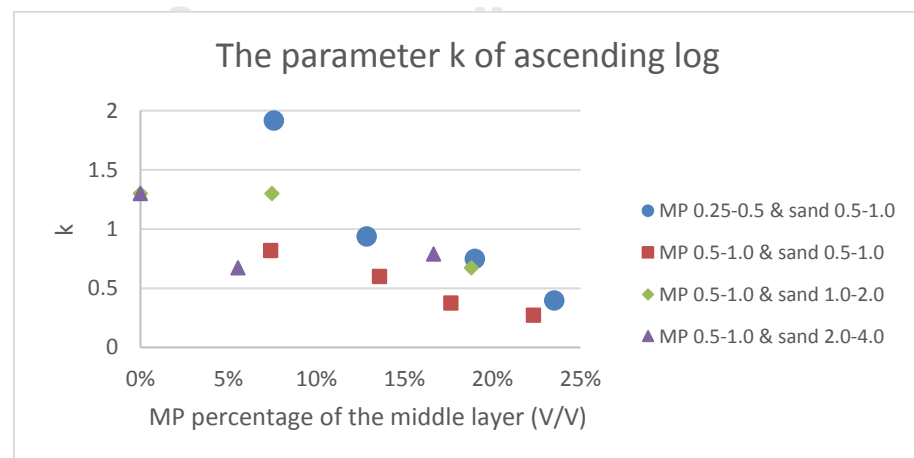


Figure D-33 The scatterplot of k (ascending) over the volume percentage of MP in the middle layer

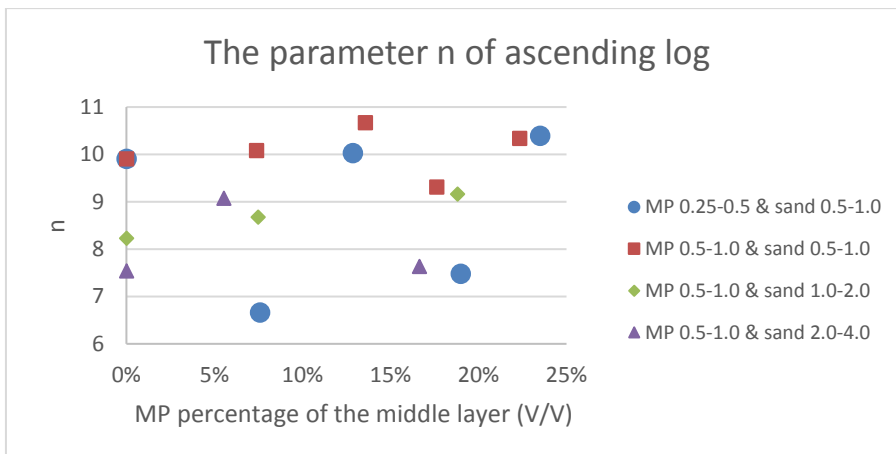


Figure D-34 The scatterplot of n (ascending) over the volume percentage of MP in the middle layer

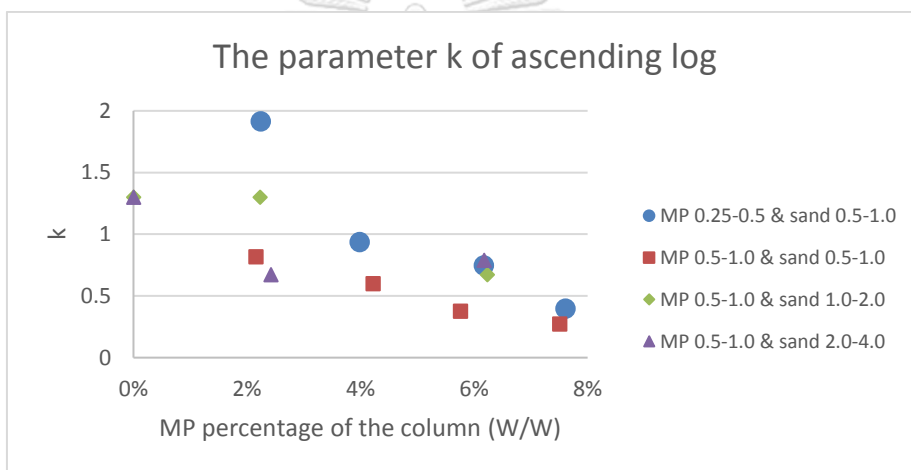


Figure D-35 The scatterplot of k (ascending) over the mass percentage of MP in the column

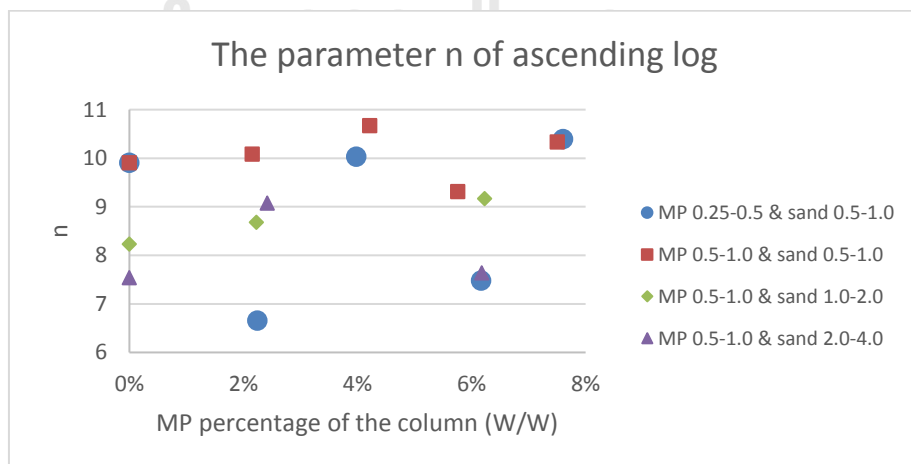


Figure D-36 The scatterplot of n (ascending) over the mass percentage of MP in the column

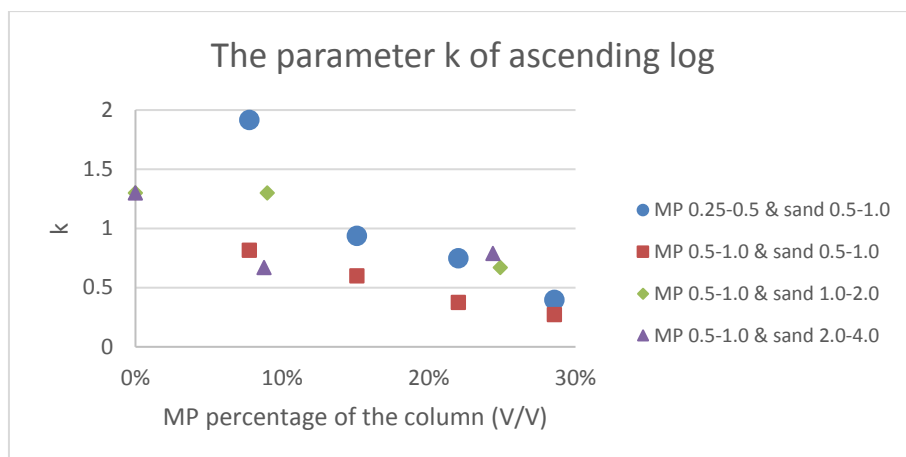


Figure D-37 The scatterplot of k (ascending) over the volume percentage of MP in the column

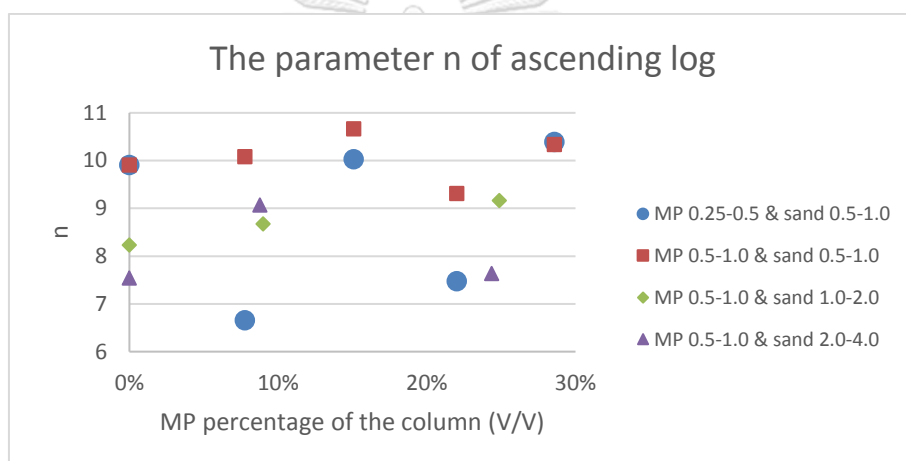


Figure D-38 The scatterplot of n (ascending) over the volume percentage of MP in the column

The parameters from fitting descending logs

Table D-2 The parameters of descending section of the breakthrough curves

MP size (mm)	Sand size (mm)	%MP	k	n	R^2
0.25-0.5	0.5-1.0	0	0.81693148	10.1637592	0.99494078
		5	0.80455038	7.88283302	0.99699797
		10	0.46704255	9.15186079	0.99671102
		15	0.38447164	7.07161787	0.9945238
		20	0.20579804	10.0636294	0.99709943
0.5-1.0	0.5-1.0	5	0.42109186	10.236378	0.98901078
		10	0.25765482	9.5772297	0.99785241

	1.0-2.0	15	0.17394953	8.74042524	0.99746342	
		20	0.06866143	9.78939429	0.99817732	
		0	0.5041046	8.53885626	0.99549634	
	2.0-4.0	5	0.36997016	8.09134947	0.993536	
		15	0.31779865	7.17943764	0.99602026	
		0	0.4096873	7.70511913	0.99595532	
		2.0-4.0	5	0.32093308	8.36506026	0.99640886
			15	0.30302601	7.84884671	0.99761573

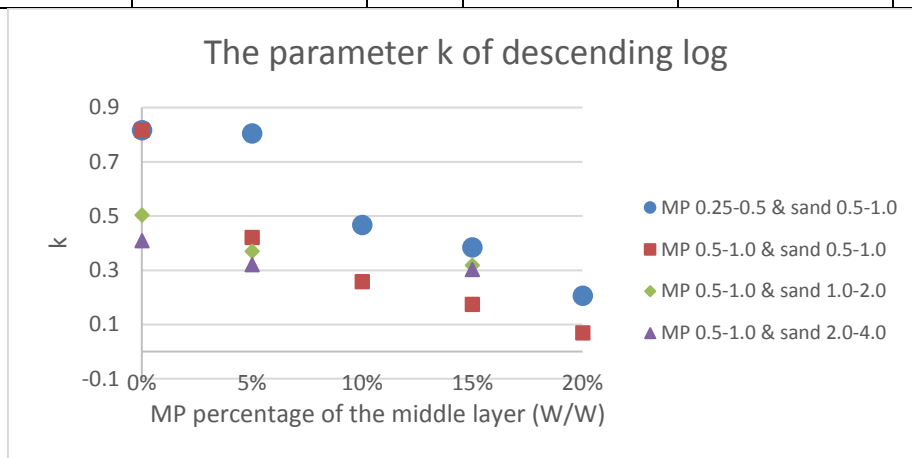


Figure D-39 The scatterplot of k (descending) over the mass percentage of MP in the middle layer

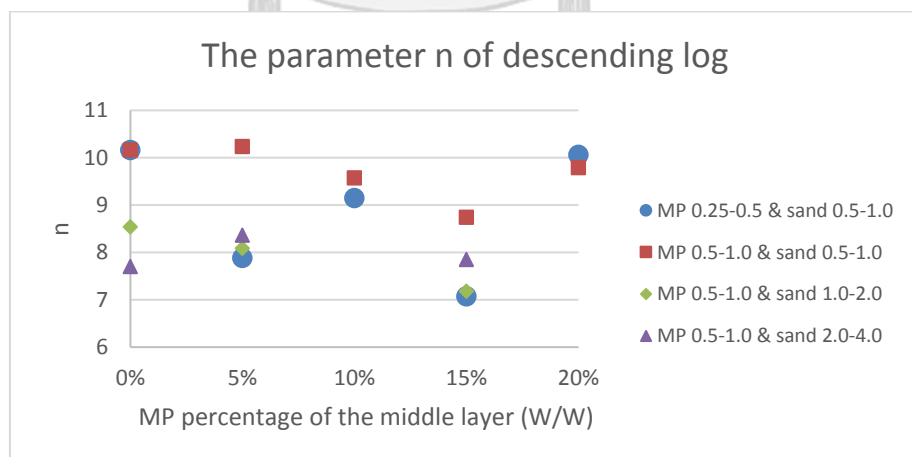


Figure D-40 The scatterplot of n (descending) over the mass percentage of MP in the middle layer

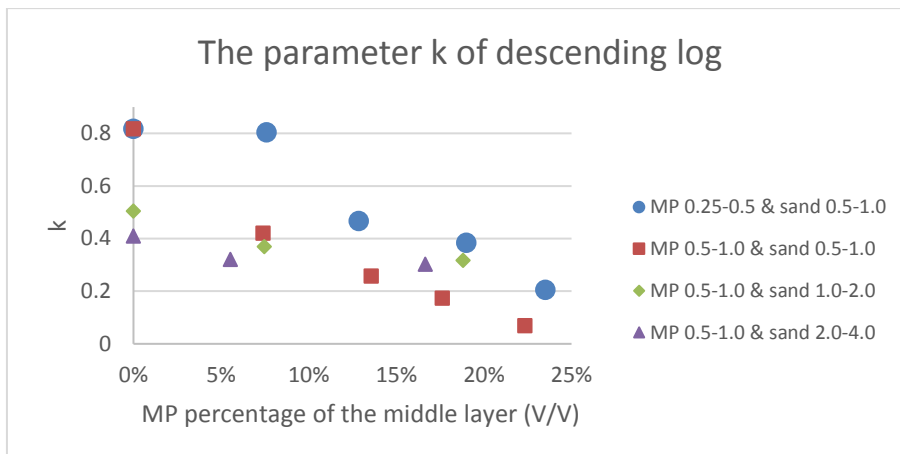


Figure D-41 The scatterplot of k (descending) over the volume percentage of MP in the middle layer

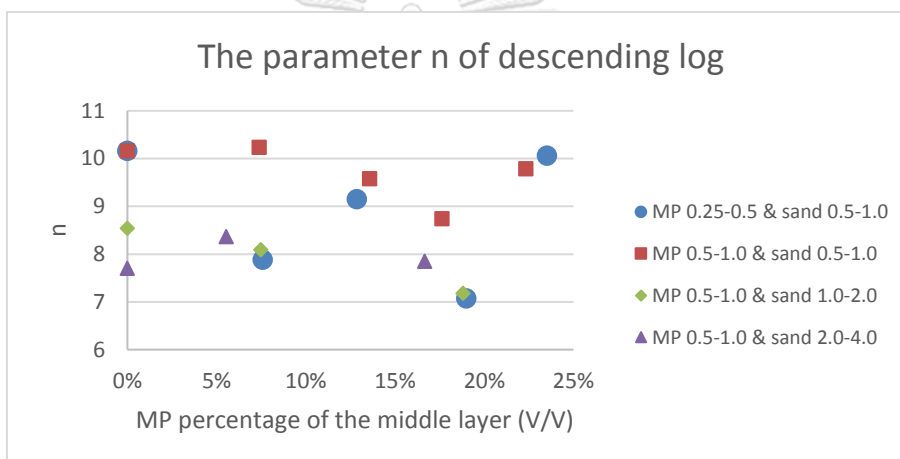


Figure D-42 The scatterplot of n (descending) over the mass percentage of MP in the middle layer

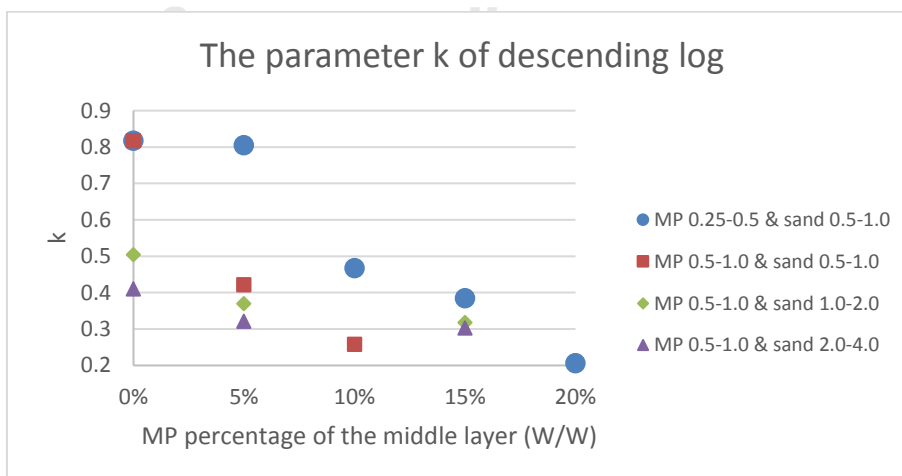


Figure D-43 The scatterplot of k (descending) over the mass percentage of MP in the column

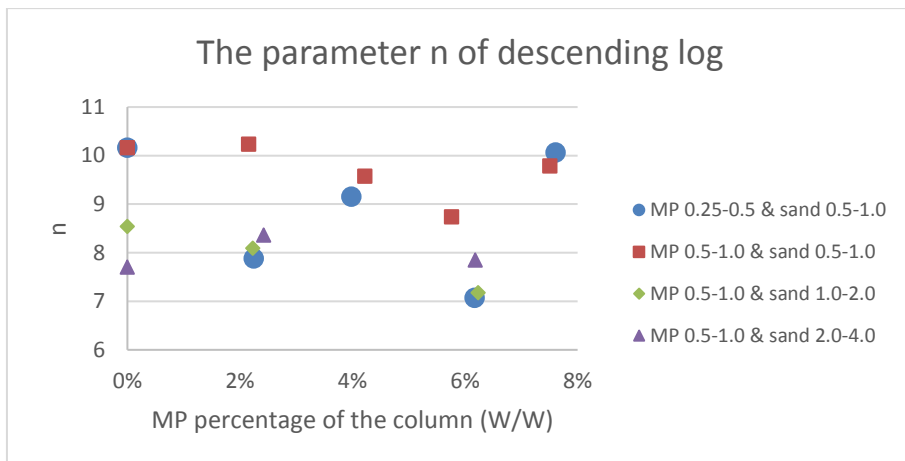


Figure D-44 The scatterplot of n (descending) over the mass percentage of MP in the column

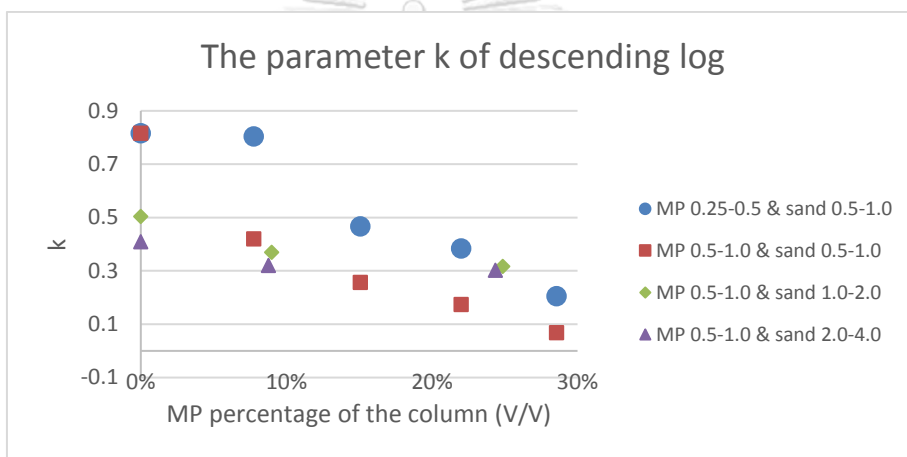


Figure D-45 The scatterplot of k (descending) over the volume percentage of MP in the column

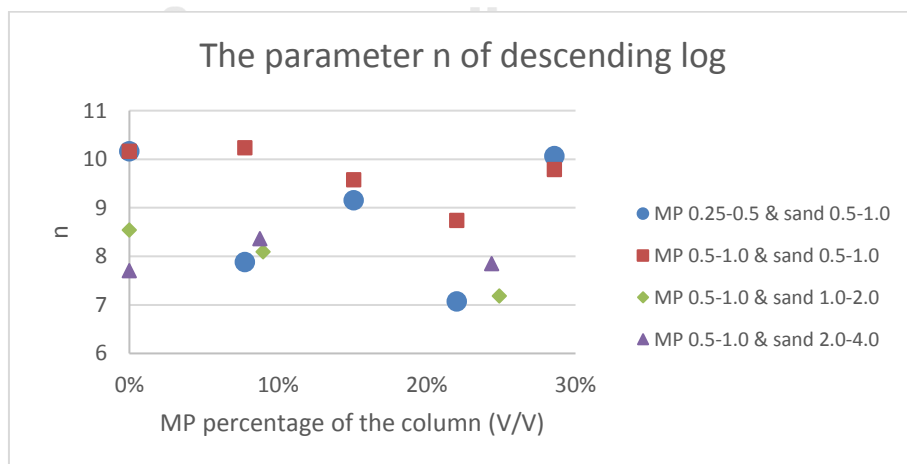


Figure D-46 The scatterplot of n (descending) and the volume percentage of MP in the column

Breakpoints of the breakthrough curve

Table D-3 The breakpoint of the breakthrough curves

MP size (mm)	Sand size (mm)	%MP	Ascending breakpoint	Descending breakpoint	
0.25-0.5	0.5-1.0	0	0.59806184	0.76159655	
		5	0.58055323	0.70524917	
		10	0.74847173	0.78556285	
		15	0.6988777	0.7521307	
		20	0.82139882	0.87105158	
0.5-1.0	0.5-1.0	5	0.75993486	0.81410416	
		10	0.79421331	0.84490479	
		15	0.80753174	0.86960302	
		20	0.85088147	0.97065051	
	1.0-2.0	1.0-2.0	0	0.69397121	0.76519349
			5	0.68896174	0.78333662
			15	0.72634242	0.77566274
	2.0-4.0	2.0-4.0	0	0.66766652	0.76363363
			5	0.75320024	0.80315592
			15	0.69931673	0.79747377

Ascending breakpoint

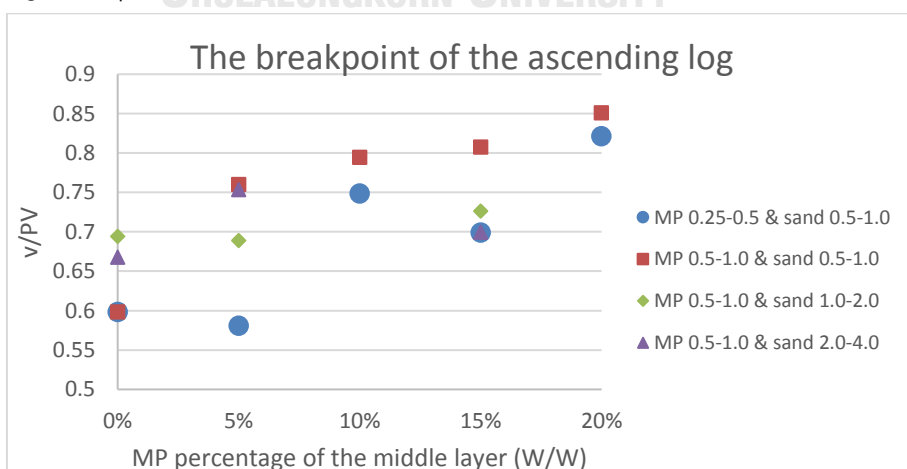


Figure D-47 The breakpoint of the ascending log over the mass percentage of MP in the middle layer

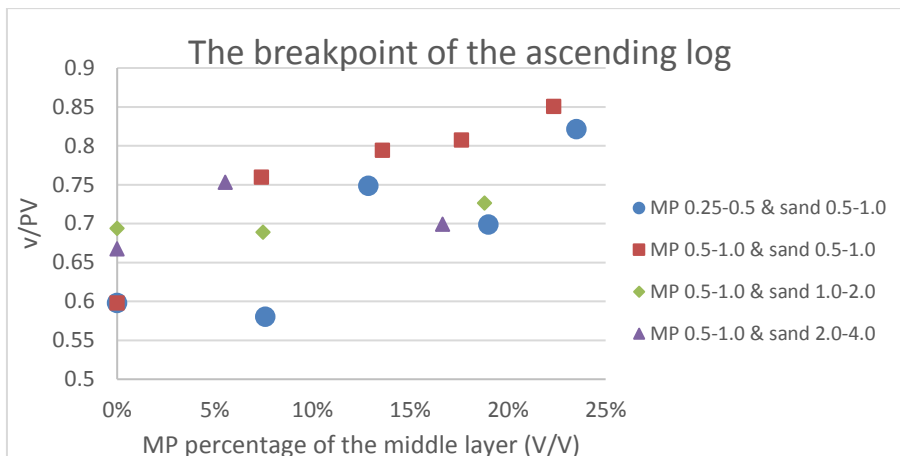


Figure D-48 The breakpoint of the ascending log over the volume percentage of MP in the middle layer

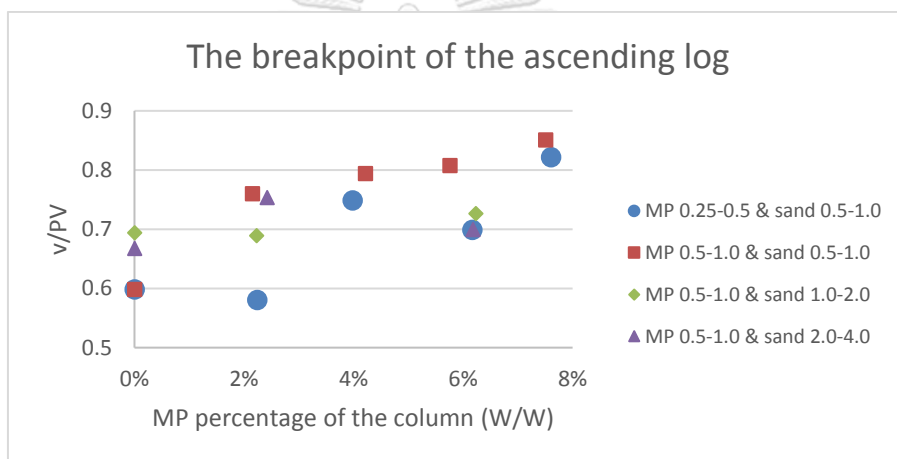


Figure D-49 The breakpoint of the ascending log over the mass percentage of MP in the column

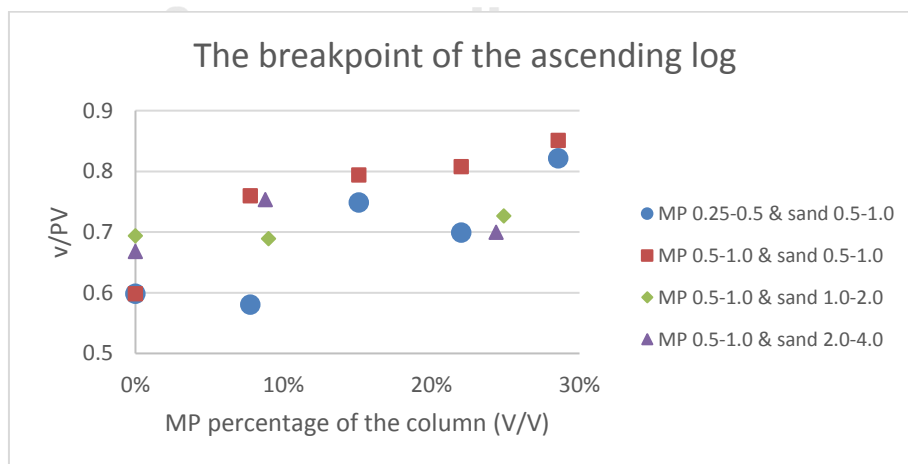


Figure D-50 The breakpoint of the ascending log over the volume percentage of MP in the column

Descending breakpoint

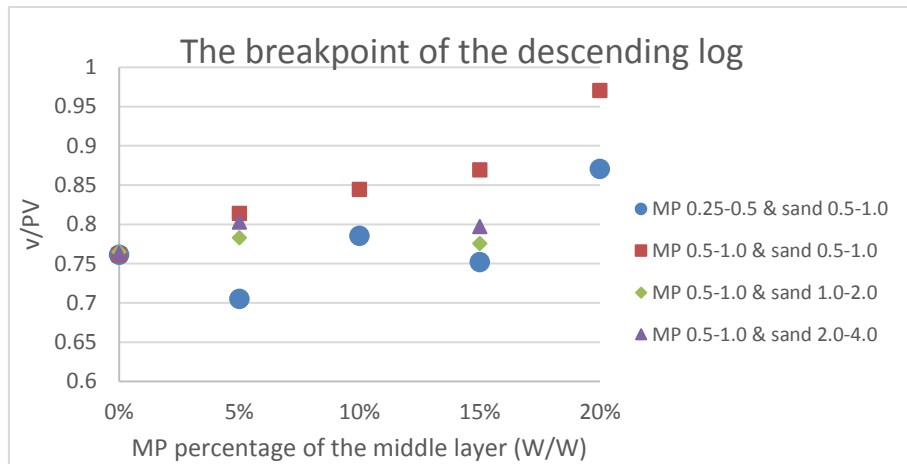


Figure D-51 The breakpoint of the descending log over the mass percentage of MP in the middle layer

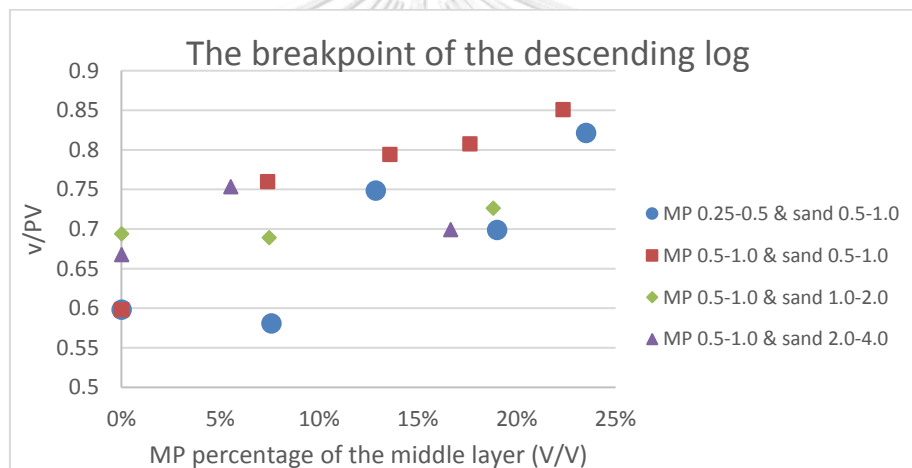


Figure D-52 The breakpoint of the descending log over the volume percentage of MP in the middle layer

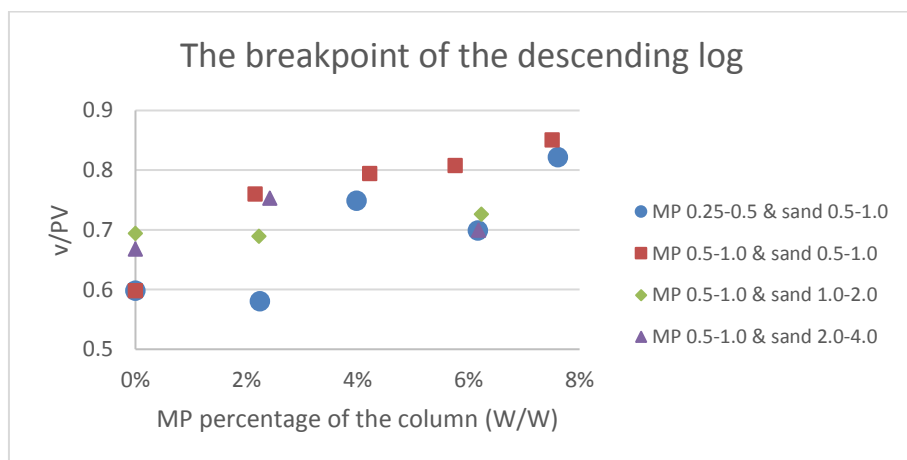


Figure D-53 The breakpoint of the descending log over the mass percentage of MP in the column

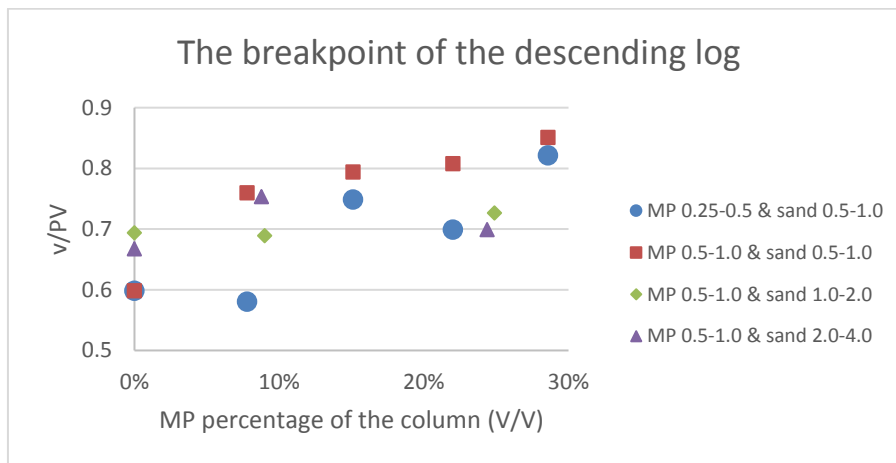


Figure D-54 The breakpoint of the descending log over the weight percentage of MP in the column



APPENDIX E

Breakthrough curve fitting (HYDRUS 1D)

The parameters

Table E-1 The parameters in the fitting of breakthrough curve derived from the column of MP 0.25-0.5 mm in sand 0.5-1.0 mm

parameter	MP percentage of the middle layer (W/W)				
	0%	5%	10%	15%	20%
θ_s (-)	0.427	0.416	0.401	0.379	0.376
K_s (cm/PV)	8.143	7.980	7.647	7.246	7.301
K_d (L/kg)	0.080	0.085	0.090	0.090	0.100
ρ_B (g/cm ³)	1.628	1.518	1.590	1.448	1.452
α (-)	0.0305	0.0301	0.0302	0.0307	0.0307
n (-)	4.4417	4.6961	4.5575	4.6608	4.6679
θ_r (-)	0.23	0.27	0.18	0.30	0.36
α_L (cm)	0.20	0.19	0.18	0.20	0.11
v_s (cm/s)	0.086	0.080	0.062	0.053	0.081
D_L (cm ² /s)	0.0173	0.0152	0.0111	0.0105	0.0089
R^2	0.9834	0.9949	0.9917	0.9892	0.9872

Table E-2 The parameters in the fitting of breakthrough curve derived from the column of MP 0.5-1.0 mm in sand 0.5-1.0 mm

parameter	MP percentage of the middle layer (W/W)				
	0%	5%	10%	15%	20%
θ_s (-)	0.427	0.409	0.383	0.393	0.372
K_s (cm/PV)	8.143	7.784	7.283	7.497	7.085
K_d (L/kg)	0.080	0.080	0.090	0.110	0.120
ρ_B (g/cm ³)	1.628	1.613	1.513	1.438	1.399
α (-)	0.0305	0.0304	0.0302	0.0304	0.0317
n (-)	4.4417	4.4892	4.6997	4.4892	4.5243
θ_r (-)	0.23	0.30	0.32	0.38	0.37

α_L (cm)	0.20	0.19	0.17	0.14	0.12
v_s (cm/s)	0.086	0.088	0.085	0.098	0.107
D_L (cm ² /s)	0.0173	0.0166	0.0145	0.0138	0.0128
R^2	0.9834	0.9855	0.9908	0.9833	0.9856

Table E-3 The parameters in the fitting of breakthrough curve derived from the column of MP 0.5-1.0 mm in sand 1.0-2.0 mm

parameter	MP percentage of the middle layer (W/W)				
	0%	5%	10%	15%	20%
θ_s (-)	0.412	0.383	-	0.355	-
K_s (cm/PV)	7.835	7.291	-	6.756	-
K_d (L/kg)	0.085	0.090	-	0.090	-
ρ_B (g/cm ³)	1.732	1.578	-	1.419	-
α (-)	0.0309	0.0302	-	0.0313	-
n (-)	4.1363	4.5897	-	4.5905	-
θ_r (-)	0.32	0.27	-	0.27	-
α_L (cm)	0.17	0.16	-	0.16	-
v_s (cm/s)	0.123	0.108	-	0.121	-
D_L (cm ² /s)	0.021	0.017	-	0.019	-
R^2	0.9930	0.9922	-	0.9910	-

Table E-4 The parameters in the fitting of breakthrough curve derived from the column of MP 0.5-1.0 mm in sand 2.0-4.0 mm

parameter	MP percentage of the middle layer (W/W)				
	0%	5%	10%	15%	20%
θ_s (-)	0.409	0.353	-	0.346	-
K_s (cm/PV)	7.782	6.736	-	6.580	-
K_d (L/kg)	0.085	0.085	-	0.085	-
ρ_B (g/cm ³)	1.640	1.604	-	1.468	-
α (-)	0.0305	0.0303	-	0.0305	-
n (-)	4.403	4.5167	-	4.6904	-
θ_r (-)	0.29	0.28	-	0.28	-

α_L (cm)	0.24	0.2	-	0.17	-
v_s (cm/s)	0.142	0.144	-	0.142	-
D_L (cm ² /s)	0.034	0.029	-	0.024	-
R^2	0.9930	0.9885	-	0.9955	-

Table E-5 The Peclet number of the column

MP size (mm)	Sand size (mm)	%MP (W/W)	Peclet number (-)
0.25-0.5	0.5-1.0	0	47.3197432
		5	38.2212331
		10	34.8722401
		15	31.5205435
		20	30.7570718
0.5-1.0	0.5-1.0	5	43.1417187
		10	38.3100198
		15	37.4058777
		20	33.8606398
	1.0-2.0	0	45.8379719
		5	38.2631287
		15	35.4358161
	2.0-4.0	0	40.8785082
		5	33.6450218
		15	32.8566679

The curve

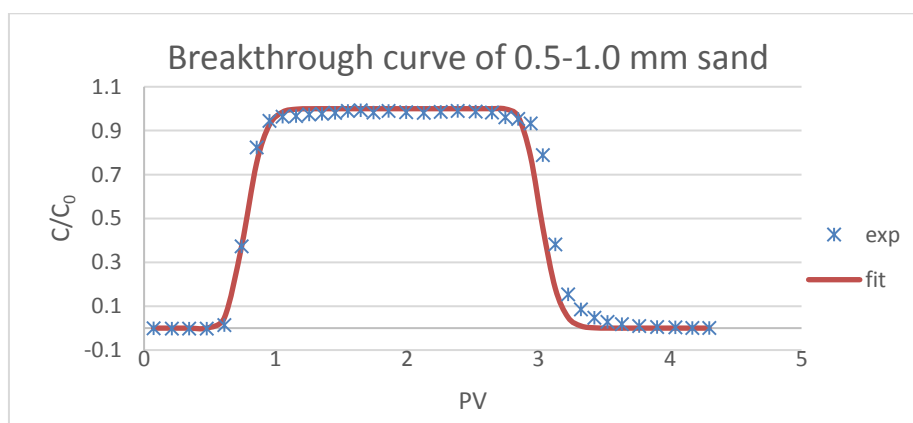


Figure E-1 Breakthrough curve fitting by HYDRUS 1D of column of sand 0.5-1.0 mm

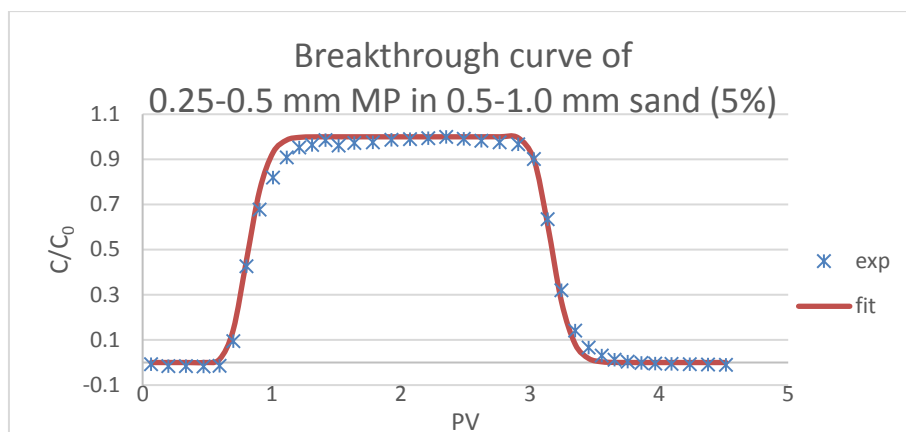


Figure E-2 Breakthrough curve fitting by HYDRUS 1D of column of
MP 0.25-0.5 mm sand 0.5-1.0 mm (5%)

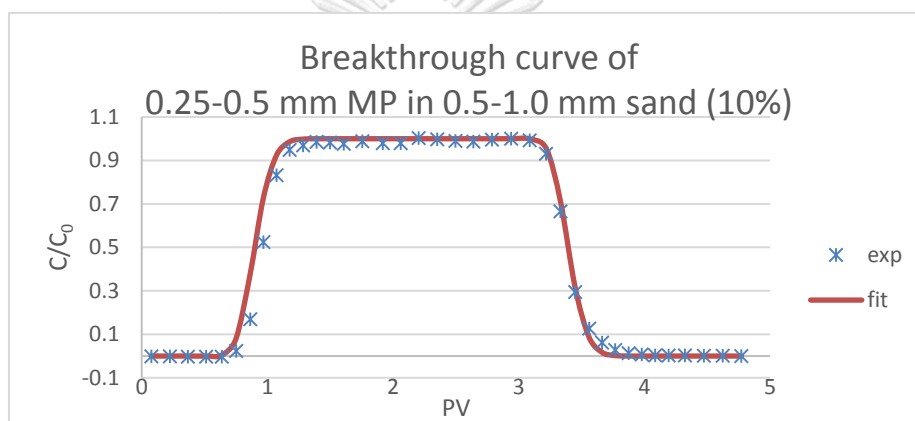


Figure E-3 Breakthrough curve fitting by HYDRUS 1D of column of
MP 0.25-0.5 mm sand 0.5-1.0 mm (10%)

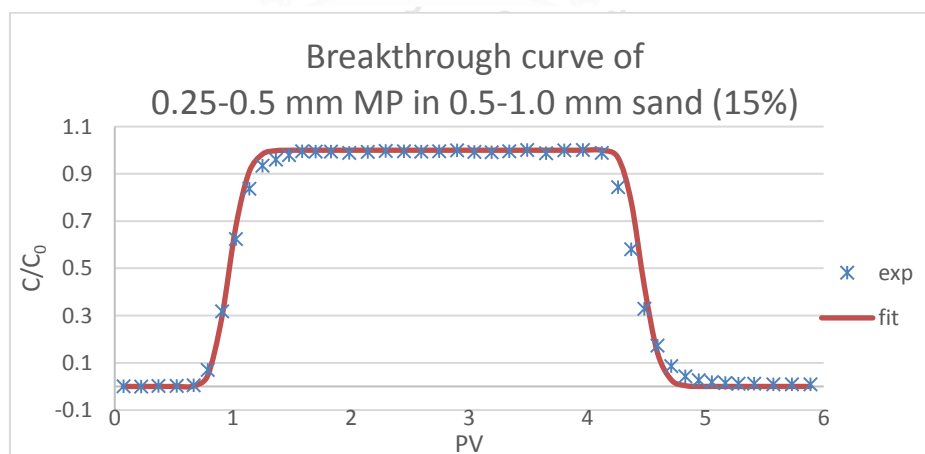


Figure E-4 Breakthrough curve fitting by HYDRUS 1D of column of
MP 0.25-0.5 mm sand 0.5-1.0 mm (15%)

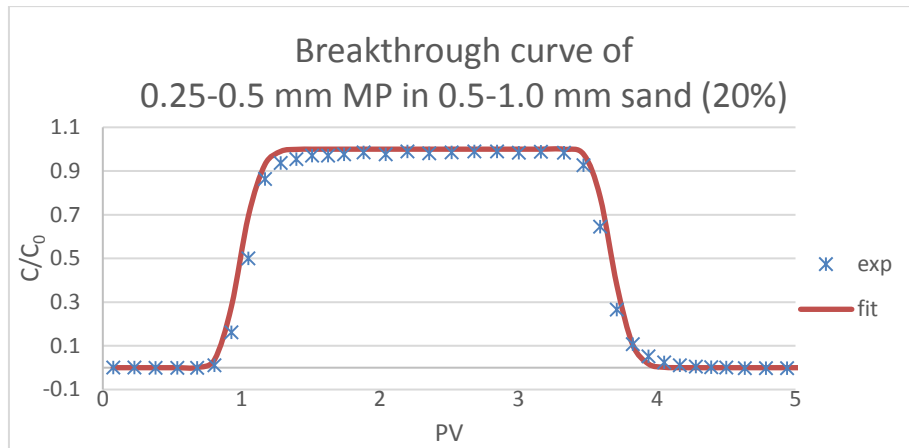


Figure E-5 Breakthrough curve fitting by HYDRUS 1D of column of MP 0.25-0.5 mm sand 0.5-1.0 mm (20%)

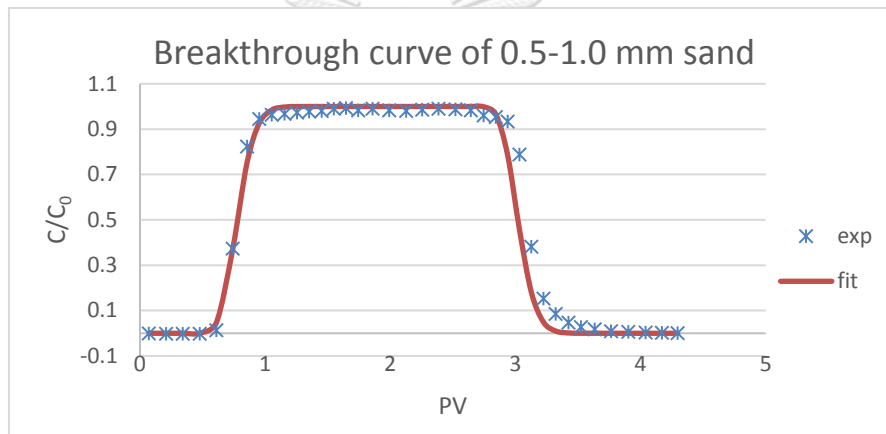


Figure E-6 Breakthrough curve fitting by HYDRUS 1D of column of MP 0.5-1.0 mm sand 0.5-1.0 mm (5%)

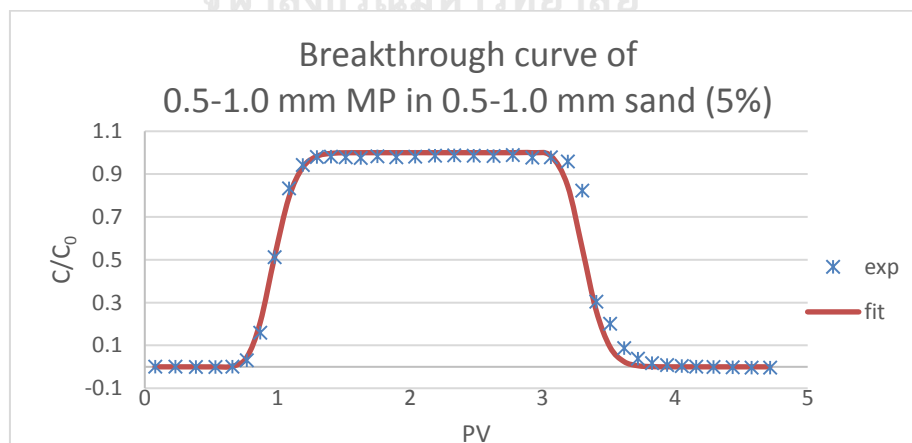


Figure E-7 Breakthrough curve fitting by HYDRUS 1D of column of MP 0.5-1.0 mm sand 0.5-1.0 mm (10%)

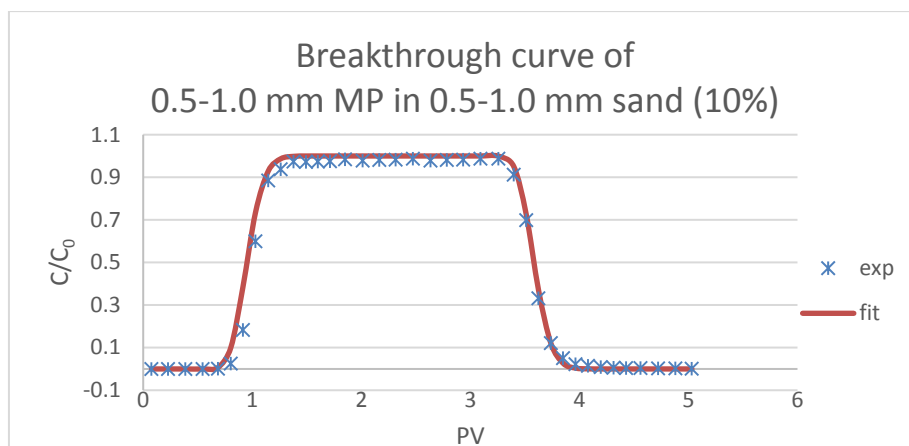


Figure E-8 Breakthrough curve fitting by HYDRUS 1D of column of
MP 0.5-1.0 mm sand 0.5-1.0 mm (15%)

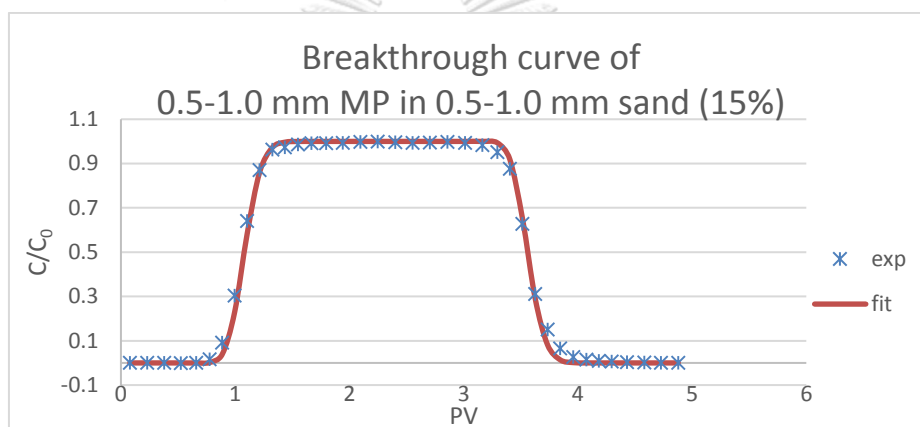


Figure E-9 Breakthrough curve fitting by HYDRUS 1D of column of
MP 0.5-1.0 mm sand 0.5-1.0 mm (15%)

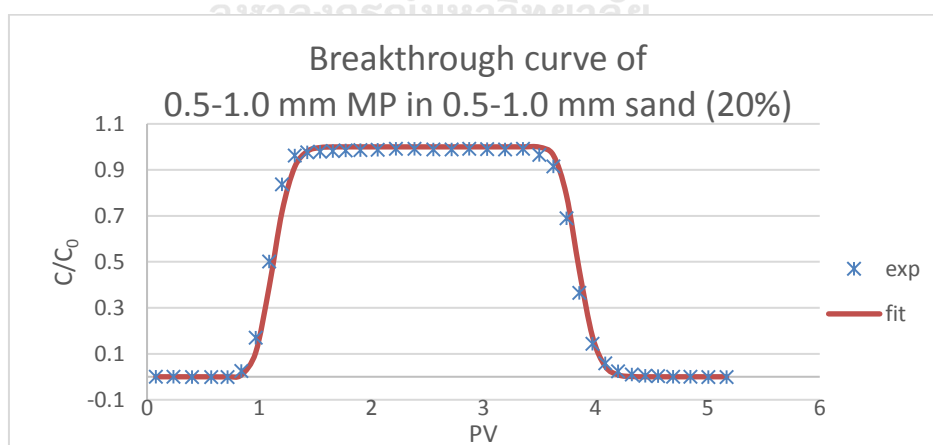


Figure E-10 Breakthrough curve fitting by HYDRUS 1D of column of
MP 0.5-1.0 mm sand 0.5-1.0 mm (20%)

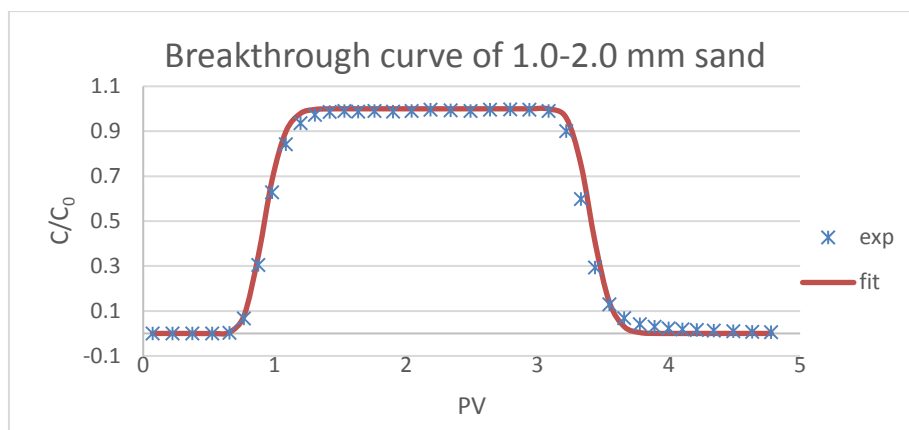


Figure E-11 Breakthrough curve fitting by HYDRUS 1D of column of sand 1.0-2.0 mm

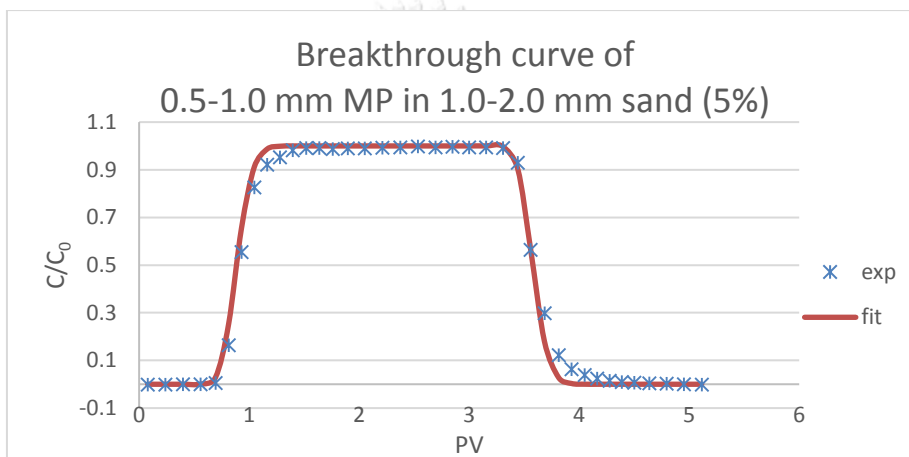


Figure E-12 Breakthrough curve fitting by HYDRUS 1D of column of MP 0.5-1.0 mm sand 1.0-2.0 mm (5%)

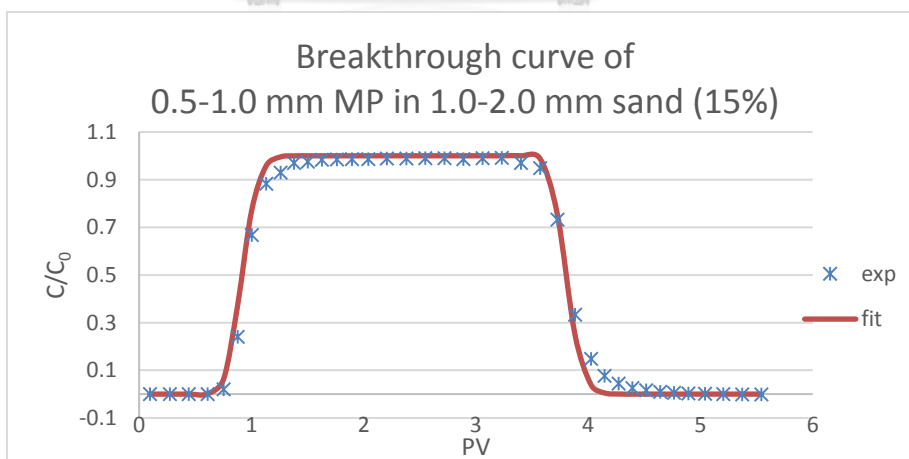


Figure E-13 Breakthrough curve fitting by HYDRUS 1D of column of MP 0.5-1.0 mm sand 1.0-2.0 mm (15%)

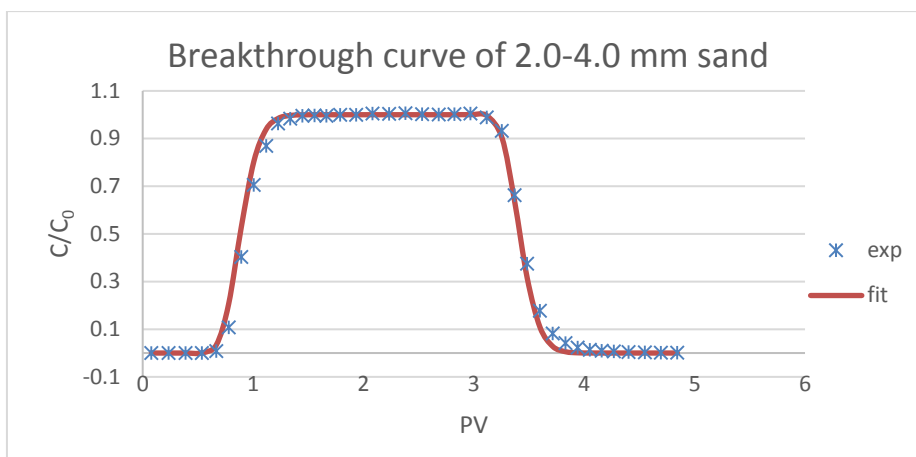


Figure E-14 Breakthrough curve fitting by HYDRUS 1D of column of sand 2.0-4.0 mm

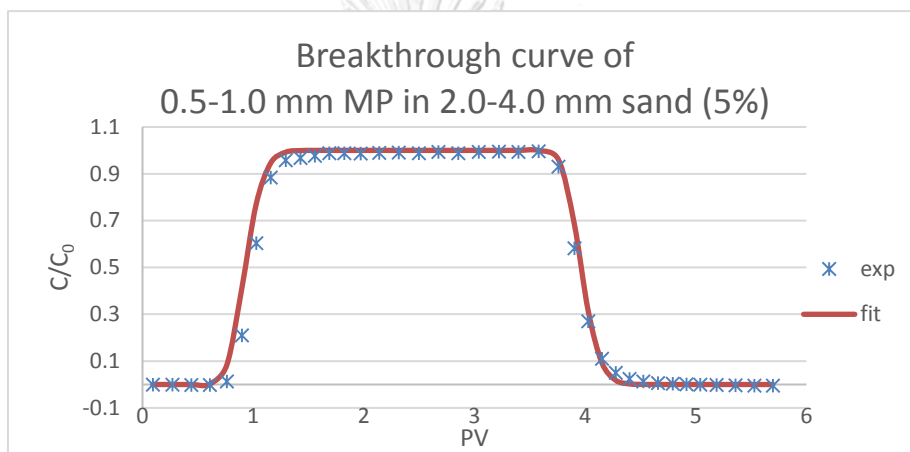


Figure E-15 Breakthrough curve fitting by HYDRUS 1D of column of MP 0.5-1.0 mm sand 2.0-4.0 mm (5%)

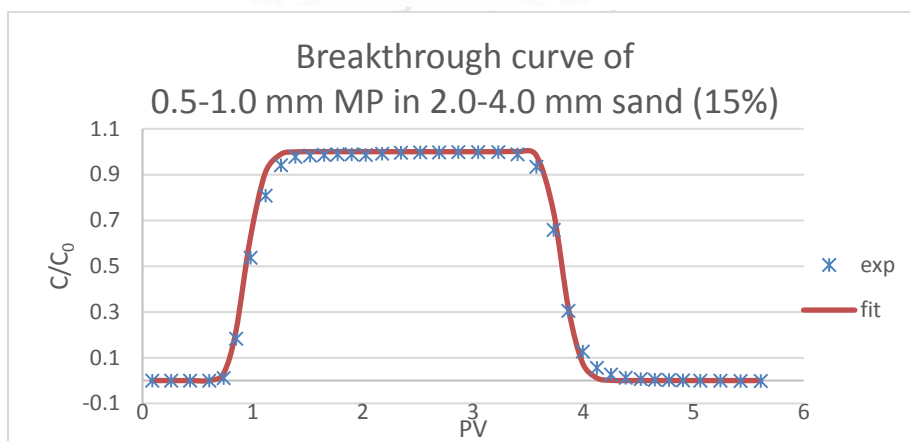


Figure E-16 Breakthrough curve fitting by HYDRUS 1D of column of MP 0.5-1.0 mm sand 2.0-4.0 mm (15%)

REFERENCES

- Ballent, Anika, Patricia L Corcoran, Odile Madden, Paul A Helm, and Fred J Longstaffe. 2016. 'Sources and sinks of microplastics in Canadian Lake Ontario nearshore, tributary and beach sediments', *Marine Pollution Bulletin*, 110: 383-95.
- Beyer, Jonny, Norman W Green, Steven Brooks, Ian J Allan, Anders Ruus, Tânia Gomes, Inger Lise N Bråte, and Merete Schøyen. 2017. 'Blue mussels (*Mytilus edulis* spp.) as sentinel organisms in coastal pollution monitoring: a review', *Marine environmental research*, 130: 338-65.
- Bissen, Raphael, and Sakonvan Chawchai. 2020. 'Microplastics on beaches along the eastern Gulf of Thailand—a preliminary study', *Marine Pollution Bulletin*, 157: 111345.
- Carman, Philip Crosbie. 1956. 'Flow of gases through porous media'.
- Cussler, Edward Lansing, and Edward Lansing Cussler. 2009. *Diffusion: mass transfer in fluid systems* (Cambridge university press).
- Fetter, Charles Willard, Thomas B Boving, and David K Kremer. 1999. *Contaminant hydrogeology* (Prentice hall Upper Saddle River, NJ).
- Firdaus, Muhammad, Yulinah Trihadiningrum, and Prieskarinda Lestari. 2020. 'Microplastic pollution in the sediment of Jagir Estuary, Surabaya City, Indonesia', *Marine Pollution Bulletin*, 150: 110790.
- Fried, Jean J. 1975. 'Chapter 2 The Theory of Dispersion in Porous Media', *Developments in Water Science*, 4.
- Gefell, Michael J, Mark Larue, and Kevin Russell. 2019. 'Vertical Hydraulic Conductivity Measurement by Gravity Drainage', *Groundwater*, 57: 511-16.
- Goodman, Alexa J, Tony R Walker, Craig J Brown, Brittany R Wilson, Vicki Gazzola, and Jessica A Sameoto. 2020. 'Benthic marine debris in the Bay of Fundy, eastern Canada: Spatial distribution and categorization using seafloor video footage', *Marine Pollution Bulletin*, 150: 110722.
- Hazen, Allen. 1983. 'Some physical properties of sand and gravel with special reference to their use in filtration', *24th Ann. Rep., Mass. State Board of Health, Boston*,

1983.

- Hossain, A.S.M.D. & Mojid, M A & Faruque, Ir. M.J. 2006. 'Determination of solute-transport parameters in three different textured soils by using time-domain reflectometry (TDR)', *Bangladesh Journal of Agricultural Research*, 33: 51-60.
- Hüffer, Thorsten, Florian Metzelder, Gabriel Sigmund, Sophie Slawek, Torsten C Schmidt, and Thilo Hofmann. 2019. 'Polyethylene microplastics influence the transport of organic contaminants in soil', *Science of the Total Environment*, 657: 242-47.
- Kakaire, Joel, George L Makokha, Majaliwa Mwanjalolo, Albert K Mensah, and Emmanuel Menya. 2015. 'Effects of mulching on soil hydro-physical properties in Kibaale Sub-catchment, South Central Uganda', *Applied Ecology and Environmental Sciences*, 3: 127-35.
- Kastrinos, John R, Andrew Chiasson, and Paul Ormond. 2019. 'Estimating groundwater heat exchange in a standing-column well by injection of a bromide tracer', *Geothermics*, 82: 121-27.
- Kozeny, Josef. 1927. 'Über kapillare leitung der wasser in boden', *Royal Academy of Science, Vienna, Proc. Class I*, 136: 271-306.
- Krumbein, WC, and GD Monk. 1943. 'Permeability as a function of the size parameters of unconsolidated sand', *Transactions of the AIME*, 151: 153-63.
- La Daana, K Kanhai, Katarina Gårdfeldt, Olga Lyashevskā, Martin Hassellöv, Richard C Thompson, and Ian O'Connor. 2018. 'Microplastics in sub-surface waters of the Arctic Central Basin', *Marine Pollution Bulletin*, 130: 8-18.
- Labrecque, Steven P, and William J Blanford. 2021. 'Fate and transport of bromide and mononuclear aromatic hydrocarbons in aqueous solutions through Berea Sandstone', *Science of the Total Environment*, 766: 141714.
- Lestari, Prieskarinda, Yulinah Trihadiningrum, Bagas Ari Wijaya, Khalda Ardelia Yunus, and Muhammad Firdaus. 2020. 'Distribution of microplastics in surabaya river, indonesia', *Science of the Total Environment*, 726: 138560.
- Masipan, Tulaya, Srilert Chotpantararat, and Satika Boonkaewwan. 2016. 'Experimental and modelling investigations of tracer transport in variably saturated agricultural soil of Thailand: Column study', *Sustainable Environment Research*, 26: 97-101.

- Naranjo, Pablo M, Edgardo L Sham, Enrique Rodríguez Castellón, Rosa M Torres Sánchez, and Elsa M Farfán Torres. 2013. 'Identification and quantification of the interaction mechanisms between the cationic surfactant HDTMA-Br and montmorillonite', *Clays and Clay Minerals*, 61: 98-106.
- O'Connor, David, Shizhen Pan, Zhengtao Shen, Yinan Song, Yuanliang Jin, Wei-Min Wu, and Deyi Hou. 2019. 'Microplastics undergo accelerated vertical migration in sand soil due to small size and wet-dry cycles', *Environmental Pollution*, 249: 527-34.
- Oleszczuk, RYSZARD, and Milena Truba. 2013. 'The analysis of some physical properties of drained peat-moorsh soil Layers', *Annals of Warsaw University of Life Sciences-SGGW. Land Reclamation*, 45.
- Peng, Guyu, Richard Bellerby, Feng Zhang, Xuerong Sun, and Daoji Li. 2020. 'The ocean's ultimate trashcan: Hadal trenches as major depositories for plastic pollution', *Water research*, 168: 115121.
- Polle, Andrea, and Shaoliang Chen. 2015. 'On the salty side of life: molecular, physiological and anatomical adaptation and acclimation of trees to extreme habitats', *Plant, Cell & Environment*, 38: 1794-816.
- Richards, Lorenzo Adolph. 1954. *Diagnosis and improvement of saline and alkali soils* (LWW).
- Royer, Sarah-Jeanne, Sara Ferrón, Samuel T Wilson, and David M Karl. 2018. 'Production of methane and ethylene from plastic in the environment', *PloS one*, 13: e0200574.
- Saliu, Francesco, Simone Montano, Maria Grazia Garavaglia, Marina Lasagni, Davide Seveso, and Paolo Galli. 2018. 'Microplastic and charred microplastic in the Faafu Atoll, Maldives', *Marine Pollution Bulletin*, 136: 464-71.
- Schmid, Kurt, Kirk O Winemiller, David Chelazzi, Alessandra Cincinelli, Luigi Dei, and Tommaso Giarrizzo. 2018. 'First evidence of microplastic ingestion by fishes from the Amazon River estuary', *Marine Pollution Bulletin*, 133: 814-21.
- Su, Lei, Yingang Xue, Lingyun Li, Dongqi Yang, Prabhu Kolandhasamy, Daoji Li, and Huahong Shi. 2016. 'Microplastics in taihu lake, China', *Environmental Pollution*, 216: 711-19.

- Thepwilai, Supakorn, Kannika Wangritthikraikul, Sakonvan Chawchai, and Raphael Bissen. 2021. 'Testing the factors controlling the numbers of microplastics on beaches along the western Gulf of Thailand', *Marine Pollution Bulletin*, 168: 112467.
- Urban-Malinga, Barbara, Mariusz Zalewski, Aneta Jakubowska, Tycjan Wodzinowski, Maja Malinga, Barbara Pałys, and Agnieszka Dąbrowska. 2020. 'Microplastics on sandy beaches of the southern Baltic Sea', *Marine Pollution Bulletin*, 155: 111170.
- Woessner, William W, and Eileen P Poeter. 2020. 'Hydrogeologic Properties of Earth Materials and Principles of Groundwater Flow', *The Groundwater Project, Guelph, Ontario, Canada*.
- Wu, Fangzhu, Youji Wang, Jonathan YS Leung, Wei Huang, Jiangning Zeng, Yanbin Tang, Jianfang Chen, Aiqin Shi, Xiang Yu, and Xiaoqun Xu. 2020. 'Accumulation of microplastics in typical commercial aquatic species: A case study at a productive aquaculture site in China', *Science of the Total Environment*, 708: 135432.
- Xu, Baile, Fei Liu, Zachary Cryder, Dan Huang, Zhijiang Lu, Yan He, Haizhen Wang, Zhenmei Lu, Philip C Brookes, and Caixian Tang. 2020. 'Microplastics in the soil environment: occurrence, risks, interactions and fate—a review', *Critical Reviews in Environmental Science and Technology*, 50: 2175-222.
- Zhang, Jiaxu, Chenglong Zhang, Yixiang Deng, Ruixue Wang, En Ma, Jingwei Wang, Jianfeng Bai, Jin Wu, and Yongjie Zhou. 2019. 'Microplastics in the surface water of small-scale estuaries in Shanghai', *Marine Pollution Bulletin*, 149: 110569.

VITA

NAME Siravit Chanprasit

DATE OF BIRTH 6 May 1995

PLACE OF BIRTH Bangkok

INSTITUTIONS ATTENDED Chulalongkorn University

HOME ADDRESS 280/1, Rama VI Soi 28, Phayathai, Phayathai, Bangkok
10400

